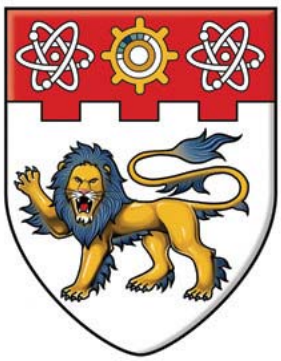

NANYANG TECHNOLOGICAL UNIVERSITY

BIOENGINEERING

BIO-FUNCTIONALISATION OF POLYELECTROLYTE MICROCAPSULES WITH BIOTINYLATED POLY (ETHYLENE GLYCOL)-GRAFTED LIPOSOMES FOR APPLICATION IN TARGETED DRUG DELIVERY

GAO JIE

GAO JIE

SCHOOL OF CHEMICAL AND BIOMEDICAL ENGINEERING

2012

2012

BIO-FUNCTIONALISATION OF POLYELECTROLYTE MICROCAPSULES WITH BIOTINYLATED POLY (ETHYLENE GLYCOL)-GRAFTED LIPOSOMES FOR APPLICATION IN TARGETED DRUG DELIVERY

GAO JIE

GAO JIE

School of Chemical and Biomedical Engineering

A thesis submitted to the Nanyang Technological University
in partial fulfilment of the requirement for the degree of
Doctor of Philosophy

2012

Acknowledgements

During my PhD study in NTU, I received tremendous help from different resources. I would like to express my sincere gratitude, in particular to:

Associate Professor Björn Holger Neu, for the opportunity to work in his research group and for his thorough scientific guidance and supervision,

Professor Edwin Donath, Dr. Uta Reibetanz, Dr. Jacqueline Leßig, for the opportunity to work in University of Leipzig and their scientific guidance during my stay in Leipzig, Germany,

Professor Changming Li, A/Professor Dong-An Wang, and their lab members, for the inspiring discussion and continuous support,

My thesis examiners, for their extremely careful review on my thesis,

NTU research assistantship, for the generously increasing financial support, SCBE faculty for the teaching and support,

My lab colleagues, Dr. Yang Yang, Dr. Zhengwen Zhang, Dr. Samar Rad, for fruitful discussions and assistance on laboratory operation,

My lab colleagues, Mr Mutukumaraswamy Shaillender and Ms Averil, Min Hui Chen, for their help to my project and their effort on proofreading of this thesis,

Office colleagues in Bioengineering division N1.3 B3-04, for providing useful information regarding to purchasing and research topics,

FYP students, for their interests in the project and for their work in this group,

SCBE officers, Dr. Shucong Yu, Ms Kah Yan Yeo, Ms Chitra Devi D/O Subramaniam, Ms Sheron Abraham Joseph, Ms Lee Sulei for their attentive help,

My parents and family members, for their continuous love and support and for believing in me all the times,

My husband, Dr. Hairong Li, for lots of intensive and fruitful discussions, for immeasurable encouragement!

Ms Meowhah Chia, friends from NTU navigator, friends from my hometown, for their friendship, encouragement and sharing their lives in different disciplines!

Table of Contents

List of Work

Publications

Samar Rad, Jie Gao, Herbert J. Meiselman, Oguz K. Baskurt, Björn Neu, *Depletion of high molecular weight dextran from the red cell surface measured by particle electrophoresis.* Electrophoresis, 2009. 30 (3): p. 450-456

Gao, J., U. Reibetanz, et al., *Bio-functionalisation of polyelectrolyte microcapsules with biotinylated polyethylene glycol - grafted liposomes.* Macromolecular Bioscience, 2011. 11(8): p. 1079-1087.

Conference presentations

10 to 12 December 2007, Singapore, Oral presentation

International conference on Cellular and Molecular Bioengineering (ICCMB1)

Jie Gao, Jianhe Wang, Haiwen Gu, Björn H. Neu, Targeting of hollow polyelectrolyte capsules to fibronectin.

2nd -4th, August 2010,Singapore, Oral presentation

International conference on Cellular and Molecular Bioengineering (ICCMB2)

Jie Gao, Uta Reibetanz, Björn Neu, Targeting ability study of bio-functional polyelectrolyte microcapsules (PEMC)

List of Figures

List of Tables

List of Abbreviations

AFM	atomic force microscopy
BSA	bovine serum albumin
CLSM	confocal laser scanning microscopy
DOX	doxorubicin
DSPE	distearylphosphatidylethanolamine
ELISA	enzyme linked immunosorbent assay
FCM	flow cytometry
FSC	forward scattering
Gmean	fluorescence intensity geometric mean
IA	immunoassay
IgG	immunoglobulin G
LbL	layer-by-layer
MF	melamine formaldehyde
MFI	mean fluorescence intensity
MPS	mononuclear phagocytic system
NA	NeutrAvidin
NCE	new chemical entity
NSB	non-specific binding
PAH	poly (allylamine hydrochloride)
PEM	polyelectrolyte multilayers

PEMC	polyelectrolyte microcapsules
PEMP	polyelectrolyte microparticles
PEG	poly(ethylene glycol)
POPC	1-palmitoyl-2-oleoyl-sn-glycero-3-phosphocholine
POPS	1-palmitoyl-2-oleoyl-sn-glycero-3-[phospho-L-serine] (sodium salt)
PPDX (X=0,1,2,5,10,20)	POPS/POPC/X%DSPE-PEG-biotin
PSS	poly (styrene sulphonate)
RGD	Arg-Gly-Asp
RMS	root mean square
SLB	supported lipid bilayers
SSC	side scattering

Summary

Progress in chemistry and biotechnology allowed the development of nanoengineered delivery systems that can encapsulate a wide variety of novel therapeutics such as proteins, chemotherapeutics, and nucleic acids. It is always interesting to functionalize the delivery systems to be "intelligent" and multi-functional, such that they can avoid the uptake by macrophages and deliver their payload at a specific position, e.g. target to a pathogen tissue. Polyelectrolyte capsules, made by layer-by-layer (LbL) coating of a sacrificial template followed by dissolution of the template, have been studied intensively as potential drug delivery carriers. LbL techniques allow the design of microcapsules using simple building blocks and assembly procedures, and provide a previously unmet control over the functionality of the microcapsules. This project was aimed to develop novel multi-functional polyelectrolyte capsules (PEMC) as targeted drug carriers using LbL techniques.

Hollow PEMC were prepared using LbL self-assembly of polyelectrolytes on melamine formaldehyde templates, followed by template dissolution, and were subsequently coated with biotinylated poly (ethylene glycol)-grafted liposomes (biotin-PEG-lipids). These potential site-specific carrier systems show a high specificity binding for NeutrAvidin and a strong resistance against unspecific serum protein binding. It is concluded that this design with NeutrAvidin as the outermost layer of such capsules provides an ideal platform for the bio-functionalisation of PEMC as drug delivery systems or as artificial cell-like structures for biomimetic studies.

PEMC modified with biotin-PEG-lipids provided the interface for developing a model microsphere immunoassay based on sequential immobilization of NeutrAvidin (NA) and biotinylated antibody (biotin-IgG). It was demonstrated that modification of biotin-PEG-lipids on PEMC has a significant effect on the apparent affinity to biotin-IgG, compared to the control sample without biotin-PEG-lipids modification and without NA presence. The results provide deep understanding of functionalisation PEMC with antibodies and thus more clear view in utilizing such PEMC in biomedical application.

The final part of the study was to investigate the targeting ability of the specific ligand (anti-CCR5 IgG) modified PEMC to a fibroblast cell line expressing antigen CCR5 (3T3.CD4.CCR5). Biotin-PEG-lipids and NeutrAvidin has been adsorbed on the PAH-ending surfaces to bind anti-CCR5 antibodies. The modified PEMC interaction with cell lines without CCR5 expression was also performed as the negative control. Under physiological conditions, a time dependent interaction was found between modified PEMC and cell line. The results are believed to shed light on the potential of bio-functional PEMC to be promising drug carriers for receptor-mediated delivery.

This work demonstrate that the structure-property of LbL multilayer films associated with surface modification is related to amplified targeting ability of PEMC and the prevention of PEMC aggregation. The results of this work have led to optimization of process parameters and proof of concept of reduction of opsonisation, and improvement of targeting both in solutions for detection purposes and in cells for delivery purposes.

Chapter 1 Introduction

Modern drug discovery has been greatly improved by the rapid development of delivery methods. The total expenditure for the research and development of every new drug (a new chemical entity, NCE) is above $500 million, and the whole process may take up to 14 years [1]. About 40% of drug candidates make their way to evaluation in humans (Phase I clinical trial), and only 10% will succeed in clinical trials [2]. In a research to analyze the high attrition rate [3], the results revealed that most failures were not due to a lack of "biological activities" defined by in vitro testing, but due to some other factors. These factors may include poor pharmacokinetics properties in humans, lack of clinical efficacy, toxicity and adverse effects, which are directly or indirectly related to drug delivery [4]. Therefore, development of drug delivery system has become major player in drug market due to economic reasons.

One of the challenges of drug delivery is to maintain the stability and solubility of therapeutic molecules from the surrounding physiochemical environment before reaching the desired site. They should prevent therapeutic molecules from distributing nonspecifically in the body and encountering both healthy and pathological cells with similar efficiency. Moreover, in order to utilize the carriers in the circulation, it is vital to prevent the rapid recognition and uptake by the mononuclear phagocytic system (MPS, e.g. monocytes or macrophages).

During past decades, a large variety of micro- and nano- drug carriers has emerged, including liposomes [5-7], micelles [8-10] and cell ghosts [11], nanoparticles [12-14],

microcapsules [15-18]. However, there still are many design and application problems, including stability, time of release, cost of preparation, and availability of the drug at the target issue. To solve these problems, it is important to develop drug delivery systems which can increase drug concentration at pathological area with minimal undesirable side-effects on healthy organs. This way therapy costs can also be reduced as less drug quantity is required.

Main attempts to achieve targeted delivery involve surface modification of drug carriers. With the rapid development of chemistry and material science, novel carriers can be designed with higher efficacy and longer life-span in circulation. The aim of this project is to make a step towards the competitive edge by developing a novel drug delivery system with multiple surface functions.

1.1 Background

1.1.1 Polyelectrolyte multilayers (PEM)

Layer-by-layer (LbL) assembly is a readily accessible, highly inexpensive process but powerful approach to produce robust films with specifically controlled film thickness and properties. There has been a growing interest in the development of thin films based on LbL polyelectrolyte multilayers (PEM) since 1990s [19-21]. Comprehensive reviews on the current progress of this field can be found in recent articles [17, 22-24]. PEM are typically formed by alternately immersing a substrate in dilute polycationic and polyanionic solutions, with ample rinsing between adsorption

steps. The PEM films allow the incorporation of a great variety of chemical and biological species, such as functional polymers, nanoparticles, lipids and enzymes [25-28].

During the electrostatic multilayer assembly, the sequential adsorption of oppositely charged polyelectrolytes is mostly directed by Coulombic forces (Figure 1.1). Additionally, secondary shorter range forces (hydrophobicity and hydrogen bonding) play a role in determining the film properties such as mechanical strength and surface functionalisation. For example, mechanical strength of the polyelectrolyte multilayer could be tailored by varying film thickness, morphology and degree of interpenetration [29, 30]. A previous study on typical polyelectrolyte pairs of poly(styrene sulphonate) sodium salt (PSS) and poly (allylamine) hydrochloride (PAH) has shown that film thickness of the pairs of adsorbed polymer polyelectrolytes on polystyrene (PS) latex particles is approximately 2 nm/layer [31]. Surface functionalisation of PEM would affect protein adsorption, cell adhesion and inflammation response [32, 33].

The outmost surface of an LbL film is irregular and penetrable with free chain ends and loops extend above the film surface. Swelling solvent and loosing chain entanglement allow newly adsorbing chains to infiltrate underlying layers [34]. Polymer backbone flexibility, degree of ionization, solvent electrostatic shielding, along with the availability of attractive surface sites, influences the conformation in which chains approach and adsorb on the surface, determining the charge density of the new surface. The resulting highly-interpenetrated film structure is exquisitely sensitive to variations in solvent conditions and polymer structures. pH variation is known to

have a strong influence during the weak polyelectrolyte LbL assembly [35-37]. Ionic concentration effects also have been studied extensively for its shielding ability during polyelectrolyte-surface and polyelectrolyte-polyelectrolyte electrostatic interactions [38, 39]. As a result, pH and ionic strength are always employed to control the film properties.

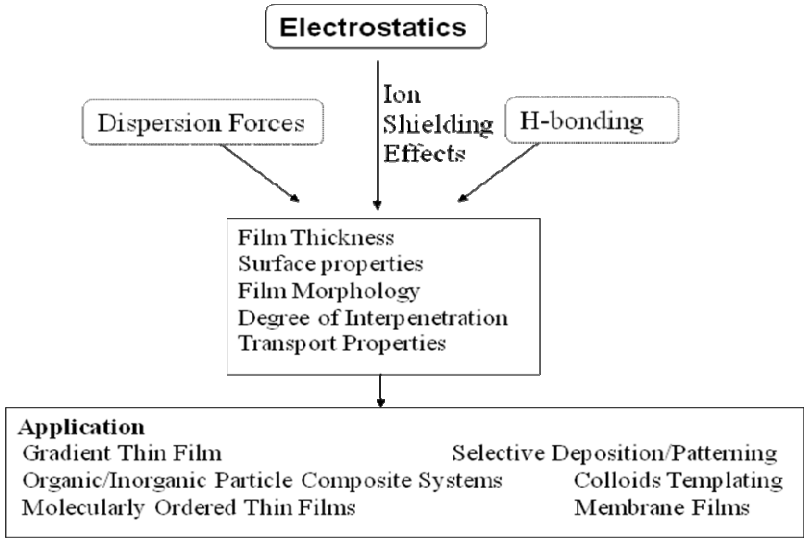

Figure 1.1 Schematic illustration of forces influencing properties of layer-by-layer films, and the applications achieved by controlling or manipulating these interactions with processing [21].

Bio-macromolecules can be used to the build-up and design of biocompatible interfaces by LbL process. These LbL films have many applications, such as (1) immobilization of biomacromolecules for smart biosensors and (2) the control of cell adhesion and cell growth for mimetics of tissue surfaces. Most of these bio-macromolecules can be classified as polysaccharides, nucleic acids, and proteins. Polysaccharides, e.g. chitosan and dextran sulfate [40-42], are mainly used by nature as building blocks or for food storage. Bearing chemical groups like carboxylic acids or

amines, they are suitable candidates for the layer-by-layer electrostatic multilayer build-up. LbL films made of polysaccharides may enhance surface biocompatibility for cell culture and human implants. Ribonucleic and desoxyribonucleic acids [43-45] can be used as polyanions for the layer-by-layer deposition process, because they have covalently linked backbones made of alternating pentoses and highly negatively charged phosphates. The conformation of the double helix is sensitive to temperature or pH changes, which is of importance for biosensing of a number of drugs intercalating in this double helix [45]. Proteins, being amphoteric, may be globally negatively or positively charged when used respectively at a pH above or under their isoelectric point. Composite protein-polyelectrolytes [46-49] multilayers have been prepared by the layer-by-layer deposition technique for potential applications from nonthrombogenic surfaces to biosensing, through the immobilization of enzymes for bio-catalysis.

1.1.2 Polyelectrolyte microcapsules (PEMC)

Novel drug delivery system that has recently emerged from cross-disciplinary scientific symbiosis is polyelectrolyte microcapsules (PEMC), fabricated by LbL assembly of PEM on 3D colloidal surfaces. Since the introduction of polyelectrolyte microcapsules (PEMC) in 1998, this technique has received great interest in material and life sciences [16, 50-52]. After the layer-by-layer (LbL) sequential adsorption of oppositely charged polyelectrolytes onto colloidal templates, hollow capsules can be obtained by dissolving the templates (Figure 1.2) [17, 53-55]. Various colloidal particles including biological as well as biodegradable materials like erythrocytes and PLGA/PLA or synthetic materials like silica or calcium carbonate have been employed

[51, 56-58]. Depending on the template PEMC can be produced in sizes ranging from a few hundred nanometers to several micrometers [59].

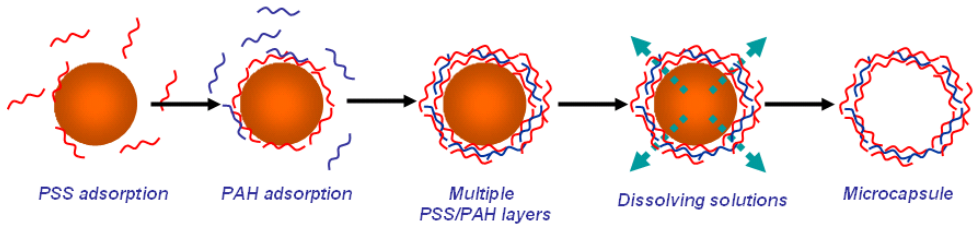

Figure 1.2 Schematic illustration of deposition of polyelectrolyte onto a sacrificial template via the LbL assembly, and formation of the hollow capsules, when the core is selectively removed through the semi-permeable polymer shells. (PSS: poly (styrene sulphonate) sodium salt; PAH: poly (allylamine) hydrochloride)

In detail, the advantages of LbL assembly techniques are described as follows:

Versatility—polyelectrolytes with a variety of compositions and structures can be fabricated on sacrificial templates with different sizes and shapes [60-64]. In addition, vast functional organic and inorganic material can be incorporated into the polyelectrolyte films or precipitated inside the hollow capsules [65-67].

Flexibility—the polyelectrolyte hollow capsules provide 3-D ultra thin shells with precisely tuned thickness of the adsorbed layers in the nanometer range. Their mechanical properties [68, 69] and the permeability of the multilayered shells can be specially controlled [37, 70-72].

In recent years there has been great interest in studying PEM particles and capsules as possible micro- or nano- drug carriers [73-77], sensor particles [78-81] and micro-reactors [82-84] for diagnostic or biological applications. Meanwhile, the fabrication

and study of the nano-organized PEMC have also enabled advances in a number of important fields in basic research such as polymer chemistry and biophysics [69, 85-89].

The initial concern of the PEMC fabrication is the colloidal templates, which have to be dissolvable and leaving the capsules completely without affecting the capsule stability. Several templates have been extensively studied for the capsule preparation, such as latex particles [53, 63, 90], inorganic crystals [27, 52, 60], and biological templates [55, 91]. Among them, weakly cross-linked melamine–formaldehyde (MF) latex particles together with polyelectrolytes PSS/PAH is the most established PEMC fabrication protocol. MF particles were coated with negatively charged PSS and positively charged PAH layer by layer until the desired layers were coated, following which the template can be dissolved into protonated MF oligomers in 0.1 M HCl. Due to its low cost and great repeatability, this procedure became a very popular model system to do further research using PEMC [16, 92], such as controlled release of encapsulated molecules and surface functionalisation of the multilayer shelf.

However, the oligomers are too large to diffuse easily out of the capsules and lead to undissolved traces of the core remaining in the interior of PSS/PAH microcapsule or the capsule shell. Meanwhile, an osmotic pressure is generated due to the temporarily high concentration of the dissolved MF oligomers in the interior. The high osmotic pressure leads to pores or weak parts in the capsule shells, which increases the permeability of the shells than the planar and unstressed polyelectrolyte films of the same material and thickness [37]. To reduce the permeability of MF capsules, further

polyelectrolyte layers can be assembled after the dissolution of the core, which results in closing of the pores and a remarkable decrease in the permeability even for small dye molecules.

As an alternative to MF particles, erythrocytes were applied as templates for LbL assembly. They are available in biconcave shapes, quasi monodisperse and very inexpensive. The decomposition of the biological templates following LbL assembly can be achieved by using a pH 12 sodium hypochlorite solution. It was observed that, under these harsh conditions, the polyelectrolyte wall is also oxidized. This oxidation causes the loss of all the positive charges and of some polyelectrolyte material, resulting in a cross-linking of the wall materials [93]. Thus using biological cells as a template would result in capsules with limited stability and uncontrolled permeability. To increase the capsules stability by closing the pores on the wall, lipids can be adsorbed after the dissolution of the template to control the permeability [54, 94].

Inorganic carbonates, such as calcium carbonate ($CaCO_3$) [17, 60, 95], manganese carbonate ($MnCO_3$) and cadmium carbonate ($CdCO_3$)[17] have recently been applied as the templates to reduce the interior residues after template dissolving. Polyelectrolyte shells are reported to be permeable to molecules with a molecular weight below 5 kDa [96]. These inorganic microparticles could be dissolved to low molecular weight of ions and diffuse easily through the wall, leaving no osmotic stress during templates dissolution.

The porous nature of these templates makes them easily loaded with relatively large amounts of biomolecules that remain entrapped within the capsule void during or after capsules fabrication. In addition, the mild dissolution conditions do not destroy

the encapsulated macromolecules, be either by EDTA (when $CaCO_3$ is used) or by a low pH (in the case of $MnCO_3$ and $CdCO_3$.). $CaCO_3$ particles coated with biodegradable polyelectrolytes poly-L-arginine and dextran sulfate, served as a low toxicity delivery system. Biodegradable polyelectrolytes are degraded through ester hydrolysis or enzymatic action [97]. For example, DNA and pronase were co-precipitated within calcium carbonate microparticles [98]. Subsequently these microparticles were LbL coated with multilayers of polypeptides (poly-L-aspartic acid and poly-L-arginine), which were susceptible to enzymatic hydrolysis by pronase. The microcapsules decomposed and subsequently released the encapsulated DNA in a temperature dependent way. Complete degradation of these capsules were found VERO cancer cells [97] and bone-marrow-derived dendritic cells [99]. The limitation of biodegradable polyelectrolytes is its low dispersity which might need further separation processes such as capsules filtration. Meanwhile, moderate inflammatory reaction was reported after PEMC subcutaneous injection to tissues [99] using PEMC coated with several types of biodegradable polyelectrolytes.

1.1.3 Polyelectrolyte microcapsules (PEMC) for drug delivery

In this chapter, we provide an overview of the important contributions in the development of PEMCs for drug-delivery purposes. Polyelectrolyte capsules have gained interest recently as potential drug carriers from different aspects, such as encapsulation and release methods [16, 92], *in vitro* and *in vivo* interaction with cells and tissues [17, 18, 51]. We will briefly explain from these two aspects and understand the strengths of LbL prepared polyelectrolyte capsules in the field of drug delivery.

1.1.3.1 Loading and release of therapeutic molecules

After dissolving the sacrificial templates such as MF particles or erythrocytes, therapeutic molecules can be loaded in to the hollow capsules through pores on the polyelectrolyte multilayers wall by varying the solvent polarity [70], salt concentration or pH [37] of the medium. Subsequently the pores are closed by reversing the conditions of the medium. If porous templates are applied, such as $CaCO_3$ [95] or SiO_2 [27] microparticles, macromolecules (e.g. proteins) can be easily entrapped in the porous structure. The latter has the advantage of keeping the integrity of polyelectrolyte multilayers wall while protecting many therapeutic macromolecules like peptides and proteins.

Permeability is one of the key properties of the LbL polyelectrolyte wall, which can be tailored by varying pH/ionic strength of the medium, the film coating thickness and wall material composition [16]. Previous studies confirmed the controlled release of encapsulated therapeutic molecules from PEMC, which respond to specific stimuli (such as pH, salt, light, redox-potential, magnetic field etc.) [92].

When the capsules have reached the intended locations, they undergo two distinct ways of release, instantly (burst release) or slowly over an extended period (sustained release). Burst release occurs when the capsules are degraded under external triggering or via intracellular uptake process, e.g., chemotherapy and gene transfection. Sustained release is achieved by either slow diffusion of the therapeutics through and intact but increasingly permeable capsule wall, or gradual release of the therapeutic through a slowly degrading capsule wall when the capsules are remain extracellular and so high doses of therapeutic may be dangerous.

Most of the triggered release of PEMC studied so far has been proved *in vitro*. There are still challenges to apply these PEMC *in vivo*. The pH values (~6.8) in extracellular matrix of tumours and intracellular vesicles are only slightly lower than that of serum (i.e. 7.4). Release of drugs from the PEMC should occur from only subtle physicochemical changes in the human body. The same challenge remains when designing PEMC sensitive to physiologically relevant changes salt concentration, glucose concentration and redox potential [92].

1.1.3.2 Cytotoxicity of PEMC

It is important to understand the *in vitro* and *in vivo* interactions of PEMC with cells to evaluate their potential as drug delivery carriers. Biocompatibility and toxicity of PEMC is the basic concern of such evaluation. Toxicity of capsules has been shown to be dependent on capsule concentrations and the materials for LbL fabricating the capsules. No acute toxicity was observed at moderate capsule concentrations.

Several research groups have reported their results of cell-viability assays such as the MTT test. At moderate capsule concentrations, no acute toxicity was observed for capsules coated with dextran sulfate and poly-L-arginine [99, 100], as well as capsules coated with PSS/PAH [101]. At elevated capsule concentrations, the metabolism of the cells was hampered due to the sedimentation of the capsules on top of the cells and their viability was affected [99] [101].

The positive polyelectrolyte outer layer could disturb cell membranes and cause cytotoxicity. An outermost polyanionic layer appeared to further decrease the toxicity

(cationic PEMCs exhibit a pronounced tendency to adhere to the cellular surface) [102, 103]. Obviously, cytotoxicity could be induced if toxic materials were embedded in polyelectrolyte multilayer walls for functionality. For example, nanoparticles incorporation to capsules has been investigated to increase the capsules mechanical strength of LbL films [101]. Toxic ions released from the nanoparticles can diffuse into the medium and cause the increased cytotoxicity.

1.1.3.3 Uptake of PEMC by cells and tissues

Extracellular material is uptaken inside a cell by membrane invagination and internalization, termed endocytosis [104]. Cellular uptake of PEMC in different cells and tissues have been studied and reviewed [17, 18, 51], which will be introduced in details below.

Complete destruction and intracellular degradation was demonstrated by De Geest et al. by using degradable polycations such as poly-L-arginine and the hydrolysis-prone charge-shifting poly (HPMA-DMAE). Incubation of VERO-1 cells with these PEMCs resulted in internalization and gradual disintegration of the capsules over a period of 60 h, after which no intact capsules could be observed [97]. Composite capsules equipped with virus envelopes on their surface have been fabricated by Fischlechner et al to facilitate cell-membrane passage. The key function of the virus surface is the binding to a host cell surface, induction of endocytosis, and subsequent fusion with the late endosome membrane. In their experiment, LbL capsules coated by lipid-enveloped rubella virus were taken up by endocytosis into Vero cells [105].

Macrophages and dendritic cells can easily phagocytose particles in the range of 0.1–10 μm [99]. Further research was done by using PEMC as delivery carriers to macrophages, e.g. U937 macrophage-like cells [106]. It is shown that activated macrophages are able to gradually degrade layer components of PEMC in phagolysosomes, facilitating the time-controlled release of active agents into immunoreactive cells [106]. It has demonstrated the feasibility of encapsulation of several scavengers or of inhibitor molecules with PEMC to increase the concentration of potential anti-inflammatory cytokines, and eventually terminate the chronic inflammations. The immune response of PEMC *in vivo* was studied by investigating tissue reaction following subcutaneous injection of microcapsules in mice [99]. The system of PEMC was $CaCO_3$ coated with dextran sulphate and poly-L-arginine. A moderate immune reaction was observed, with an acute phase characterized by recruitment of polymorphonuclear cells and a more chronic phase in which microspheres are phagocytosed by macrophages and the injection site is surrounded by fibroblasts.

The adhesion and internalization of capsules in breast cancer cells have been investigated *in vitro* by Sukhorukov et al [107]. In their experiment, the capsules labeled with quantum dots (QDs) were utilized as fluorescent markers to monitor the adhesion and interaction pathway of capsules to cells. Studies on in vitro cancer cell lines by De Geest et al. and Kreft et al. indicated that PEMCs end up in intracellular acidic vesicles, which corresponds to an endo/lysosomal environment with the pH value 5.2 [18]. The results from Ai et al. [108] confirmed that LbL capsules were mostly internalized into the cytoplasm of MCF-7 cells, but not into the cell nuclei.

Apoptosis of hepatoma carcinoma cells have been studied *in vivo* and *in vitro* using doxorubicin (DOX) encapsulated PEMC [109].

Biotechnological drug molecules, such as proteins and nucleic acids, or cancer therapeutics often have a specific target tissue [18]. Nonspecific uptake of the therapeutic molecules might be hazardous to healthy cells or cause undesired death of the healthy cells, for example, chemotherapeutics for cancer. With functional capsules, direction and control of the uptake of drugs by pathological cells is possible. The first method is called receptor mediated uptake. There are receptors present at high density on the pathological cells from the diseased tissue [104]. Some peptides (e.g., RGD [110]), proteins (e.g., antibodies, transferrins [111]), co-polymers (styrene-maleic acid providing targeting to solid tumors [112]), or a large variety of oligosaccharides [113] are known ligands to promote receptor mediated cellular adhesion and endocytosis. The modification of PEMC with these ligands would increase the affinity of capsules to the surface of cells and to achieve a higher number of uptaken capsules with encapsulated therapeutic molecules. Recent research confirmed the feasibility of functionalizing PEMCs with antibodies and their targeting to colorectal cancer cells [114, 115].

Another method of controlling the targeting of capsules is to load the polymer capsules with magnetic nanoparticles, which can be directed by magnetic fields to pathogenic parts of a tissue, such as tumors. Zebli et al. incorporated magnetic nanoparticles on to the multilayer shells of capsules and observed increased uptake of capsules by breast cancer cells in the magnetic field [116]. Site-specific release has been achieved by other magnetic-responsive delivery systems. Doxorubicin loaded

magnetoliposomes have been targeted into tumours by a static magnetic field [7]. Consequently, massive release of the doxorubicin was achieved upon application of an oscillating magnetic field. Alginate spheres containing insulin and ferrite microparticles exhibited a 50-fold increase in insulin release in the presence of an oscillating magnetic field [117]. However, so far no successful results have been reported regarding magnetically induced drug loading and release from polyelectrolyte capsules [92].

The third method lies in shielding the capsules from unwanted uptake while also enhancing their uptake by the target cells. Unspecific and undesirable phagocytosis should be avoided for prolonged circulation times and the targeted delivery of PEMCs. It would be beneficial to minimize the adsorption of proteins onto the capsule surface, since opsonic proteins rapidly adsorb onto the particle surface, thereby causing particle clearance by phagocytic cells [118]. Recent progress has been made in controlling the cell internalization and thus the *in vivo* lifetimes of PEMC via functionalizing them with lipids and poly (ethylene glycol) (PEG) [94, 99, 108, 119]. Bio-functionalisation of PEMC will be discussed in greater depth in the following section **1.2.3**. The immobilization of functional materials onto the PEM is a highly potential way to combine all three methods of targeting and produce novel modified PEMC. By combining two or three of the above-mentioned methods of targeting in one carrier system, improved protection of normal tissue can be an achievable task.

1.2 Bio-functionalisation of PEMC for targeted drug delivery

1.2.1 Antibodies incorporation on PEMC

1.2.1.1 Surface immobilization for antibody immobilization

Protein adsorption on surfaces of synthetic materials is an area of great interest in tissue engineering substrates, biosensing surfaces, and drug delivery vehicles [120]. In the field of targeted drug delivery, it is necessary to develop drug or drug carriers, which limit the distribution of toxic drugs to only pathological cells. By modifying the drug and drug carriers with certain ligands (e.g. antibodies), it would enable them to be recognized by the receptors on pathological cells.

There are many immobilization methods for maintaining antibody's activity and optimizing its accessibility/orientation on the surface. An overview of the advantages and disadvantages of various immobilization strategies is presented in **Table 1.1**[121]. Each of the categories is discussed in greater detail in the following sections.

Table 1.1 Advantages and disadvantages of different immobilization strategies[121]

Method	Advantages	Disadvantages
Adsorption	Simple, inexpensive Good for single-use application	Relatively unstable proteins denature on hydrophobic surfaces Adsorption is highly pH, temperature, solvent, surface and bio-molecule dependent – may need extensive optimization

Method	Advantages	Disadvantages
Entrapment: In polymer gel	Simple universal approach for macromolecules	
	High loading of protein can be trapped Prolonged protein activity	Protein denaturation during gel preparation
Covalent coupling	Stable coupling	Complexity and cost of derivatisation steps
	Intimate contact with transducer Low diffusion barrier – rapid response	Limited sites for attachment leads to shorter lifetime
Use of 'capture system'	Generic surfaces where specificity can be switched Many options for regeneration Opportunities for antibody orientation	Expensive and complex multi-step derivatisation procedures Multi-layer structure may reduce signal Non-specific binding to components of capture system

Adsorption to the hydrophobic surface

Proteins adsorb strongly to hydrophobic surfaces, e.g. plastic surface or carbon electrodes, due to hydrophobic, ionic and Van der Waals interactions. Physical adsorption is a simple method to immobilize proteins, which has often been used in immunological techniques such as enzyme linked immunosorbent assay (ELISA). For

many types of hydrophobic surfaces, e.g. polystyrene in ELISA, non-specific binding (NSB) often leads to high background signals. The most favorable type of surface to prevent NSB and denaturation seems to be one most closely mimicking an aqueous solution, i.e. a flexible uncharged environment rich in hydroxyl groups. These do not ionize under any physiological conditions and are also highly hydrated, thus minimizing the possibility of hydrophobic effects. In much antibody-based assay techniques, such surfaces are usually post-treated with a protein solution such as albumin to block any remaining adsorption sites. The blocking procedure reduces background signals in subsequent assay steps.

Entrapment methods

Enzymes and antibodies can be physically entrapped within the volume of a polymer hydrogel, such as agarose. Different types of polymer come in many molecular weights and degrees of hydrolysis. Some can be dissolved in boiling water and become insoluble in cool water. Proteins can be mixed with the polymer solutions and deposited on surfaces by printing, droplet deposition, etc. The film is then dried, entrapping the enzyme. When subsequently rehydrated, the film swells rapidly and the protein becomes active, but cannot diffuse out of the polymer. If required, a large amount of proteins can be included in the volume of hydrogel. The approach is limited to certain type of transducers requiring a large amount of proteins or even cells. And it would be not appropriate for systems only requiring 2D surface modification.

The hydrogel can also be made by free-radical polymerization of monomers and cross-linkers in the presence of the protein. The proteins can be covalently linked to the growing polymer chains. This would help to prevent leaching of the protein out of the

entrapped hydrogel. Some protein activity is usually lost during the polymerization procedure but the remaining activity is often stable in the gel.

Covalent coupling chemistry

In covalent coupling procedures, the surface is first activated with functional groups and followed by immobilization of the soluble protein. If an antibody is used, the linkages will be made to surface amine groups. The surface functional groups include carboxylic acids, thiol, hydroxyl groups, etc. Vast immunoassay literature provides many insights into each categories of reaction. Briefly, covalent coupling provides stable and intimated contact of protein to the surface. However, the complexity and cost of multiple derivatisation steps limit the popularity of these methods.

Protein can be covalently immobilized to reduce or eliminate the non-specific binding [122-124]. Usually surface modification is necessary to generate functional groups, e.g. –COOH, -NH2, -SH [125]. Cross linkers such as dextran [126] or PVA [122] have served as chemical linker between surfaces and proteins. However, an efficient bio-interface not only needs a high loading of antibody but also requires retaining the antibody affinity to its antigen. Protein immobilized by covalent binding often suffers from unfavorable orientations, structural changes, or steric hindrance after immobilization [127, 128].

Avidin/streptavidin capture system

Another approach, biotin-avidin-biotin linking, has been applied to reduce the denaturation of bound proteins caused by coupling them directly using chemical covalent binding. Biotin is a natural vitamin with small size (244 Da). It has been

conjugated to a variety of ligands including carbohydrates, peptides, proteins, antibodies, or DNA/RNA without significantly altering their structure or biological function [129]. These biotin conjugates bind to avidin with high affinity and produce binding sites for subsequently biotin conjugates. Thus they have been used for various fields such as bioanalytical assay [129], artificial cell membrane [130], drug delivery system [8], transplantation [131].

The use of the interaction between biotin and avidin/streptavidin is widespread in assay and labeling methodology. The extremely high affinity of avidin/biotin interaction is essentially non-reversible under normal assay conditions. More interesting is the ability of avidin to form two-dimensional crystalline arrays on suitable surfaces. Avidin is protein with 'block-shaped' structure with four binding sites [132]. The binding sites are distributed with two on each of the near-parallel faces of the molecule. If an appropriated surface is prepared with immobilized biotin molecules, avidin can bind to this surface to form a tightly-anchored array, with a high site density for biotin binding. This should be an ideal surface for capture of biotinylated antibodies, using mild conditions that cause little denaturation. This will lead to capture of biotinylated antibodies in a more controlled orientation.

Avidin, Streptavidin, and NeutrAvidin are three common proteins showing strong non-covalent binding interactions with biotin. Avidin demonstrates the highest bonding strength with a dissociation constant of $K_D=10^{-15}$ M. However, Avidin also shows non-specific binding due to its carbohydrate content and a basic isoelectric point (pI≈10) [133]. Streptavidin has a slightly lower biotin binding strength with a dissociation constant of $K_D=10^{-13}$ M and a mildly acidic pI of ~5. NeutrAvidin is a deglycosylated

Avidin exhibiting a more neutral pI of 6.3. Therefore, NeutrAvidin demonstrates much less nonspecific binding compared to Avidin but still has the same binding affinity to biotin as Avidin [129]. As a result, NeutrAvidin was chosen as the most popular protein for binding biotin in recent applications [129, 132, 134].

1.2.1.2 Antibodies incorporation on PEMC

The incorporation of biomolecules on PEM has experienced an explosion of growth in both application and theoretical advances [20, 46, 135]. This area has progressed to include biosensing surfaces, drug delivery vehicles, tissue engineering substrates [136], and fundamental biomimetic studies [47]. The incorporation of antibodies into PEMC shells has been used to develop strategies that allow specific targeting of these carriers to enhance receptor mediated cellular internalization and thereby the accumulation of the encapsulated agent in the targeted tissue.

Monoclonal immunoglobulin G (IgG) antibodies were coupled via electrostatic interaction to the surface of MF core–PSS–PAH shell particles coated with the phospholipid DLPE. These particles were demonstrated to be covered homogeneously with a FITC-labeled secondary antibody (rabbit anti-mouse IgG) [137]. Further investigation was performed by functionalizing the capsules' surfaces with a humanized A33 monoclonal antibody [114]. Human A33 antigen is expressed by 95% of all human colorectal tumor cells. The modified PEMC were readily recognized and internalized by colorectal cells expressing the A33 antigen, while colorectal tumor cells that do not express the A33 antigen fail to take up the particles.

The physical adsorption relies on electrostatic interaction of charged protein in buffer and oppositely charged surface. Besides electrostatic interaction, hydrophobic attraction also plays important role in the protein-surface interaction [138]. Physically adsorbing proteins to PEM provide a way to incorporate proteins in non-denaturing conditions. Study indicates that antibodies incorporated in a polyelectrolyte multilayer retain their reactivity with respect to their antigens [46]. Being amphiphilic molecules, proteins bear patches of positively and negatively charged zones. When proteins start to adsorb on PEM, there is a combination of simultaneously acting forces, including hydrophobic and electrostatic interactions or entrapment in the porous structure.

It is possible to adjust the porosity of the PEM film by changing pH and ionic strength, and thus tune its surface property, loading capacity, and antigen binding activity [35]. In these porous PEM structure, the embedded proteins can preserve not only their native like secondary structures but their enzymatic activities as well [139]. PEM provides semiwet environment which keep protein probes in an active form and thereby prevent protein unfolding. This application has been extended to protein microarray substrate fabrication to increase the microarray intensity [140]. This remarkable property has the potential to construct multilayers incorporating specific ligands that keep the biological activity and promote the adhesion of specific cells.

1.2.1.3 Methods for measuring protein binding interaction

Binding affinities / avidities of antibody-antigen interaction

One topic of studying protein immobilization on surfaces is to know their binding ability to the proteins (e.g. antibodies) and the stability of the complex (e.g. antibodies

bound to particle surfaces). This binding strength is based on a large number of noncovalent interactions including hydrogen bonds, ionic bonds, hydrophobic interactions, and van der Waals interactions. Affinity is a quantitative measure of the binding strength between the receptor–ligand (i.e., single antibody-antigen or multiple ligands in the case of avidin-biotin interaction) [141]. The true strength of the receptor-ligand interaction is complicated within biological systems, which cannot be reflected by the affinity at one site. An example is the reaction of an antibody with antigenic determinants on a virus or bacterial cell. Complex antigens are present on cells with repeating antigenic determinants providing multiple binding sites for the antibody. Typically, the presence of these multiple binding sites can have a cooperative effect on the binding of the antibody to the cell. The strength of such complex receptor-ligand interactions is referred to as avidity of the interaction [141].

Affinity represents the balance between association and dissociation of the overall interaction. Assuming the reaction is monovalent binding, the interaction of the receptor-ligand complex can be described by the equation [141, 142]:

$$R + L \Leftrightarrow RL \tag{1.1}$$

At equilibrium, the equation can be written as:

$$k_a[R][L] = k_d[RL] \tag{1.2}$$

where [R], [L], and [RL] are the molar concentrations of unbound receptors, free ligands and bound receptor-ligand complexes respectively. k_a is the forward (association) rate constant and k_d is the reverse (dissociation) rate constant. From this equation, equilibrium constant can be calculated as:

$$K_d = \frac{k_d}{k_a} = \frac{[R][L]}{[RL]} = \frac{1}{K_a} \quad 1.3$$

The equilibrium constant for that reaction K_d, the reciprocal of K_a, is a quantitative indicator of the stability of an R-L complex [141]. Low values of K_d indicate very stable complexes and higher values weak interaction. For example, strong Avidin-Biotin binding has low K_d of 10^{-15}, while antibody-antigen binding can range from 10^{-7} to 10^{-11} [143].

The mass balance of receptor-ligand interaction can be written as:

$$[R]_{Total} = [R] + [RL] \quad 1.4$$

Substitute Equation 1.3 to 1.4, one would obtain single-site Langmuir isotherm equation:

$$[RL] = \frac{[R]_{Total}[L]}{K_d + [L]} \quad 1.5$$

When the receptor or the ligand is bound to a solid surface or support (such as cells or ELISA plate), the assumption of above mentioned freely suspended antibodies, ligands, and antibody–ligand conjugates is not valid. Given the added complexity of such heterogeneous phase systems, a typical approach is to use the term “apparent binding constants”, which may have different values compared to the true binding constants obtained in suspension. This apparent binding constant takes into consideration the potential of antibody valence, steric hindrance, or other non-ideal effects [144].

Methods for measuring antibody-antigen interaction

Methods for measuring rate constants and affinities of interaction can be grouped according to interaction phase. In homogeneous phase, the measurements are performed in a protein solution. While in heterogeneous phase, the measurements are monitored through binding to a surface-immobilized protein. Probing the interaction homogeneous phase involves techniques such as optical spectroscopy, activity (or inhibition) measurement. Heterogeneous phase measurements include heterogeneous immunoassays or biosensors based techniques [145]. In this section, heterogeneous immunoassays measurements will be the focus.

Immunoassay (IA) is widely used in selective and sensitive measurement of biomolecule analytes through specific binding abilities of antibodies and antigens. In heterogeneous phase measurements, molecules from solutions are immobilized onto a surface before recognizing specific targeted antigens. With the development of detection technology and surface conjugated chemistry, different types of immunoassays have emerged over the past few decades, e.g. biosensors on 2D planar surfaces or beads assay on 3D surfaces. They are widely used for clinical disease diagnoses, environment monitoring. For example, proteins and peptides [146] have been immobilized on microspheres for the detection and quantification of the antibodies, using standard flow cytometric microsphere based assay.

In this project, microsphere immunoassay will be applied for studying the affinity between the antibodies immobilized drug carrier and the targeted molecules. The theory behind is no different with that of 2-D protein-protein affinity measurement. The detection technique used to measure antibody-antigen interactions is flow cytometry.

Briefly, antibodies are immobilized on the microsphere and bound with fluorescently labeled antigens from samples. The complex of fluorescent microsphere will then be counted by flow cytometry and the fluorescence intensity will be recorded and analyzed.

One of the applications of flow cytometry (FCM) is to determine the binding affinity between cellular receptors and fluorescently labeled ligands. The fluorescence of the ligand bound to the cell surface can be quantified using FCM and the Mean Fluorescence Intensity (MFI) of the cells can be analyzed from FCM software. The relationship of MFI and the ligand-receptor concentration has been described in the following equation [142, 147]:

$$MFI = \varepsilon \log_{10}[RL] + MFI_{bg} \quad 1.6$$

$$MFI = \varepsilon[RL] + MFI_{bg} \quad 1.7$$

Equation 1.6 and 1.7 describe the relationship using logarithmic amplification and linear amplification respectively, depending on the FCM equipment type. ε is the conversion factor between MFI and the amount of receptor-ligand complexes formed per cell. The value of ε depends on the FCM instrument settings (e.g. the laser intensity and the photomultiplier voltage), as well as intrinsic characteristics of the fluorescent dyes. MFI_{bg} is the background MFI of unlabeled cells, which is often referred to as cellular autofluorescence [142]. In this work, the MFI_{bg} was set close to zero by decreasing the laser intensity of the flow cytometer. Thus, Equation 1.7

becomes $MFI = \varepsilon[RL]$. Combine Equation 1.7 and 1.5, the single-site Langmuir isotherm equation can be written as:

$$MFI = \frac{MFI_{\max}[L]}{K_{app} + [L]}$$

MFI_{max} is the maximum MFI of the saturated binding with labeled ligand to the receptor. K_{app} is the apparent molar dissociation constant for ligand binding on the cell or microspheres. The concentration of ligands ([L]) should be always in excess to make sure the reaction is in equilibrium status. The fitting of Langmuir curve using MFI v.s. ligand concentration gives the estimation of MFI_{max} and K_{app}.

1.2.2 Lipid adsorption on PEMC

Liposome is one type of drug delivery system which has long been used in pharmaceutical industry and remains popular with gene delivery and cancer therapy. One shortcoming of liposomes is that they have a rather low stability and exhibit structural fluctuations. In nature, biomembranes are supported by a polymer network, the cell cytoskeleton. Thus combination of lipids and synthetic materials has been applied to fabricate biomimetic membranes. Liposomes are rather unstable and undergo fusion when coming in contact with solid surfaces [148]. This leads to spreading of vesicles on solid support and formation of so-called supported lipid bilayers (SLBs) [14, 149]. Liposome adsorption is mainly driven by electrostatic forces. Within 5 minutes of the addition of the solution to a substrate, a uniform lipid bilayer forms very quickly and covers more than 95% of the surface [32, 150].

SLB membrane retains natural fluidity and biological functionality and can be implanted with membrane proteins for functional studies [151]. The amphiphilic character of lipids facilitates, on one hand, the adsorption of hydrophilic compounds on bilayer surface via hydrophilic interactions, and on the other hand, the insertion of hydrophobic molecules in the bilayer hydrocarbon chain region via hydrophobic effects [152]. These features have attracted interest for using SLB as models of cell membranes for research as well as for their potential biotechnological applications [153-155], e.g., fabrication of these interfaces reconstitutes of a membrane environment for enzymes or cell receptors [156].

Lipid bilayer formed on LbL surfaces has been used for combining advantages of LbL assembly and liposome technology (*Figure 1.3*). Lipid bilayer coated on LbL surfaces formed complexation between the lipid and polyelectrolyte multilayers, attributing the high morphological stability of such coatings. A lot of studies of the composite lipid-layer–polyelectrolyte shell have been done for biomimetic research, e.g. artificial cell membranes [15, 16, 28, 32, 157-159].

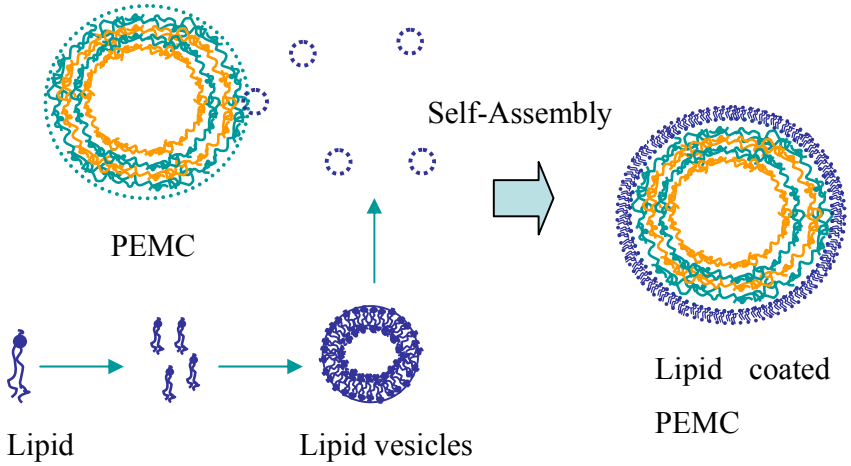

Figure 1.3 Scheme of lipid layer formation onto polyelectrolyte capsules via adsorption and spreading of self assembled lipid vesicles

Lipid coated PEMC offers the possibility to control vesicle size, monodispersity and lipid-layer number, compared to the conventional liposome preparation methods (sonication, rapid injection, swelling, reverse evaporation, inverted emulsion and electroformation) [157]. Fusion of viral nanoparticles has been investigated on LbL SLBs on colloidal particles to form membranes to facilitate the cell membrane passage [105]. By adsorption of lipid layers on polyelectrolyte multilayer coated colloidal surfaces, the modified capsules resembled endogenous carrier systems (e.g. lipoproteins) with significantly prolonged life times [160]. Furthermore, the lipid layers allow control of the permeability of PEMC [150, 157, 161, 162]. Lipid/protein [161] and lipid/polyelectrolyte [150] have been used to fabricate microcapsules with controlled permeation features. These features have been intensively applied to develop capsules as potential drug carrier to retard diffusion of drug from the core.

1.2.3 PEG modified PEMC

1.2.3.1 PEG as protein-resistant material for long circulating delivery system

Protein-resistant surfaces are desirable for many biomedical applications, such as reduced adsorption of proteins as well as the bacterial colonization of implanted materials [163-165]. Particularly in the drug delivery field, protein-resistant drug carriers are desirable to achieve long circulation times in blood. Protein-resistant surfaces reduce the adsorption of certain plasma proteins (opsonins) on to the carriers and thus help them escaping from rapid phagocytosis.

Polymers have been extensively used to modify surfaces against protein adsorption and internalization by phagocytic cells [166-169], which is to impact Stealth function [119] in drug delivery systems. These polymers share common properties such as hydrophilicity, neutrality and hydrogen bond acceptor character [170]. Poly (ethylene glycol) (PEG) is by far the preferred strategy for imparting protein adsorption to surfaces [163, 171, 172], due to its low toxicity and low immunogenicity. It has been widely applied to reduce bacterial adhesion [173, 174] and control cell patterning [175-177]. It has been approved by the Food and Drug Administration for in-vivo use in humans as coatings for long circulating usage.

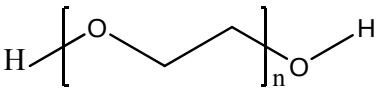

Figure 1.4 Molecular structure of poly (ethylene glycol)

The mechanism underlying the protein resistance of PEGylated, brush-type surfaces is frequently attributed to this "exclusion effect" or "steric stabilization effect" as well as to osmotic repulsion [163, 178]. PEG (Figure 1.4) constructs higher-order intrachain structure in water when the EG monomer units form hydrogen bond with water molecules [179]. Extensive hydration, good conformational flexibility and high chain mobility contribute to the steric effect when PEG chains are densely packed on a surface. Theoretically, the nominal size of PEG was given by Flory radius [180], e.g. PEG[2000] ($R_{PEG} \approx 3.4$ nm, $R_{PEG} = aN^{3/5}$; N = 45 and a = 0.35 nm for –CH2CH2O-). By experiments, it has been confirmed that the thickness of 2000 kD PEG is to be on the order of about 5 nm (almost 4 nm by zeta potential measurement and 6 nm by steric pressure measurement) [6].

Experimental studies related to PEG surface coverage indicate that both grafting density and chain length affect the protein-resistant property of PEG based coatings. The concentration of protein adsorbed on the surface decreased as the surface density of the grafted PEO increased, but surface protein concentration never reached zero [181]. A sufficiently high surface density of EG monomer units is required to achieve protein resistance of PEGylated surfaces for both long PEG chains (e.g., MW 5000) and shorter chains (e.g., MW 2000) [182]. As the length of the PEG chains increases from 10 to 120 EG units, protein resistance increases with larger excluded volumes, higher conformational entropy and more pronounced steric repulsion[183]. If the initial grafting density is too low, the use of longer PEG chains can lead to protein resistance; however with longer chains the use of a high density surface is not required [169].

The PEG chains would form a layer of “mushroom” or “brush” on the grafted surface to prevent the adsorption of serum proteins. The conformation of the grafted PEG chain and the thickness of the layer depend on the grafting density or distance between the chains (D) and on the length of the chain, which is related to the radius of gyration in solution (R_G) (Figure 1.5). At very low surface coverage ($D >> R_G$), the polymer molecules form a "pancake" or "mushroom" structure, depending whether the interaction between the polymer segments and the surface is attractive or repulsive, respectively [184]. At $D \sim 2\ R_G$, the mushrooms start to encounter their neighbors. When the grafted PEG reaches a high surface density ($D < R_G$), the polymer chains forms a spiky surface resembling the brush structure forced by extension of PEG chains. The brush thickness is determined by the balance between the excluded volume within the PEGs, which tends to stretch the chains out, and the chain elasticity, which opposes the stretching [184].

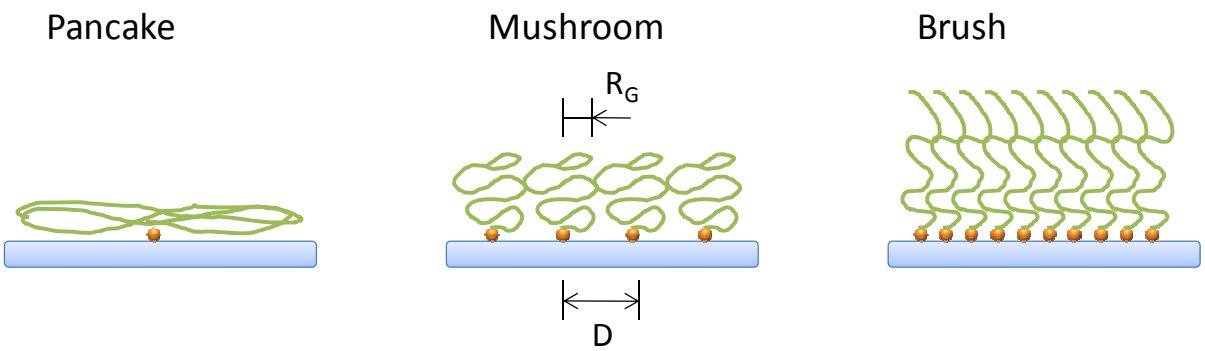

Figure 1.5 Schematic representation of the conformation of end-grafted PEG chains at the interface. D represents the distance between the PEG chains. R_G represents the radius of PEG gyration in solution. There are three conformation structures: pancake ($D >> R_G$), mushroom ($D \sim 2\ R_G$) and brush ($D < R_G$).

1.2.3.2 Adsorption of PEG conjugated copolymers on PEM

To produce surfaces with dense arrays of PEG brushes, it is popular to apply PEG-grafted conjugates by spontaneous assembly on surfaces. Polymers, proteins and lipids have been immobilized with PEG by covalent coupling to the end functionalized PEG [9, 163, 168, 185]. Functional PEG can be coated on solid surfaces [186] or soft cushion surfaces (e.g. PEM). Recent research has attracted a lot of interests in coating PEG or PEG-grafted copolymers on PEM to create novel functional and tunable surfaces [49, 172]. For example, cationic polyelectrolytes, such as poly (ethylene imine) or poly (L-lysine) has been grafted with PEG side chains, offering densely packed PEG brushes when immobilized on negatively charged PEM surfaces [132, 171, 187]. In the field of drug delivery, this poly (L-lysine) grafted PEG has been adsorbed on polyelectrolyte microparticles/capsules to reduce unspecific uptake by MPS, prolonging the life time in the circulation [118, 188].

PEG conjugates have a strong impact in the development of multifunctional polyelectrolyte microcapsules as potential drug carrier systems. Poly-(ethylene glycol) (PEG) phospholipid derivatives, e.g. PEG2000-DSPE (distearylphosphatidylethanolamine), have been coated on LbL colloids. By adsorption of this PEG2000-DSPE onto PEMC, capsules can be fabricated that more closely resemble the endogenous carrier system thereby resulting in significantly prolonged life times [160]. Biotinylated PLL-g-PEG adsorbed to the outlayer of PEMC has been studied as functional PEMC [118], which has demonstrated capable of recognizing and binding to streptavidin. Stable and biofunctional capsules that are resistant to protein adsorption and opsonization by macrophages in combination with surface immobilized

specific bioligands are believed to be a promising platform for drug carrier systems [118].

1.3 Scope of the thesis

The main function of targeted drug delivery system is to protect therapeutic molecules and direct ligand-drug conjugate to only the pathological cells and minimize the damage to normal cells. The principle for a PEMC-based system for targeted drug delivery has been successfully demonstrated from previous work. However, enormous hurdles still have to be overcome before applying polymer capsules to clinical practice. The interested area includes the amplified targeting ability, the prevention of capsule aggregation in blood vessels, the control of capsule opsonisation and macrophage scavenging. The immobilization of functional materials onto the PEM is a highly potential way to produce novel modified PEMC to increase the targeting ability of the drug delivery and to reduce the side effects to normal cells. A deeper understanding of the structure-property relationship of LbL multilayer films is required to develop highly sophisticated drug delivery systems.

The overall objective of this project was to develop multifunctional polyelectrolyte microcapsules (PEMC) as potential targeted drug carriers with enhanced targeting property and circulation time. The focus of our methodology was to design a PEMC-antibody (IgG) composite on common PEMC model. Hollow PEMC was fabricated under economical and mild conditions. This work demonstrates for the first time modification of nano-engineered polyelectrolyte films with biotin-PEG-lipid using

electrostatic LbL assembly. Further, Immunoglobulin G (IgG) was chosen as the model ligand to modify the PEMC. The hypothesis and the specific aims will be thoroughly discussed in the following section.

Specific aim I

The first part of this project involves successful fabrication and modification of the PEMC under suitable conditions, e.g. temperature, assembly buffers, and centrifuge speed. Dissolvable templates need to be chosen if hollow PEMC is required for further encapsulation of certain therapeutic molecules. Although biopolymers as PEMC wall materials could offer better biocompatibility, experiments can be started from the synthetic polyelectrolytes to establish the feasibility and concept. As a proof-of-principle, synthetic melamine formaldehyde (MF) particles were coated via the LbL method with PAH and PSS followed by core dissolution.

The modification of PEGylated phospholipids with functional moieties could be another promising direction to functionalize lipid coated PEMC. In this way it will be possible to target PEMC to specific molecules, while still enhancing their *in vivo* lifetime as well as their permeability. One approach for such functionalisation is to utilize the non-covalent specific interaction between biotin and Avidin. In this project, biotin-PEG-lipid was proposed to coat on the PEMC surface as the modification layer.

Biotin-PEG-lipid has three function moieties, one is biotin for catching IgG using biotin-avidin interaction, the other is PEG for reduced protein binding and undesired cellular uptake, the last is the lipid for controlling surface permeability. The hypothesis

is that the above described functions would be retained after biotin-PEG-lipid adsorption on PEMC. PEMC can be modified using LbL assembly techniques under mild conditions. The modified PEMC should demonstrate high affinity to targeted molecules, while remaining low non-specific binding to serum protein. The PEMC shall remain monodispersity by preventing aggregation.

The optimization of biotin-PEG-lipid composition is an essential step for studying corresponding LbL film properties. The optimized PEMC can be effectively used to design and test targeting ability and the non-specific protein binding of such films. The characterization of NeutrAvidin as the outermost layer of PEMC provides possibility for further coating with biotin-antibodies. The characterization of modified LbL PEM on 2D surface is used to understand the structure property of the surface.

Specific aim II

After we prove the specific binding of biotin-PEG-lipid modified PEMC to NeutrAvidin, we should continue with coating the surface with biotin-antibody. NeutrAvidin is a tetrameric protein containing four identical homotetramers with two on opposite sides thereby providing two biotin binding sites on each side. Therefore, NeutrAvidin immobilized on the outmost layer of bio-functional PEMC creates a surface site for subsequent binding of biotinylated antibodies or other bio-molecules. The hypothesis is that the NeutrAvidin ending PEMC will be able to catch biotin-antibodies.

As potential drug carriers for targeted delivery, it is interesting to know their binding ability to the antibodies and the stability of the complex (PEMC/NA/Biotin-Ab). This information can be obtained by quantitative measurement of the interaction between PEMC/NA and Biotin-Ab. Microsphere-based assays using immobilized surface bound interaction partners are routinely used with flow cytometry as a readout platform to detect analytes, such as proteins, nucleic acids, or small molecule entities. In this work, the microsphere-based assay is proposed to measure binding ability and dissociation constants of PEMC with and without biotin-PEG-lipid modification.

Specific aim III

PEMC with specific antibodies can be used for targeting to the corresponding antigen expressing cells. In the final part of this project, the interaction of antibody modified biofunctional PEMC with the cells will be elucidated. Cell lines with and without the antigen expressed will be chosen as the positive and control cell lines respectively. The hypothesis is that antibody modified biofunctional PEMC would be able to specifically bind to antigen presenting cells. A deeper understanding of cell and PEMC interaction is investigated to optimize the interaction conditions.

1.4 Chapters Organization

In summary, this dissertation demonstrates the development of advanced targeted drug delivery system with emphasis on layer-by-layer (LbL) electrostatic assembly

technique. Successful fabrication and investigation of this PEMC could elucidate whether it would be potential targeted drug delivery systems with enhanced efficacy in the circulation. The dissertation has been organized in five chapters.

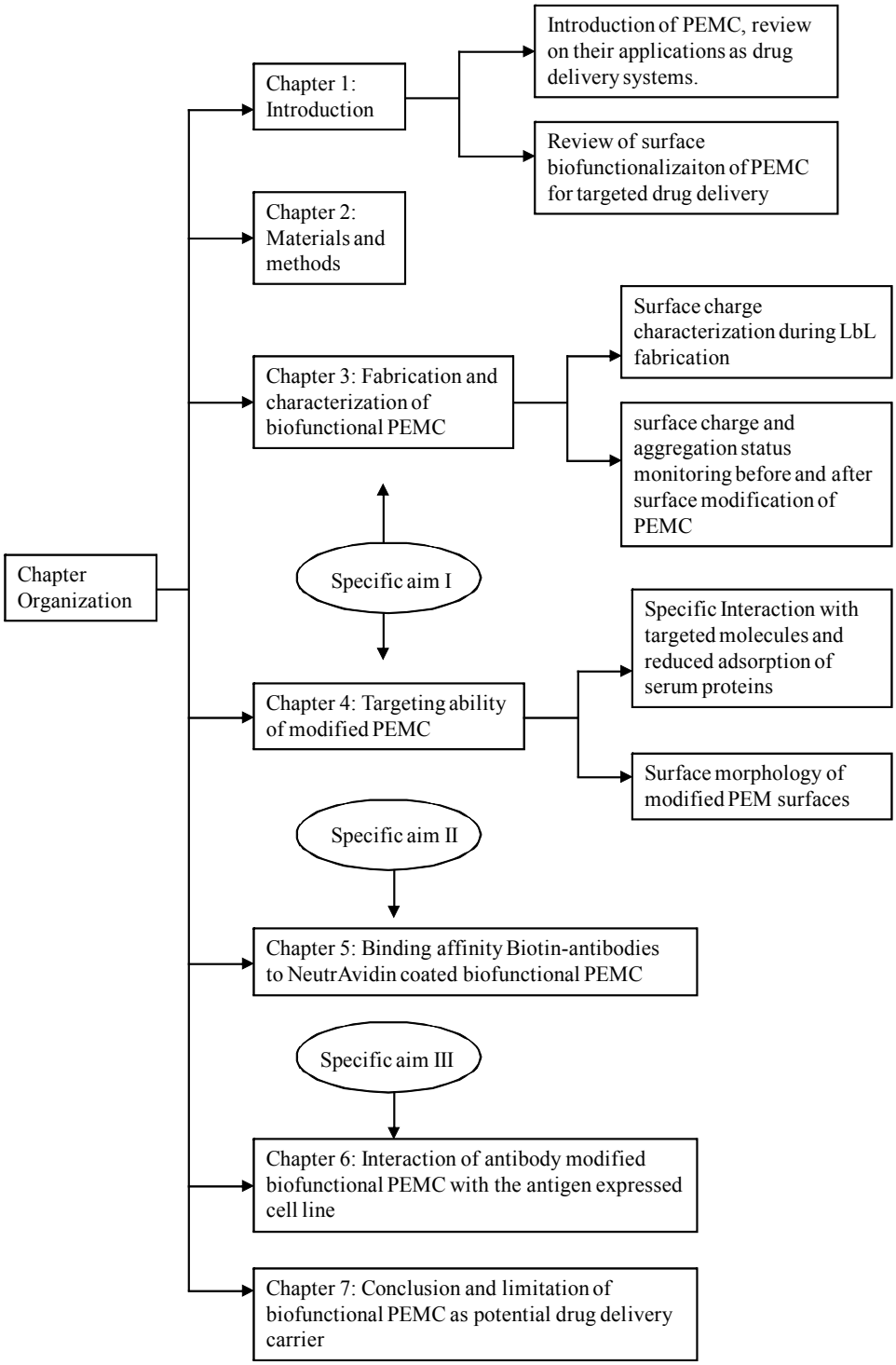
Chapter Organization
Chapter 1: Introduction
Introduction of PEMC, review on their applications as drug delivery systems.
Review of surface biofunctionalizaiton of PEMC for targeted drug delivery
Chapter 2: Materials and methods
Chapter 3: Fabrication and characterization of biofunctional PEMC
Surface charge characterization during LbL fabrication
surface charge and aggregation status monitoring before and after surface modification of PEMC
Specific aim I
Chapter 4: Targeting ability of modified PEMC
Specific Interaction with targeted molecules and reduced adsorption of serum proteins
Surface morphology of modified PEM surfaces
Specific aim II
Chapter 5: Binding affinity Biotin-antibodies to NeutrAvidin coated biofunctional PEMC
Specific aim III
Chapter 6: Interaction of antibody modified biofunctional PEMC with the antigen expressed cell line
Chapter 7: Conclusion and limitation of biofunctional PEMC as potential drug delivery carrier

Chapter 2 Materials and methods

2.1 Chemical products

2.1.1 Solutions

Double distilled water (Milli-Q, Millipore, USA, (MP)) was used for the preparation of all aqueous buffers. 0.5 M and 0.01 M sodium chloride (NaCl) solutions were obtained from diluting 5 M NaCl solution (Sigma-Aldrich, USA) in MP water. Phosphate buffered saline (PBS, dry powder, Sigma-Aldrich, USA) with a pH of 7.4 at 25°C was used. 0.1 M hydrochloric acid (HCl) was obtained by diluting 37% HCl (Sigma-Aldrich, USA). All solutions described above were sterilized via filtration with 0.2 μm filters (TPP, Switzerland). NeutrAvidin (molecular weight [MW] = 60 kDa, Pierce, USA) was labeled with FluoroLink™-Ab carbocyanine (Cy3) labeling kit (GE healthcare, USA). Bovine serum albumin (BSA, 66 kDa) and fluorescein isothiocyanate- (FITC-) BSA were purchased from Sigma-Aldrich. 1% BSA blocking buffer was prepared in PBS and stored at -20°C in 0.5 ml aliquots. All NeutrAvidin solutions (250 μg/ml NeutrAvidin and Cy3-NeutrAvidin) were prepared in 1% BSA.

2.1.2 Polyelectrolytes and template

Negatively charged poly(styrene sulphonate) sodium salt (PSS, MW=70 kDa) and positively-charged poly (allylamine) hydrochloride (PAH, MW= 70 kDa) were

purchased from Sigma-Aldrich (*Figure 2.1*). Melamine formaldehyde particles (MF particles 10%w/v, d = 7.2 ± 0.09 μm) were purchased from microParticles GmbH, Germany.

PAH was labeled with FITC as described elsewhere [106]. In brief, FITC (dissolved in dimethyl sulfoxide, DMSO) was added to PAH in 0.1 M sodium hydrogen carbonate buffer (pH 8.5) and incubated for 2 days. FITC-PAH solution was dialyzed against double distilled water. Free FITC molecules were removed by gel chromatography. The labeled polyelectrolytes were aliquoted, lyophilized, and stored at 4°C.

Figure 2.1 Molecular structure of polyelectrolytes: left, PSS; right, PAH.

2.1.3 Lipids

All phospholipids stored in chloroform were purchased from Avanti Polar Lipids, USA. The details of lipids are listed in *Table 2.1*. The molecular structures of the lipids are shown in Figure 2.2.

Table 2.1 Lipids used in surface modification of PEMC

Product Name	Abbreviation
1-Palmitoyl-2-Oleoyl-sn-Glycero-3-[Phospho-L-Serine] (Sodium Salt)	POPS
1-Palmitoyl-2-Oleoyl-sn-Glycero-3-Phosphocholine	POPC
Egg Lissamine Rhodamine Phosphatidylethanolamine	Rhod-PE
1,2-Distearoyl-sn-Glycero-3-Phosphoethanolamine-N-[Biotinyl(Polyethyleneglycol) 2000] (Ammonium Sallt)	DSPE-PEG[2000]Biotin

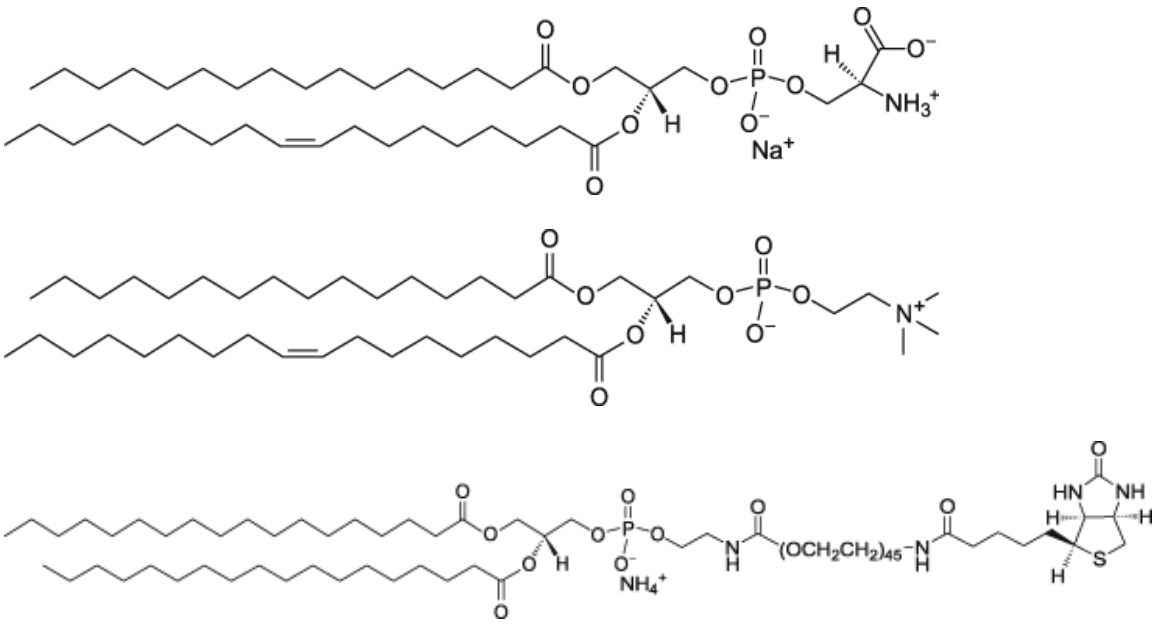

Figure 2.2 Molecular structure of lipids: top, POPS; middle, POPC; bottom, DSPE-PEG [2000] Biotin

2.1.4 Antibodies

The details of antibodies, including product name and supplier, were listed as follows (Table 2.2). These antibodies were received in the form of freeze-dried powder and stored according to product instructions.

Table 2.2 Antibodies used to study protein binding on modified PEMC

Product Name	Supplier
Cy3 AffiniPure Goat Anti-Rabbit IgG	Jackson ImmunoResearch Laboratories, USA
Biotin-SP-AffiniPure Rabbit Anti-Goat IgG	
Biotin Rat Anti-Human CCR5 IgG	Abcam, USA
FITC Goat Anti-Rat IgG	Sigma-Aldrich, USA
FITC anti-cytokeratin	Sigma-Aldrich, USA

2.2 PEMC fabrication and functionalization

2.2.1 Fabrication of hollow PEMC

The LbL preparation of PEMC has been described elsewhere.[63, 118] In brief, MF particles were alternatively incubated with PSS and PAH solution (2 mg/ml in 0.5 M NaCl) at a final concentration of 3% for 10 min under gentle stirring. Thereafter, the particles were centrifuged and washed three times with 0.01 M NaCl solution to remove non-adsorbed polyelectrolytes. For preparing hollow capsules, MF particles were coated with 9 layers ($(PSS/PAH)_4/PSS$) before dissolving the template via

incubation in 0.2 M HCl (pH=1.2) for 2 min. The hollow capsules were then washed with 0.01 M NaCl solution and coated with one additional layer of PAH. FITC-PAH replaced PAH as the positively charged polyelectrolyte layers for fluorescence detection.

2.2.2 Surface modification of PEMC

Procedures of obtaining liposomes have been reported elsewhere.[134, 161, 189] POPS and POPC were mixed at a 1:1 molar ratio with varying molar ratios of DSPE-PEG[2000]biotin ranging from 0 to 20%. The surfaces with POPS/POPC/X% DSPE-PEG[2000]biotin are abbreviated as PPDX with X indicating the percentage of DSPE-PEG[2000]biotin (see Table 2.3, layer 1-11). Chloroform in lipid solutions was removed using a rotary evaporator. The dried lipid films on the round-bottom flask were hydrated using PBS to form 1 mg/ml lipid multi-lamellar vesicle suspension under vortexing. Small unilamellar liposome suspension was produced through an extruder (Avestin Inc., Canada) using a polycarbonate membrane with 100 nm pores (Avestin Inc., Canada). PEMC were incubated with the unilamellar liposome suspension at a volume ratio of 1:2 at 37^{o}C for 45 min under constant stirring to induce liposome spreading and bilayer formation.

2.2.3 Protein binding for studying specificity of modified PEMC

The above modified PEMC were further incubated with Cy3-Neutravidin (250 μg/ml) or FITC-BSA (250 μg/ml) for 20 min at room temperature. 1% BSA was used

to block the non-reactive sites on the PEMC surface. After incubation with proteins, the PEMC were subsequently washed three times with PBS.

Table 2.3 Layer deposition design of modified PEMC

layer number	PAH	PPD0	PPDX
1 - 10	(PSS/PAH)5	(PSS/PAH)5	(PSS/PAH)5
11	-	POPS/POPC	POPS/POPC/ X% DSPE-PEG[2000]Biotin
12		NeutrAvidin	NeutrAvidin
13		Biotin-IgG	Biotin-IgG
14		Cy3-secondary antibody	Cy3-secondary antibody

2.2.4 Biotin labeled antibodies binding on NeutrAvidin coated PEMC

The surface modified PEMC was classified in three groups, in which PEMC was modified with different concentration of biotin-PEG-lipid (i.e. PPD0, PPD10 and PPD20). The modified PEMC (4.7×10^4 per ml) were further incubated with NeutrAvidin (250 μg/ml) for 20 min at room temperature. Each group of PEMC was titrated with different concentrations of biotin-IgG (Biotin-Rabbit IgG, Jackson ImmunoResearch). The biotin-IgG solutions was added with double dilute

concentration, starting from 100 μg/ml to 3.125 μg/ml. These would convert to molar concentrations of 667 nM to 21 nM (nano molar, 10^{-9} M). These antibodies were incubated with the above described NeutrAvidin coated PEMC (NA-PEMC) for 20 min at room temperature (Table 2.3, layer 12-14). To detect antibodies by flow cytometry, Cy3 labeled Goat Anti-Rabbit IgG with the same concentration (1:100 in 1% BSA) were then incubated with above PEMC for 1 hr at 37°C. To check the simultaneous coating of NeutrAvidin and biotin-IgG, Cy3-NeutrAvidin and FITC secondary antibody were applied during the coating procedure. To block unspecific adsorption, the indicated primary and secondary antibodies were prepared in 1% BSA solution. Three rinses with PBS (pH 7.4) were performed after each antibody adsorption.

2.2.5 Cells interaction with biofunctional PEMC

25 μg/ml anti-human CCR5 IgG (biotin labeled, from Rat, Abcam, US) was incubated with the above NeutrAvidin coated PEMC for 20min at room temperature. To confirm the coating of the biotin antibody, a secondary antibody FITC-goat-anti-rat IgG (1:100 in 1% BSA, Sigma, US) was added and incubated for 1hr at 37^{o}C. Three rinses with PBS (pH 7.4) were performed after each protein adsorption. The control sample (NeutrAvidin coated PEMC without biotin-antiCCR5 IgG) was prepared with the same steps as described above.

The biotin-antiCCR5 IgG coated PEMC and control samples were employed in cell incubation experiments. In this case, the PEMC was coated with two layers of FITC-PAH for subsequent flow cytometry detection. These PEMC were incubated with

cells attached on planar surface of 24-well microplate at 37^{o}C for different time intervals. For each experiment, PEMC were interacted with control cells 3T3.CD4.CXCR4 and positive cells 3T3.CD4.CCR5. The incubated PEMC is tenfold concentration of cells. After incubation, cells on the microplate surfaces were detached using trypsin and washed with PBS. Flow cytometry was used to analyze the number of FITC-PEMC attached to the cells.

To investigate the interaction of PEMC with antigen expressed cell lines under fluorescent microscopy, the cell lines were labeled with FITC anti-cytokeratin. The PEMC were pre-coated with polyelectrolyte multilayers (PSS/PAH)5 and POPS/POPC/X% biotin-PEG-lipid (PPDX, X = 0, and 10). The modified PEMC were incubated with Cy3 labeled NeutrAvidin. Subsequently the modified PEMC were incubated with biotin-isotype antibody as a control and biotin-antiCCR5 IgG.

2.3 Characterization methods

2.3.1 Zeta potential measurement using laser Doppler electrophoresis (LDE)

Most particles dispersed in an aqueous system will acquire a surface charge, principally either by ionization of surface groups, or adsorption of charged species. These surface charges modify the distribution of the surrounding ions, resulting in a layer around the particle that is different from the bulk solution. If the particle moves, under Brownian motion for example, this layer moves as part of the particle. The zeta potential is the potential at the point in this layer where it moves past the bulk solution

(Figure 2.3). Zeta potential is very sensitive to the concentration and type of ions in solution, e.g. pH and ionic strength of the solution.

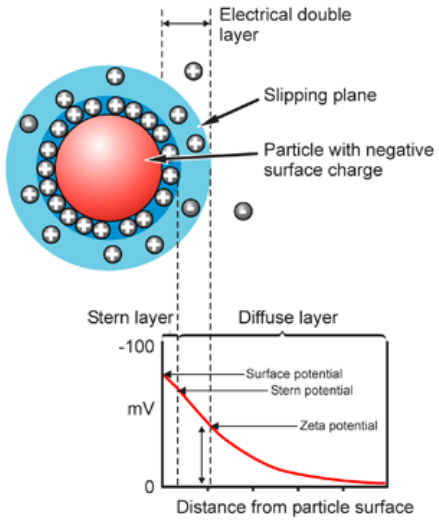

Figure 2.3 Schematic representation of zeta potential [190]

The zeta potential (ζ) can be related to the velocity of charged particles in an electric field. The electrophoretic mobility describes the motion of charged species in a fluid due to an external electric field. From the Henry equation and the Smoluchowski approximation, ζ can be calculated by $\zeta = u\eta/\varepsilon$, where η and ε are the viscosity and dielectric constant of the sample, respectively [190]. The electrophoretic mobility (u) is determined by a combination of laser Doppler velocimetry and phase analysis light scattering techniques (Zetasizer).

During the coating procedure, zeta potential of PEMC (e.g. PSS/PAH multilayer growth on particles or the lipid/protein adsorption on the surface) can be analyzed by a Zetasizer (Zetasizer Nano Z, Malvern Instruments, UK, with software named

Dispersion Technology Software 4.20). All measurements were performed with three replicates in 0.01 M NaCl or PBS at room temperature.

2.3.2 Flow cytometry (FCM)

Flow cytometry for particle and cell analysis has been routinely applied in research, diagnostics and therapy [79, 191]. Flow cytometry involves the counting, examining and sorting of single particles or cells suspended in a stream of fluid. Any suspended particle or cell from 0.2–150 micrometers in size is suitable for analysis [192]. The multiple characteristics of particles are obtained based on light scattering and fluorescent properties of the sample. The properties measured include the relative size, granularity and fluorescence intensity.

The details of flow cytometry technology can be obtained from suppliers, e.g. BD Biosciences. Briefly, after a sample is injected into a flow cytometer, the sample core will be kept separated and coaxial in sheath fluid (Figure 2.4). As the particles or cells pass single file through the sample core, they will be excited by lasers. The resulting scattered laser light and fluorescent signals are collected by lenses and directed by optical filters to detectors.

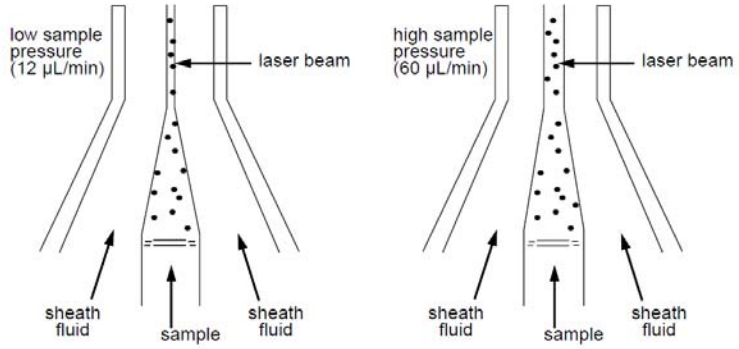

Figure 2.4 Scheme of flow cytometry when the laser detects the single file of particles or cells [192].

The light scattering signals are divided into two categories: forward-scattered light (FSC) and side-scattered light (SSC). FSC is proportional to cell-surface area or size. It is a measurement of mostly diffracted light off the axis of the incident laser beam in the forward direction. SSC is proportional to cell granularity or internal complexity. It is a measurement of mostly refracted and reflected light that occurs at any interface within the cell where there is a change in refractive index [192]. By applying fluorescently labeled antibodies on the cell surfaces, combined with light scattering data, different cell types can be identified and sorted based on corresponding cell surface markers. More than one surface marker can be identified by applying different fluorochromes simultaneously, if each is excited at 488 nm and if the peak emission wavelengths are not extremely close to each other. The excitation and emission wavelengths of different fluorochromes are provided at BD Biosciences's website.

As the single file of particles or cells pass through the laser beam, the scattered and emitted light are collected from a system of lens and optical mirrors and filters. FSC is detected by a photodiode in the forward direction of the incident laser beam. SSC is

collected at approximately 90 degrees to the laser beam and then redirected to the appropriate detector. Emitted SSC and fluorescence signals, which are often weak, are diverted to the photomultiplier tubes (PMTs). Emitted fluorescence signals are collected by placing a filter, which allows only a narrow range of wavelengths to reach the detector. Such filters are called bandpass (BP) filters. For example, the filter used in front of the FITC detector is labeled 530/30. This number gives the characteristics of the spectral band transmitted: 530 ±15 nm, or wavelengths of light that are between 515 nm and 545 nm.

For the experiments in Chapter 3, binding of fluorescently labeled proteins (NeutrAvidin-Cy3, BSA-FITC) on PEMC were investigated by flow cytometry (FACSCalibur, Becton Dickinson, USA) with a laser excitation wavelength of 488 nm (FITC detection in FL1, Cy3 detection in FL2). 10^4 capsules were detected in each measurement and the data were analyzed by WinMDI 2.9 software. Flow cytometry was than performed to detect fluorescence intensity and scattering signals of these capsules. The fluorescence intensity was displayed as geometric mean value (Gmean) of the fluorescence intensity obtained via flow cytometry and analyzed using WinMDI 2.9.

2.3.3 UV-Vis Spectroscopy for 2-[(4'-hydroxybenzyl)azo]benzoic acid (HABA) assay

Ultraviolet and visible spectrometers have become the most important analytical instrument in the modern day laboratory for the last 35 years. Many molecules or ions exhibit absorption in the visible or ultraviolet region when radiation causes an

electronic transition within the molecule structure. The absorbance of a solution increases as attenuation of the beam increases. Absorbance is directly proportional to the path length and concentration of the absorbing species, as stated in Beer's Law (Absorbance A = constant x concentration x path length).

The quantity of DSPE-PEG-biotin attached to the surface was determined by HABA assay as described elsewhere.[130] In brief, a suspension containing biotinylated PEMC was added to a mixture of HABA and Avidin. Since biotin has a higher affinity for Avidin, it prevents the interaction of HABA with Avidin, resulting in a decrease of the absorbance at 500 nm (EX-Link NHS-PEO_4-biotinylation kit instructions, Pierce). The HABA assay buffer (BupH™ PBS, Pierce) contained 0.1 M sodium phosphate and 150 mM sodium chloride. DSPE-PEG[2000] tethered PEMC served as a negative control. A HABA/Avidin solution was prepared by dissolving 600 µl of 10 mM HABA and 10mg Avidin into 19.4 ml HABA assay buffer. 100 µl PEMC/PPDX were each suspended in 900 µl of HABA/Avidin solution. After 5 min of incubation with gentle mixing, the PEMC samples were centrifuged and absorption of the supernatant solutions at 500 nm was measured employing a UV visible spectrophotometer (Shimadzu UV-2450, software UV Probe Version 2.10).

2.3.4 Atomic force microscopy (AFM)

Atomic force microscopy (AFM) origin lies in scanning tunneling microscopy, which won its inventors the Nobel prize in 1985. The microscope itself has hardly anything to do with optical microscopy. There are no lenses, eyepiece and no

requirement for a light source to illuminate the sample. AFM is particularly suited for biological applications [35, 189], as there is no need for staining or coating, and no requirement that the sample should conduct electrons. The samples can be imaged in physiological condition buffer or medium with high resolution. The force contrast gives 3-dimensional topography information, as well as the possibility to access other information such as mechanical properties or adhesion.

AFM consists of a flexible cantilever as a type of spring (Figure 2.5). The basic idea is that the cantilever is able to measure very small forces between the tip and the sample when the tip travels the landscape. The cantilever will bend, or deflect, towards or away from the surface, depending on whether the interaction at the tip is attractive or repulsive. The force appears when atoms or molecules come close together, thus it was named atomic force microscopy.

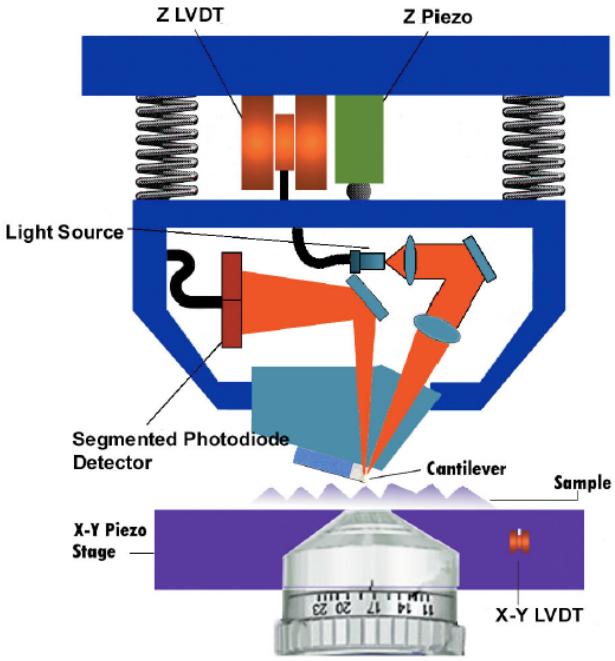

Figure 2.5 Schematic presentation of AFM detection method: the cantilever deflection is detected using a laser beam that is reflected from the back of the cantilever onto a detector [193].

The extension of springs described by Hooke's Law (F = - k * s) can be used on the AFM cantilever. The force F depends in linear manner on the extending range s; k is the spring constant of the cantilever. The spring constants of commercially available cantilevers vary over four orders of magnitude between 0.005 N/m and 40 N/m. Thicker and shorter ones tend to be stiffer and have higher resonant frequencies.

Using the optical lever principle, a small change in the bending angle of the cantilever can be converted to a measurably large deflection in the position of the reflected spot. The movements of the reflected spots are monitored by the current in different parts of a photodiode, which provides three-dimensional images of the sample.

The position of the laser spot is measured by comparing the signals from different sections of the detector. Most AFMs use a photodiode that is made of four quadrants, so that the laser spot position can be calculated in two directions. The vertical deflection (measuring the interaction force) can be calculated by comparing the amount of signal from the "top" and "bottom" halves of the detector. The lateral twisting of the cantilever can also be calculated by comparing the "left" and "right" halves of the detector.

AFM can be mainly performed in contact mode or in tapping mode for imaging. In contact mode, value of the cantilever deflection (the force between the tip and the sample) is selected. The feedback loop system adjusts the height of the cantilever base to keep this deflection constant as the tip moves over the surface. In this mode lateral deflection of the cantilever can provide further information on the chemistry of the surface (friction properties).

Tapping mode has been developed to minimize the interacting forces during scanning, and uses near-resonance, vertical oscillation of the cantilever. A set point amplitude is chosen, and the height adjusted to match this amplitude through the feedback system. Topographical changes on the surface result in a change in the amplitude of the cantilever oscillation. While scanning, the amplitude of the cantilever oscillation is kept constant, allowing imaging of the topography of delicate sample. Phase shift of the oscillation can be recorded for information on the surface chemistry (damping properties).

In our experiment, Silicon wafers were cut into small slides and sonicated in 1:1 (v/v) isopropyl alcohol/water for 5min. They were then immersed in $H_2O/H_2O_2/NH_3$=5:1:1 (v/v) at 70^oC for 15min followed by a thorough rinse with Millipore water. Since the cleaned silicon surfaces have a negative surface charge, the step-wise deposition of polyelectrolytes was initiated using positively charged PAH. All polyelectrolyte solutions were prepared at a concentration of 2 mg/ml in 0.5M NaCl. The silicon wafers were coated by immersing them in polyelectrolyte solutions for 20 min followed by a thorough rinse with 10 mM NaCl. Thereafter the wafer was incubated with liposomes for 45min at 37^oC and unfused lipid aggregates were removed by washing the wafer thrice with PBS. All AFM experiments were conducted in liquid using a Molecular Force Probe (MFP)-3D instrument (Asylum Research, Santa Barbara, CA, USA) in tapping mode. Pyrex-Nitride Probe-Triangular Cantilevers (PNP-TR, force constant: 0.32 N/m, resonance frequency: 67 kHz) were purchased from NanoWorld AG (Switzerland).

The obtained AFM images were analyzed for surface roughness and 2D section using the software Igor Pro 5.05A (Asylum Research, USA). Generally, section analysis proves most useful for making direct depth measurements of surface features, for example, when measuring vertical distance (depth), horizontal distance and angle between two or more points. The section analysis can be used to depict the sectional profile of the studied surface.

The roughness analysis generates a wide variety of statistics for surfaces. In this study, the roughness analysis gives root mean square roughness (RMS), which can be used to represent the roughness of scanned surfaces. The standard deviation of the

surface roughness for all Z_{ij} (surface heights) is calculated according to the equation: $RMS = \sqrt{\sum_{j=1}^{N}\sum_{i=1}^{N}\frac{(Z_{ave} - Z_{ij})^2}{N^2}}$, where Z_{ave} and N are the average value and the number (512) of Z_{ij}, respectively [194].

2.3.5 Fluorescence Microscopy

An inverted Olympus IX71 (Figure 2.6) microscope equipped with a 10× objective lens (Olympus UPlanFLNph 10/0.3 NA, W.D. 10mm) was used to view the PEMC. The fluorescently labeled PEMC was visualized with fluorescence system (U-LH100HG, Manual Imotorized Reflected Fluorescence System, Fluorescence Mirror Unit U-MWB2, Excitation wavelength 490 nm). Note that the fluorescent lamp (Mercury Burner Power Supply Unit BH2-RFL-T3, Olympus Corporation) was switched on 30 minutes before use to allow for stabilization. All images were captured using a CCD camera (DP30BW with the softwares DP Controller and DP Manager, Olympus Corporation, Japan), mounted on the left-hand port of the microscope.

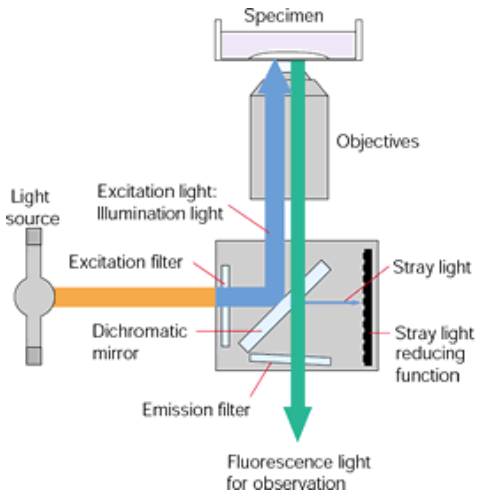

Figure 2.6 Olympus IX71 inverted fluorescence microscopy

2.3.6 Confocal Laser Scanning Microscopy (CLSM)

There has been a tremendous explosion in the popularity of confocal microscopy in recent years, due in part to the relative ease with which extremely high-resolution 3-D images can be obtained from specimens prepared for conventional optical microscopy, and in its great number of applications in numerous biological and medical research interest. Confocal microscopy offers several advantages over conventional optical microscopy, including controllable depth of field, the elimination of image degrading out-of-focus information, and the ability to collect serial optical sections from thick specimens. The key to the confocal approach is the use of spatial filtering to eliminate out-of-focus light or flare in specimens that are thicker than the plane of focus.

In a confocal laser scanning microscope, the light source is a laser that produces high intensity and defined wavelength. The laser beam passes through an excitation aperture and then is focused by an objective lens into a small focal volume within a fluorescent specimen. As the laser scans over the plane of interest, a whole image is

obtained pixel-by-pixel and line-by-line, whereas the brightness of a resulting image pixel corresponds to the relative intensity of detected fluorescent light. A mixture of emitted fluorescent light as well as reflected laser light from the illuminated spot is then recollected by the objective lens. A beam splitter separates the light mixture by allowing only the laser light to pass through and reflecting the fluorescent light into the detection apparatus. After passing a detection pinhole, the fluorescent light is detected by a photodetection device (a photomultiplier tube (PMT) or avalanche photodiode), transforming the light signal into an electrical one that is recorded by a computer. The detection pinhole is conjugated to the focal plane so that only this excited pixel can be detected.

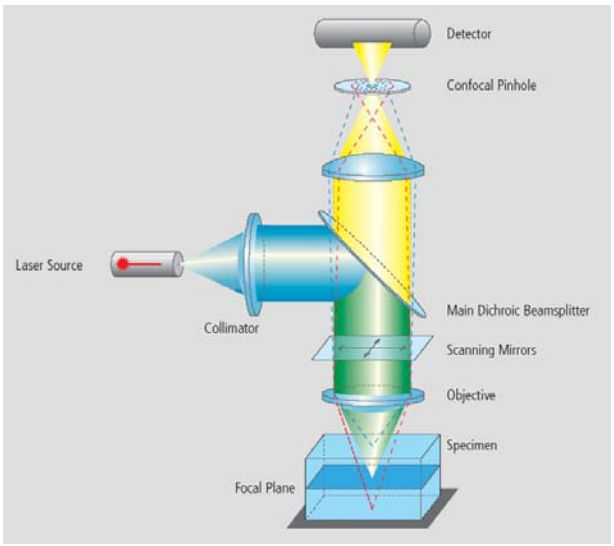

Figure 2.7 Schematic illustration of Zeiss LSM 510 Confocal systems [195]

Confocal micrographs were taken by Zeiss LSM 510 Confocal systems (Zeiss, Germany) with Ar laser (488 nm) and HeNe laser (543nm) as the excitation source

(Figure 2.7). The modified particles were imaged in x-y mode with a 63X/1.4 DIC Plan-Apochromatic oil immersion objective using a high gain photomultiplier tube (PMT). A series of fluorescence images as a function of time were taken using the 'Series Scan' function. Images in transmission mode were taken in parallel. The capsule sizes were obtained from the images. Fluorescence intensity profiles along a line were calculated using the `Profile' function provided with the LSM 510Meta program.

Chapter 3 Fabrication and characterization of biofunctional PEMC

3.1 Introduction

The modification of PEGylated phospholipids with functional moieties could be another promising direction to functionalize lipid coated PEMC. In this way it will be possible to target PEMC to specific molecules, while still enhancing their *in vivo* lifetime as well as their permeability. One approach for such functionalisation is to utilize the non-covalent specific interaction between biotin and Avidin. Avidin, Streptavidin, and NeutrAvidin are three common proteins showing strong non-covalent binding interactions with biotin. Avidin demonstrates the highest bonding strength with a dissociation constant of $K_D=10^{-15}$ M. However, Avidin also shows non-specific binding due to its carbohydrate content and a basic isoelectric point (pI≈10) [133]. Streptavidin has a slightly lower biotin binding strength with a dissociation constant of $K_D=10^{-13}$ M and a mildly acidic pI of ~5. NeutrAvidin is a deglycosylated Avidin exhibiting a more neutral pI of 6.3. Therefore, NeutrAvidin demonstrates much less nonspecific binding compared to Avidin but still has the same binding affinity to biotin as Avidin [129].

In this chapter, we report results of fabricating PEMC and coating them with a lipid bilayer containing lipids equipped with PEG side chains and end-conjugated with biotin. As a proof-of-principle, synthetic melamine formaldehyde (MF) particles were

coated via the LbL method with PAH and PSS followed by core dissolution. Subsequently a phospholipid bilayer, containing different concentrations of PEG-biotin, was assembled as the outermost layer and functionalized with NeutrAvidin. The fabrication and modification of PEMC was monitored using surface charge measurement. The increment of polyelectrolyte multilayers was demonstrated by flow cytometer. The dissolving of PEMC templates was displayed from a series of real time confocal laser scanning microscopy (CLSM) images. PEMC morphology was visualized using CLSM and fluorescence microscopy.

3.2 Results

3.2.1 Fabrication and characterization of hollow PEMC

Since the surface potential of MF particles is positive, the step-wise deposition of polyelectrolytes was initiated using negatively charged PSS. The surface potential effects of this step-wise process are shown in Figure 3.1, which presents ζ-potential measurements for MF particles with different layers of PAH and PSS. With repeated application of layers of PAH and PSS a reversal of the ζ-potential is observed with every new deposition of an oppositely charged polyelectrolyte layer. After completing the ninth adsorption cycle, the template (i.e. the MF core) was removed via incubation in HCl. The ζ -potential of the tenth layer in Figure 3.1 represents the measurement after coating with an additional PAH layer onto the hollow PEMC. The light

microscopy images (inserts) demonstrate that the shape and size of the hollow capsules closely resembles that of the particles.

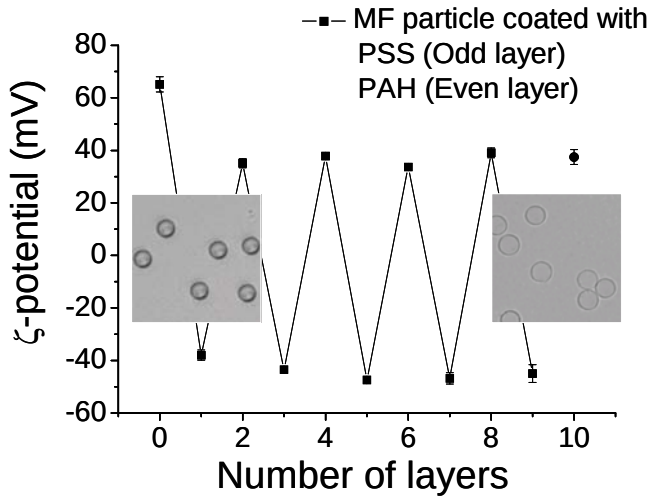

Figure 3.1 ζ-potential of MF microparticles as a function of the number of polymer layers formed by consecutive adsorption of poly-anionic poly (styrenesulfonate) sodium salt (PSS) and poly-cationic poly (allylamine)hydrochloride (PAH). The odd numbers correspond to PSS and the even numbers to PAH as the outermost layer. The tenth layer represents the ζ-potential of PEMC with the additional PAH coating after the dissolution of the MF core. The inserts show light microscopy images (50 μm × 50 μm) of particles (left) and hollow capsules (right). The picture of hollow capsules was positioned on the 10^{th} layer, because the hollow capsules were obtained after coating the 10^{th} layer of polyelectrolyte.

Fluorescence intensity was measured as a function of the number of FITC-PAH to verify that, the layer thickness increased with each deposition of the charged polymers. Figure 3.2a displays dot plots of forward scattering (FSC-H) vs. FL1 fluorescence intensity. For better data comparison, Figure 3.2a displays only the dot plots of MF particles coated with none and 5 layers of FITC-PAH. The dot plots of MF particles coated with 1-4 layers of FITC-PAH were not shown because of the overlapping plots.

R1 regions represent single particles and R2 aggregates of particles. The fluorescence histograms of respective R1 singlets are shown in Figure 3.2b. The Gmean intensity of each fluorescence histogram is given as a function of the number of FITC-PAH in Figure 3.2c. The dot straight line in Figure 3.2c represents the expected theoretical linearity of the fluorescence vs. layer numbers in double log scale, showing an increase in fluorescence intensity with each additional layer.

a

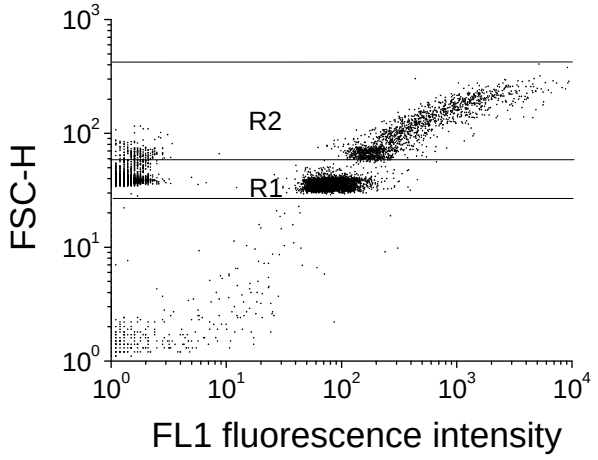

b

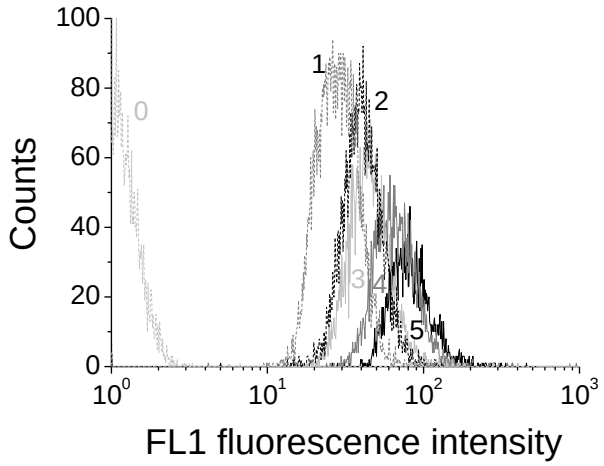

c

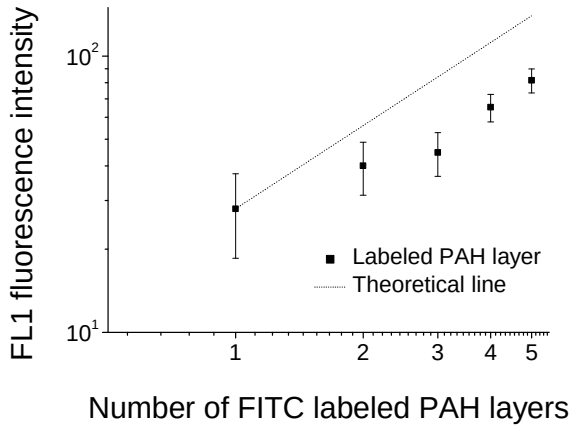

Figure 3.2 Flow cytometric analysis of MF particles coated with increasing FITC-PAH layers. Graph (a) displays dot plots of MF particles coated with none and 5 layers of FITC-PAH. Graph (b) displays fluorescence histograms of the gated R1 regions (singlets) from the respective dot plots. The numbers displayed on the histogram represent the layer number of FITC-PAH. Graph (c) represents mean fluorescence intensity of single particles as a function of the number of labelled PAH layers. The straight dot line is a theoretical prediction assuming fluorescence intensity is doubled in each coating.

In this work, the dissolving process of MF cores was captured by CLSM. Figure 3.3 displays one example for visualization. The core was decomposed completely in 18 seconds. The shells are swelling and the increase in diameter is the result of shells flattened and spreading after the dissolving of the core.

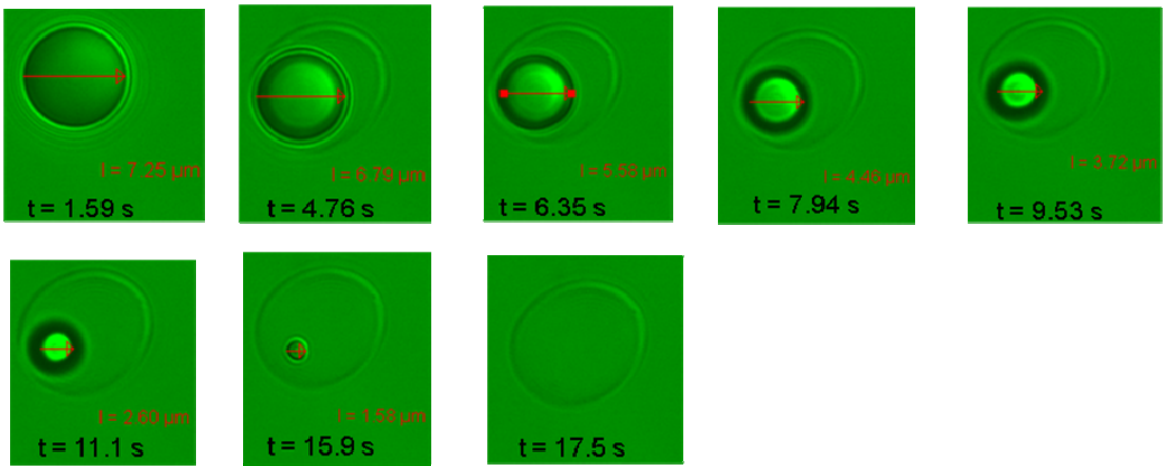

Figure 3.3 CLSM images of the digestion process of MF core as a function of time. The size of MF core at each dissolving time is shown in the graph.

The morphology of the polyelectrolyte shells was also characterized by CLSM. FITC labeled PAH was adsorbed to the surface of the polyelectrolyte microparticles and filled into the hollow PEMC to investigate the morphology of them under CLSM. CLSM images confirmed that the shape of the capsules clearly resembles the shape of MF particles (Figure 3.4a) and the interior of the capsules is hollow (Figure 3.4b).

a

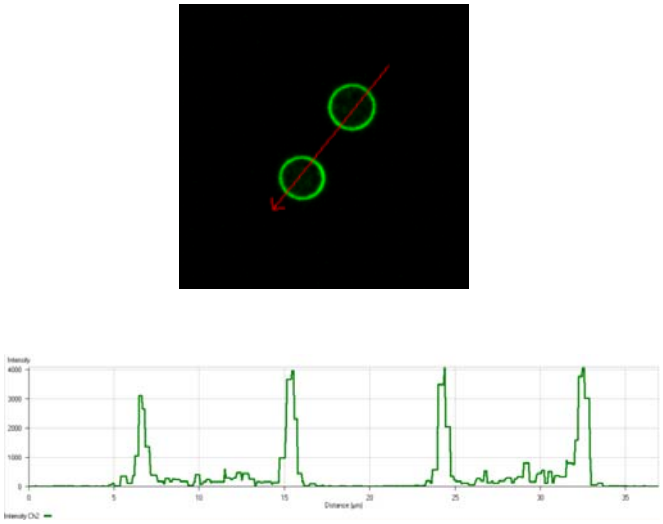

b

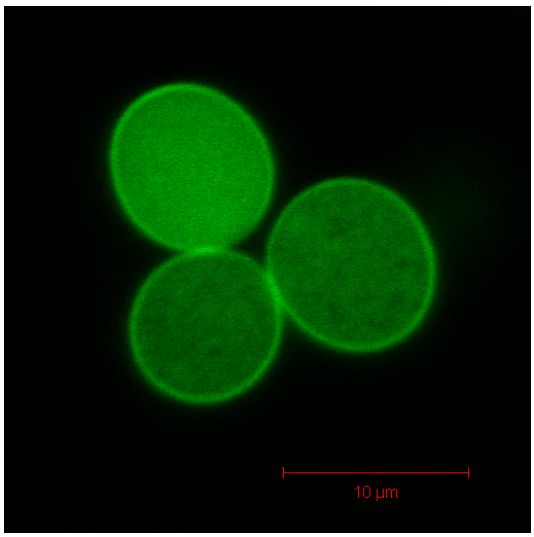

Figure 3.4 CLSM images representing microparticles labeled with FITC-PAH (a) and images of the hollow PEMC filled with FITC (b)

3.2.2 Surface modification of hollow PEMC

After fabrication of PEMC with PAH as the outermost layer, the hollow capsules were coated with POPS/POPC/DSPE-PEG-biotin forming the outermost layer of the PEMC surface. The arrangement of the capsule layers employed in this study is summarized in Table 3.1. The 1:1 mixture of POPS and POPC (PPD0) resulted in a negatively charged surface at pH 7.4, due to the negative charge of POPS and the zwitterionic appearance of POPC. The ζ-potential measurement in Figure 3.5 reveal a charge reversal from 37.4 ± 2.8 mV (PAH, layer 10) to -11.0 ± 0.4 mV (PPD0, layer11), thereby confirming the successful lipid bilayer coating in PBS.

Table 3.1: Layer deposition design of modified PEMC.

layer number	**PAH**	**PPD0**	**PPDX**
1 - 10	$(PSS/PAH)_5$	$(PSS/PAH)_5$	$(PSS/PAH)_5$
11	-	POPS/POPC	POPS/POPC/ X% DSPE-PEG[2000]Biotin

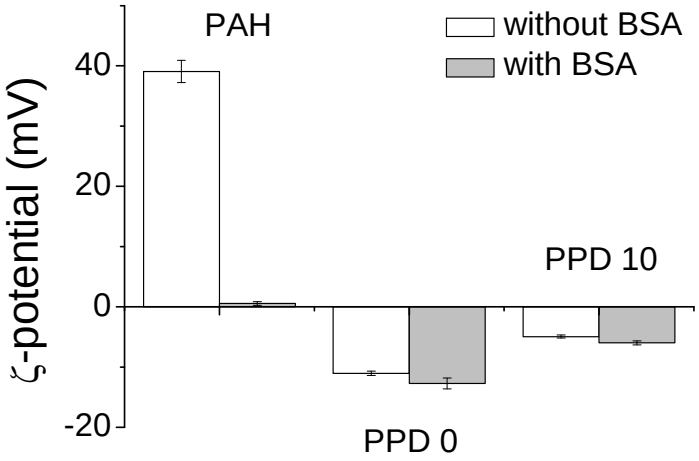

Figure 3.5 ζ-potential of PEMC with different outermost layers before and after incubation with 1% BSA. The PEMC were first coated with $(PSS/PAH)_5$ followed by different outermost layers: PAH, PPD0, and PPD10.

3.3 Discussion

In this chapter, hollow polyelectrolyte microcapsules (PEMC) were fabricated using layer-by-layer self-assembly of polyelectrolytes on sacrificing templates. Polyelectrolyte adsorption and accumulation on the surface of the microparticle were confirmed using ζ-potential measurement and flow cytometry. There is a discrepancy between theoretical growth of flow cytometer fluorescence intensity and experimental findings (Figure 3.2c), which can be explained that if the different adsorption behavior of PSS and PAH for the first two layers compared with the additional layers is considered. Usually, after 3 layers a linear increase of fluorescence can be obtained in agreement with the theoretical prediction.

In this chapter, we fabricated functional hollow polyelectrolyte microcapsules based on surface coating with POPS/POPC and DSPE-PEG-biotin as illustrated in Figure 3.6. Driven by electrostatic forces, negatively charged POPS/POPC liposomes (Figure 3.6b) adsorb and spread onto positively charged polyelectrolyte multilayer surfaces (Figure 3.6a) to form a uniform lipid bilayer by direct vesicle fusion (Figure 3.6c).[82, 93, 181] These findings are in good agreement with a previous report by Fischlechner et al.[188] demonstrating that PAH as the outermost layer combined with POPS/POPC mixture is an ideal system to study lipid bilayer adsorption onto LbL multilayers making this system suitable for further functionalisation. After adsorption, the microcapsules displayed a negative potential of -11.0 ± 0.4 mV, indicating the successful surface modification. After coating with PPD10, the negative charge decreased to -5.0 ± 0.3 mV, clearly demonstrating the effect of the neutral DSPE-PEG-biotin on the electrostatic surface potential. NeutrAvidin attachment was acquired via biotin-Avidin binding to provide a specific coupling mechanism for functional molecules to the PEMC surface (Figure 3.6c). NeutrAvidin is a tetrameric protein containing four identical homotetramers with two on opposite sides thereby providing two biotin binding sites on each side [189]. Therefore, NeutrAvidin can be immobilized with one side attached to the DSPE-PEG-biotin and the other side creating a surface site for subsequent binding of biotinylated antibodies or other bio-molecules.

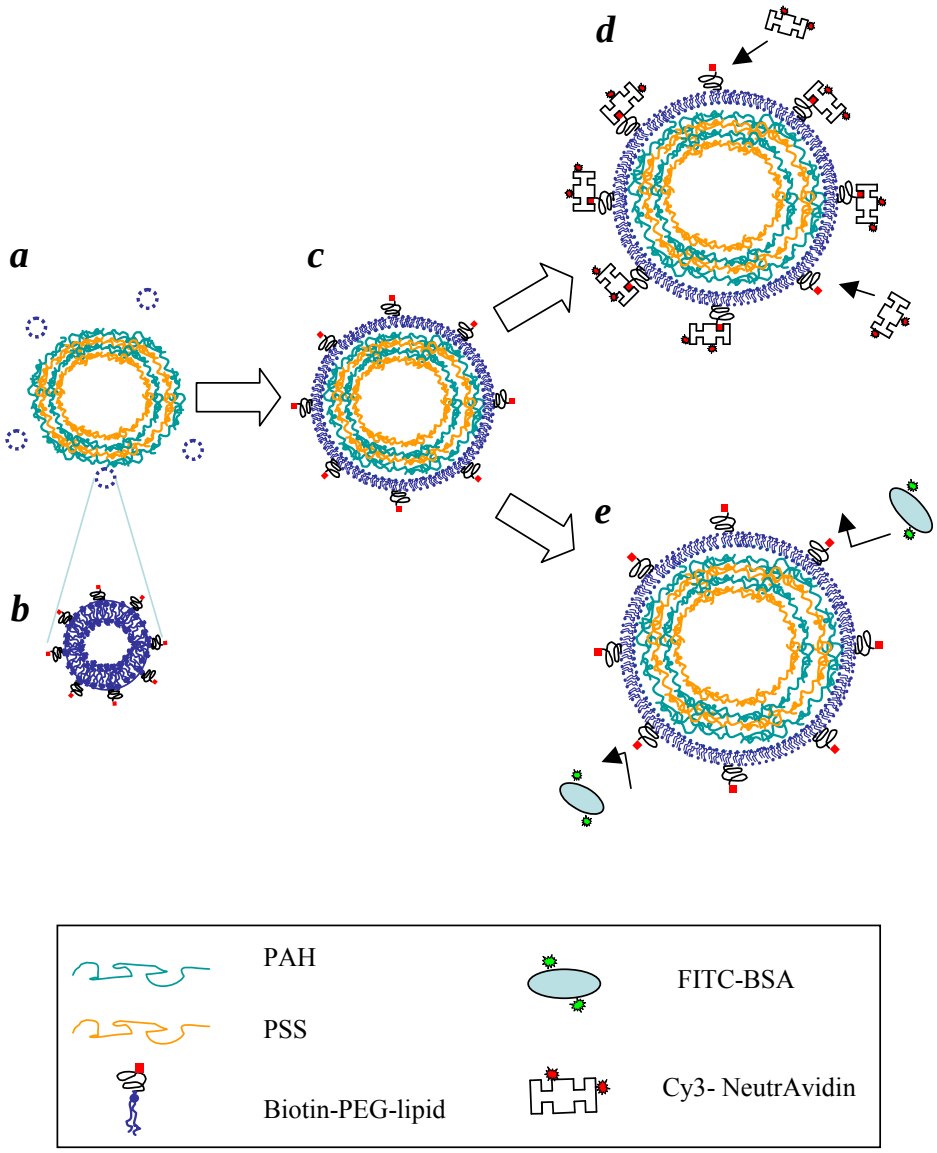

Figure 3.6 Simplified scheme for the preparation of (a) PEMC coated with (b) liposomes containing DSPE-PEG-biotin. c) The functionalisation of the PEMC facilitates d) specific binding to Cy3-labeled NeutrAvidin and reduces e) non-specific binding of FITC- labeled BSA.

Chapter 4 Targeting ability of polyelectrolyte microcapsules modified with biotinylated poly (ethylene glycol)-grafted liposomes

4.1 Introduction

This work presents the specific binding of modified bio-functional PEMC to NeutrAvidin and resistance to serum proteins such as albumin (bovine serum albumin, BSA) adsorption. A sandwich strategy of biotin-avidin-biotin binding can help to assemble specific biotinylated molecules such as antibodies or penetrating peptides onto the microcarrier surface to enhance the specific adsorption and uptake by the target cells. The protein binding was monitored by means of flow cytometry. The morphology of the biotinylated PEG phospholipids was investigated via atomic force microscopy.

4.2 Results

4.2.1 Specific interaction with Cy3-NeutrAvidin

As described in the previous section, after the LbL assembly of PEMC the capsules were modified with POPS/POPC/DSPE-PEG-biotin with different concentrations of biotin PEG-lipid between zero and twenty percent. Afterwards these modified PEMC as well as the control samples (PPD0 and PAH) were incubated with Cy3-NeutrAvidin and the specific binding of NeutrAvidin was investigated by flow cytometry. Figure

4.1 shows the forward scattering signal (FSC-H) versus the fluorescence intensity (FL2-H). The different regions in these plots indicate that the PEMC form aggregates of different sizes with the different regions corresponding to singlets, doublets, and triplets. Comparing the graphs in Figure 4.1 also shows that the percentage of single capsules differs considerably between the different samples. For the PAH-ending PEMC, the singlets only account for 48% of the total sample, whereas for lipid coated PEMC up to 90% of the capsules are singlets.

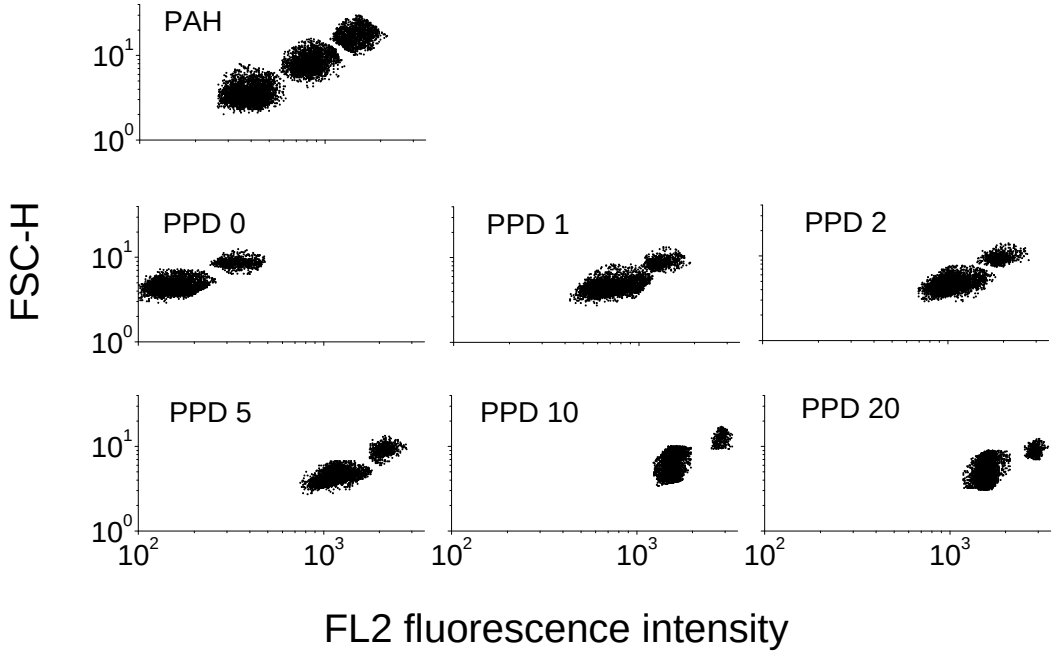

Figure 4.1 Flow cytometry dot plots of PEMC after incubation with Cy3 labeled NeutrAvidin showing the forward scattering signal (FSC-H) versus the fluorescence intensity of the Cy3 labeled NeutrAvidin (FL2). The PEMC were first coated with $(PSS/PAH)_5$ followed by various outermost layers: PAH, PPD0, PPD1, PPD2, PPD5, PPD10 and PPD20. In each gate, the selected events always account for at least 85% of the total events.

The specific binding of Cy3 labeled NeutrAvidin in the presence of 1% BSA to DSPE-PEG-biotin as POPS/POPC surface bilayer constituent was compared to control samples. Figure 4.2*a* shows the FL2 intensity histograms extracted from the single capsule regions in Figure 4.1. A significant increase of fluorescence intensity can be observed with increasing percentages of DSPE-PEG-biotin within the lipid bilayer indicating an increase in NeutrAvidin binding. In addition, it can be seen that PEMC with PAH ending show a higher intensity than those coated with PPD0, but lower than those coated with DSPE-PEG-biotin. PEMC modified with PPD20 (light gray curve) and PPD10 display the same fluorescence intensity indicating a saturation in NeutrAvidin binding. The CLSM image (inserts in Figure 4.2a) also confirms the homogeneous Cy3-NeutrAvidin coating of the PEMC. In summary, these results demonstrate that PEMC modified with DSPE-PEG-biotin show a much greater affinity for NeutrAvidin than the control samples (i.e. PPD0 and PAH).

The same set of experiments was done on the PEMP modified with different concentrations of biotin-PEG-lipid. The peak of each intensity histogram is shown in Figure 4.2b. The trends of the mean fluorescence intensity versus DSPE-PEG-biotin concentration from both PEMP and PEMC data is demonstrated in Figure 4.2c. The trends are the same as demonstrated, with a higher intensity from each of the PEMC data point.

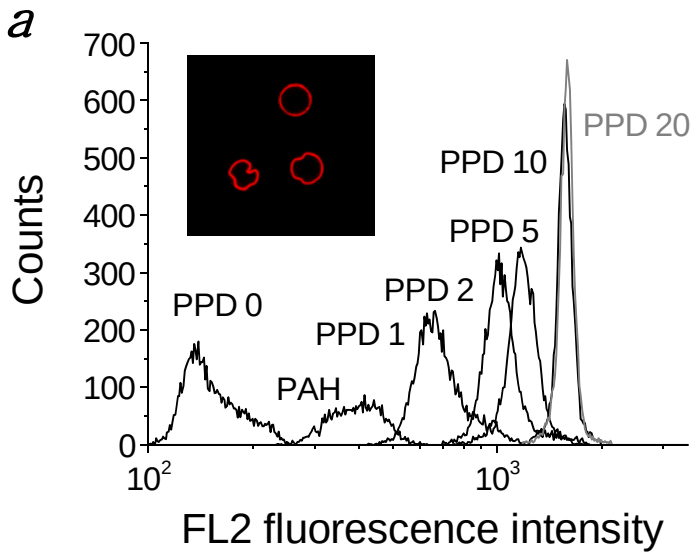
a
700
600
500
400
300
200
100
0
Counts
PPD 0
PAH
PPD 1
PPD 2
PPD 5
PPD 10
PPD 20
10^2
10^3
FL2 fluorescence intensity

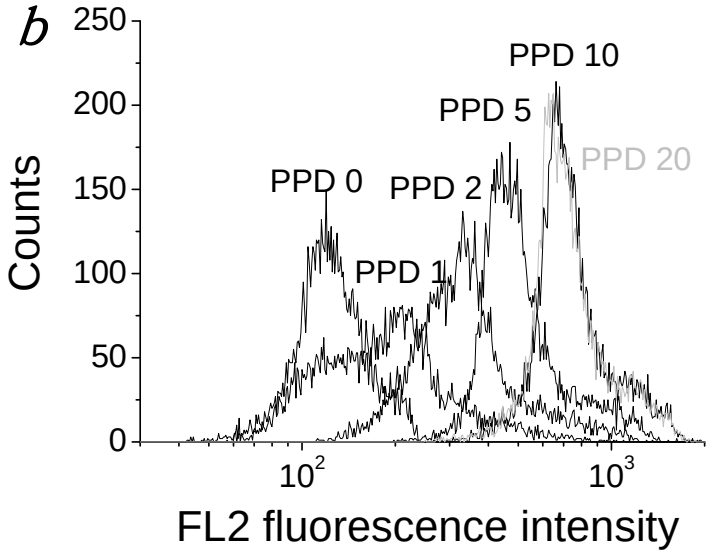
b
250
200
150
100
50
0
Counts
PPD 0
PPD 1
PPD 2
PPD 5
PPD 10
PPD 20
10^2
10^3
FL2 fluorescence intensity

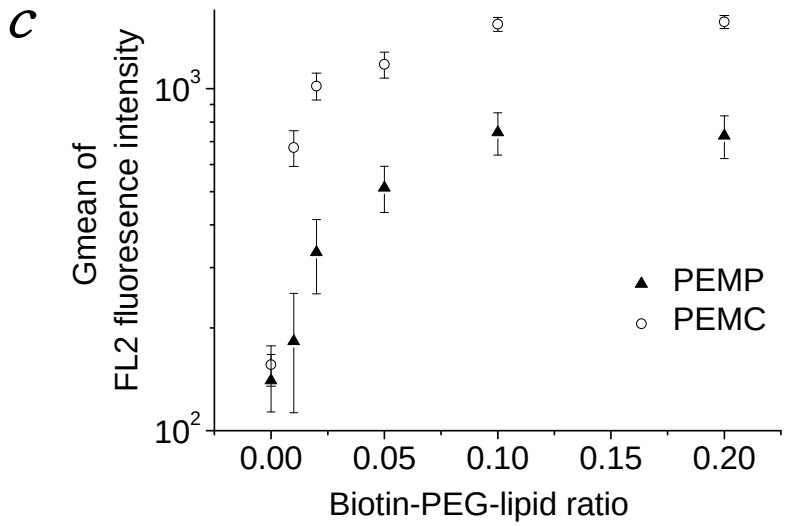

Figure 4.2 (a) and (b) Fluorescent intensities (FL2) of PEMC and PEMP and (c) mean fluorescence intensities of PEMP and PEMC after incubation with Cy3 labeled NeutrAvidin. The CLSM image (40 μm × 40 μm) demonstrates the homogeneous coating of the capsules (s.a. Figure 4.1).

4.2.2 Non-specific Interaction with FITC-BSA

BSA is an abundant protein and is often employed to test the protein resistance of biomaterials [118, 196]. In this work, 1% BSA was employed as a model plasma protein to test non-specific protein binding to functionalized PEMC. PEMC modified with PPD10 and PPD20 as well as control samples, i.e. PEMC with PPD0 and PAH as the outermost layer were incubated in 250 μg/ml of FITC labeled BSA and mixed with a 1% unlabelled BSA solution, followed by fluorescence detection by flow cytometry. The flow cytometric measurements presented in Figure 4.3 demonstrates that the trend of capsule aggregation in the presence of BSA shows a strong dependence on the

outermost layer. For the control sample with PAH as the outermost layer, about 43% of the detected capsules are single capsules whereas for the lipid coated PEMC the percentage of single capsules increases to more than 90%. Figure 4.4 shows the fluorescence intensity (FL1) of the single capsules as well as the mean intensity. The FITC intensity of the control PEMC, i.e. with a PAH ending, clearly shows the highest fluorescence intensity whereas PEMC coated with PPD0, PPD10 and PPD20 demonstrate a significant reduction of the fluorescent intensities with increasing concentrations of the DSPE-PEG-biotin.

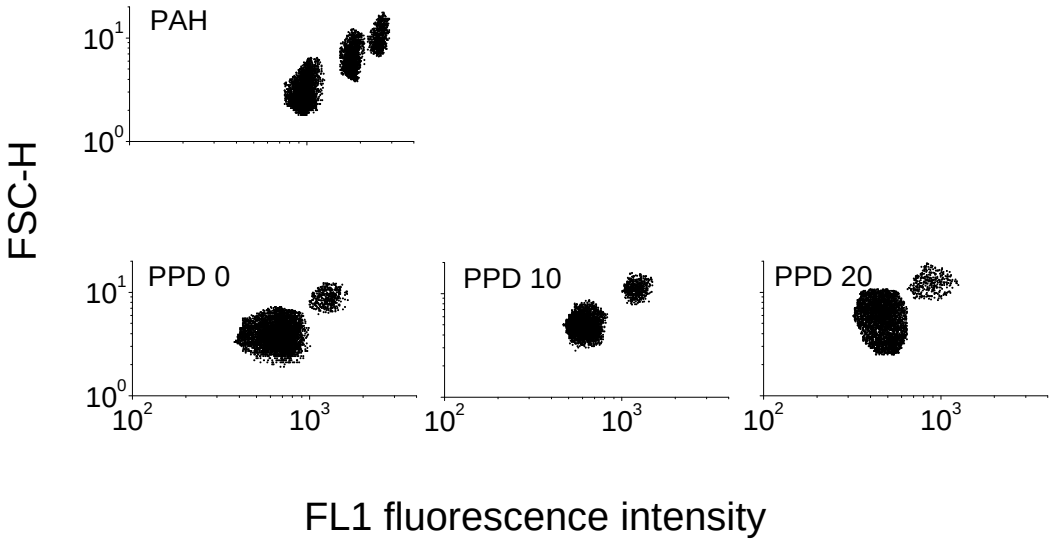

Figure 4.3 Flow cytometry dot plots of PEMC after incubation with FITC labeled BSA showing the forward scattering signal (FSC-H) versus the fluorescence intensity (FL1). The PEMC were first coated with $(PSS/PAH)_5$ followed by different outermost layers: PAH, PPD0, PPD10 and PPD20.

a

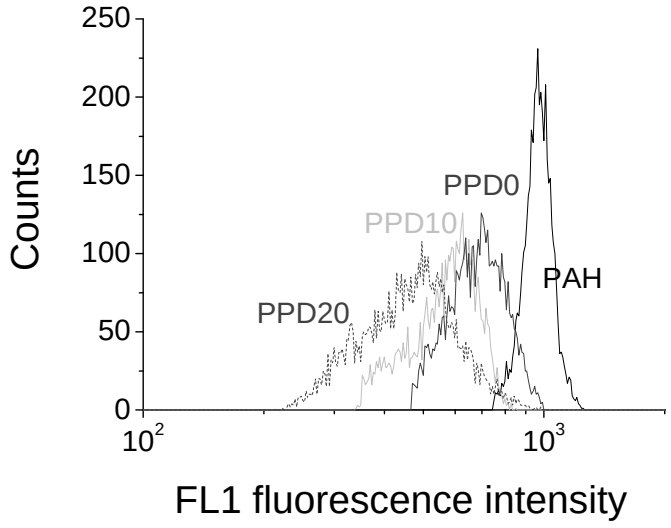

b

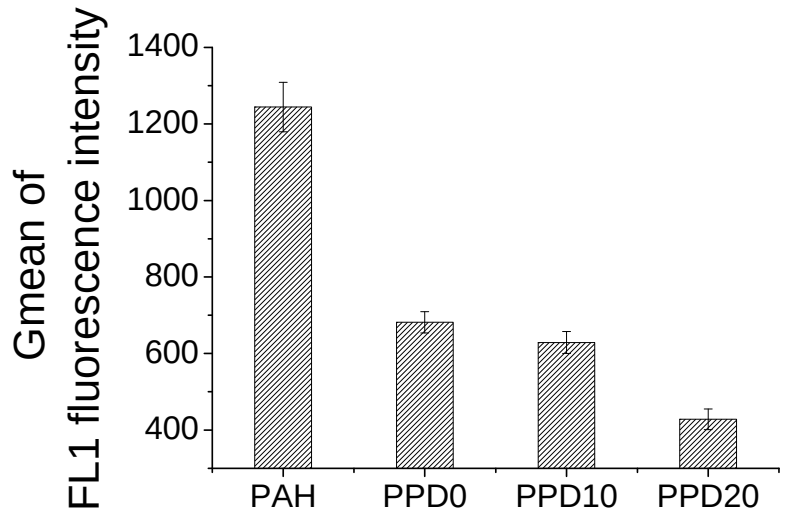

Figure 4.4 a) Fluorescent intensities (FL1) and b) mean fluorescence intensities of PEMC after incubation with FITC labeled BSA (s.a. *Figure 4.3*). The error bars mean the standard deviations of the mean values.

4.2.3 Quantification of DSPE-PEG [2000]Biotin

The surface density of attached DSPE-PEG-biotin on PEMC was determined by HABA assay, which is commonly used for the quantitative measurement of biotin concentrations. PEMC coated with lipid served as a negative control. For PEMC modified with PPD10 and PPD20, the calculated surface density was one DSPE-PEG-biotin molecule per 3.92 nm^2 and 2.26 nm^2 respectively (0.2551±0.0083 nm^{-2} and 0.4434±0.004 nm^{-2}).

The example of formula to calculate surface density of PPD10 modified PEMC was shown as the following.

$$M_{DSPE\text{-}PEG\text{-}Biotin\ 10\%} \bullet N_0 = 3.26471 \times 10^{-6}\,(mol/l) \times 6.023 \times 10^{23}\,molecules/mol$$
$$= 19.665 \times 10^{17}\,molecules/l = 19.665 \times 10^{14}\,molecules/ml$$

$$DSPE\text{-}PEG\text{-}Biotin\ per\ PEMC = \frac{19.665 \times 10^{14}\,molecules/ml}{4.733 \times 10^{7}\,PEMC/ml} = 4.155 \times 10^{7}\,molecules/PEMC$$

$$Surface\ area\ per\ PEMC = 4\pi r^2 = 4\pi(7.2\,\mu m/2)^2 = 4\pi(3.6 \times 10^{3}\,nm)^2 = 1.629 \times 10^{8}\,nm^2$$

$$\frac{DSPE\text{-}PEG\text{-}Biotin\ per\ PEMC}{Surface\ area\ per\ PEMC} = \frac{4.155 \times 10^{7}\,molecules/PEMC}{1.629 \times 10^{8}\,nm^2} = 0.2551 \approx 1\,molecule\ /\ 3.92\,nm^2$$

4.2.4 Surface morphology of biofunctional polyelectrolyte multilayers

The surface morphology of the polyelectrolyte multilayers was characterized via atomic force microscopy (AFM). Polyelectrolyte multilayers (PEM) and lipid layers were coated on planar silicon substrates. Figure 4.5 shows AFM images of $(PAH/PSS)_4$/PAH PEM films modified with PPD0, PPD10, and PPD20. The

morphology of the $(PAH/PSS)_4/PAH/PPD0$ PEM films without any DSPE-PEG-biotin (Figure 4.5a) is fairly smooth with a root mean square (RMS) roughness of 0.77 nm. With the addition of 10% DSPE-PEG-biotin, the surface becomes spiky and the RMS roughness increases to 1.85 nm (Figure 4.5b). In addition, Figure 4.5b also indicates a uniform distribution of the spikes with no significant clustering. Coating the surface with 20% DSPE-PEG-biotin results in the formation of large aggregates and an RMS of 3.01 nm (Figure 4.5c).

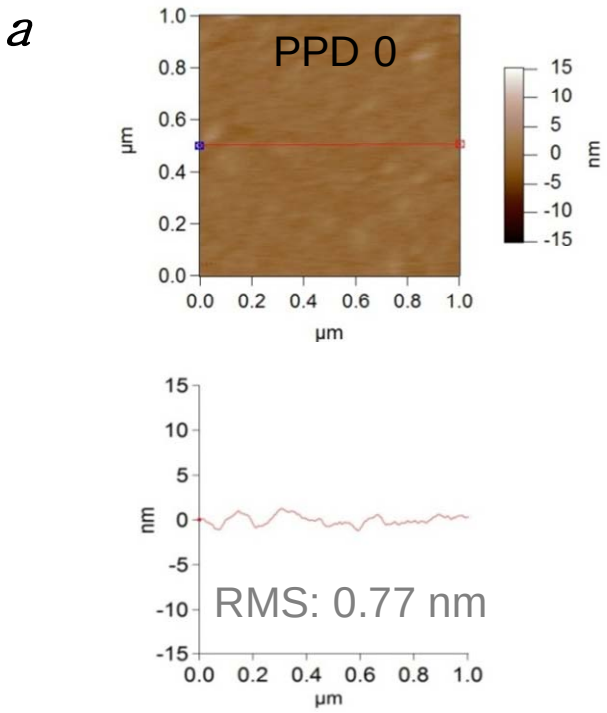

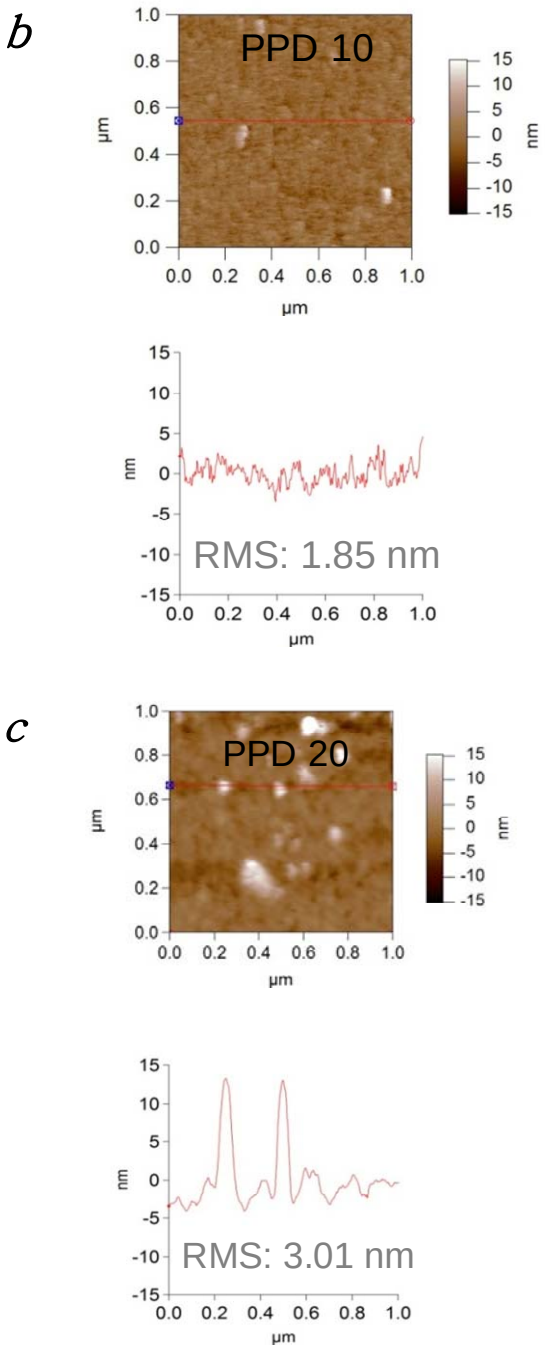

Figure 4.5 AFM images of a) $(PAH/PSS)_4/PAH/PPD0$, b) $(PAH/PSS)_4/PAH/PPD10$, and c) $(PAH/PSS)_4/PAH/PPD20$ coated onto planar silicon surfaces.

4.3 Discussion

It was demonstrated that PEMC modified with DSPE-PEG-biotin resulted in a significant decrease in the number of aggregates after incubation with either only BSA (Figure 4.3) or with NeutrAvidin (Figure 4.1). BSA is negatively charged at pH 7.4 and the ζ-potential change after BSA exposure to PEMC with PAH as outermost layer (Figure 3.1) confirmed its adsorption to the positively charged macromolecules. The surface charge became nearly zero (0.6 ± 0.3 mV) after protein incubation whereas the value of the ζ -potential of POPS/POPC surfaces remains almost constant after BSA incubation. Thus, the reduced aggregation of the PPD0 coated capsules as compared to PAH ending capsules might be at least partly due to the relatively high negative surface charge. For surfaces coated with PPD10, the value of the surface charge reduced to -6.0 ± 0.4 mV. These capsules show a further reduced aggregation rate as compared to the surfaces modified with PPD0 despite the more than 50% lower ζ-potential and thus lower surface charge, which is most likely due to the steric repulsion of the PEG chain structures. Therefore, these functionalized lipid bilayer surfaces should not only provide a platform for specific functional molecules, but also facilitate the stabilization of these carriers.

The binding of Cy3-NeutrAvidin to control samples and DSPE-PEG-biotin coated PEMC was compared via flow cytometry. The geometric mean value of fluorescence intensity of PPD20 modified PEMC increased tenfold as compared to PEMC modified with PPD0, and fourfold as compared to that with PAH-ending PEMC. The scale of this difference is thus set as 0-10 fold. Ten fold is given by the highest increase fold in

the results. The difference will be considered significant if it is above fivefold. The difference between PPD0 and PAH can be explained by electrostatic interaction. The isoelectric point (pI) of NeutraAvidin is at 6.3 and it is thus negatively charged in PBS (pH=7.2). Therefore, it can be expected that NeutrAvidin binds stronger to the positively charged PAH-ending surface as compared to the negatively charged PPD0 surface. With increasing DSPE-PEG-biotin concentration within the POPS/POPC bilayer, the amount of bound NeutrAvidin is also increasing, reaching saturation at 20% DSPE-PEG-biotin. The same trend is observed for modification on polyelectrolyte microparticles (PEMP). However, there was about twice NeutrAvidin coated on capsules than on particles with the same biotin-PEG-lipid modification. The reason might be that PEMC provided porous and rough surface after template dissolving and thus adsorbed more biotin-lipid-PEG, compared to the surface of PEMP.

From the AFM images and their RMS roughness values (Figure 4.5), it can be concluded that the surface morphology became rougher after coating the PEMC with the DSPE-PEG-biotin layer. Via the quantification of the biotin concentration using HABA assay, the calculated DSPE-PEG-biotin surface density on PPD10 is one molecule per 3.92 nm^2. Therefore the mean distance between the PEG molecules should be around 2.0 nm, which in turn is slightly less than the calculated Flory radius of PEG[2000] of about 3.4 nm.[180] Thus a brush structure can be expected for PPD10 capsules.[180] For PPD20 the roughness of the surface increased with the AFM data indicating some aggregation (Figure 4.5c). This also demonstrates that the lipid layers eventually reached a limit leading to micelle or liposome formation on the surface.

Lastly, it should be emphasized that these biofunctional capsules also demonstrate a significant reduction of non-specific protein binding (Figure 3.6e). Utilizing BSA-FITC as the reporter protein, it was demonstrated that an increase in the DSPE-PEG-biotin amount within the POPS/POPC bilayer results in a gradual reduction of protein binding. Taking into consideration the above AFM analysis it can be concluded that the densely packed PEG chains prevent unspecific BSA adsorption via providing a steric exclusion layer. This reduced nonspecific adsorption should help to prevent the detection of such biofunctional PEMC in vivo and thus the early uptake by the mononuclear phagocytic system (MPS) through endocytosis and phagocytosis.

Chapter 5 Binding affinities of biotin-antibody to NeutrAvidin on biofunctional polyelectrolyte microcapsules

5.1 Introduction

The LbL PEMC modified with biotin-PEG-lipid and NeutrAvidin as the outmost layer (PEMC/NA) was incubated with biotin-antibodies (Biotin-Ab). As potential drug carriers for targeted delivery, it is interesting to know their binding ability to the antibodies and the stability of the complex (PEMC/NA/Biotin-Ab). This chapter was aimed to provide quantitative measurement of the interaction between PEMC/NA and Biotin-Ab. The binding ability and apparent dissociation constant of PEMC/NA to biotin-antibody were determined using flow cytometric microsphere based assay.

Bioaffinity interactions are successfully adapted from nature for use in separation and detection applications that range from affinity chromatography to detection technology for human diagnostics. For example, proteins and peptides [146] have been immobilized on microspheres for the detection and quantification of the antibodies, using standard flow cytometric microsphere based assay. Microsphere-based assays using immobilized surface bound interaction partners are routinely used with flow cytometry as a readout platform to detect analytes, such as proteins, nucleic acids, or small molecule entities [142, 197]. In this work, the PEMC serves as the microsphere immobilized with NA, and the molecular partners are NA and Biotin-Ab.

The same population of PEMC/NA microcapsules was incubated with different concentrations of Biotin-Ab to obtain binding curves for the estimation of binding ability and dissociation constants. Fluorescent labeled secondary antibodies were bound to the outlayer of the complex (PEMC/NA/Biotin-Ab) for the detection by flow cytometry. The binding ability and dissociation constants were compared between PEMC with and without biotin-PEG-lipid modification. Fluorescent microscopy was employed for visualizing the PEMC after coating with biotin-antibody.

5.2 Results

5.2.1 Flow cytometry characterization of biotin-IgG coated biofunctional PEMC

The fabrication and modification of hollow PEMC has been successfully completed and described in our previous work [198]. Briefly, the coating on MF particles was initiated from PAH and the particles were subsequently coated repeatedly with PSS and PAH for nine layers. The coating of PAH and PSS was confirmed by zeta potential measurement, which exhibited a reversal of surface charge every new deposition of an oppositely charged polyelectrolyte layer. The template, i.e. the MF core, was removed via incubation in HCl to obtain hollow PEMC. The hollow PEMC were modified with POPS/POPC/DSPE-PEG-biotin with different concentrations of biotin PEG between zero and twenty percent (i.e. PPD0, PPD10 and PPD20). NeutrAvidin (NA) has been shown specifically bind to biotin-PEG-lipid modified PEMC.

In this work, after LbL fabrication and modification of PEMC, these PEMC capsules with NA as the outmost layer (i.e. PEMC/PPDX/NA, X=0, 10, 20) were incubated biotin-IgG. A serial of double diluted biotin-IgG solutions were incubated with these modified PEMC/PPDX/NA as well as the control samples (PEMC/PPD0/NA). Cy3-labeled secondary antibody was subsequently coated for fluorescent detection by flow cytometry. There were three population of PEMC, i.e. PEMC/PPD0/NA, PEMC/PPD10/NA and PEMC/PPD20/NA. Each population was incubated with six concentrations of biotin-IgG solutions. Six flow cytometry data were obtained for each population of PEMC complex (PEMC/PPDX/NA/Biotin-Ab). For example, Figure 5.1 shows the forward scattering signal (FSC-H) versus the fluorescence intensity (FL2-H) from PEMC complex (PEMC/PPD10/NA/Biotin-Ab). The different regions in each graph indicate that the PEMC form aggregates of different sizes with the different regions corresponding to singlets (main region, left), and doublets (right). In this figure, different graphs demonstrate the aggregation status of PEMC/PPD10/NA after coating with double diluted concentrations of biotin-IgG. On each graph, the singlets account for at least 80% of the total number of PEMC complex.

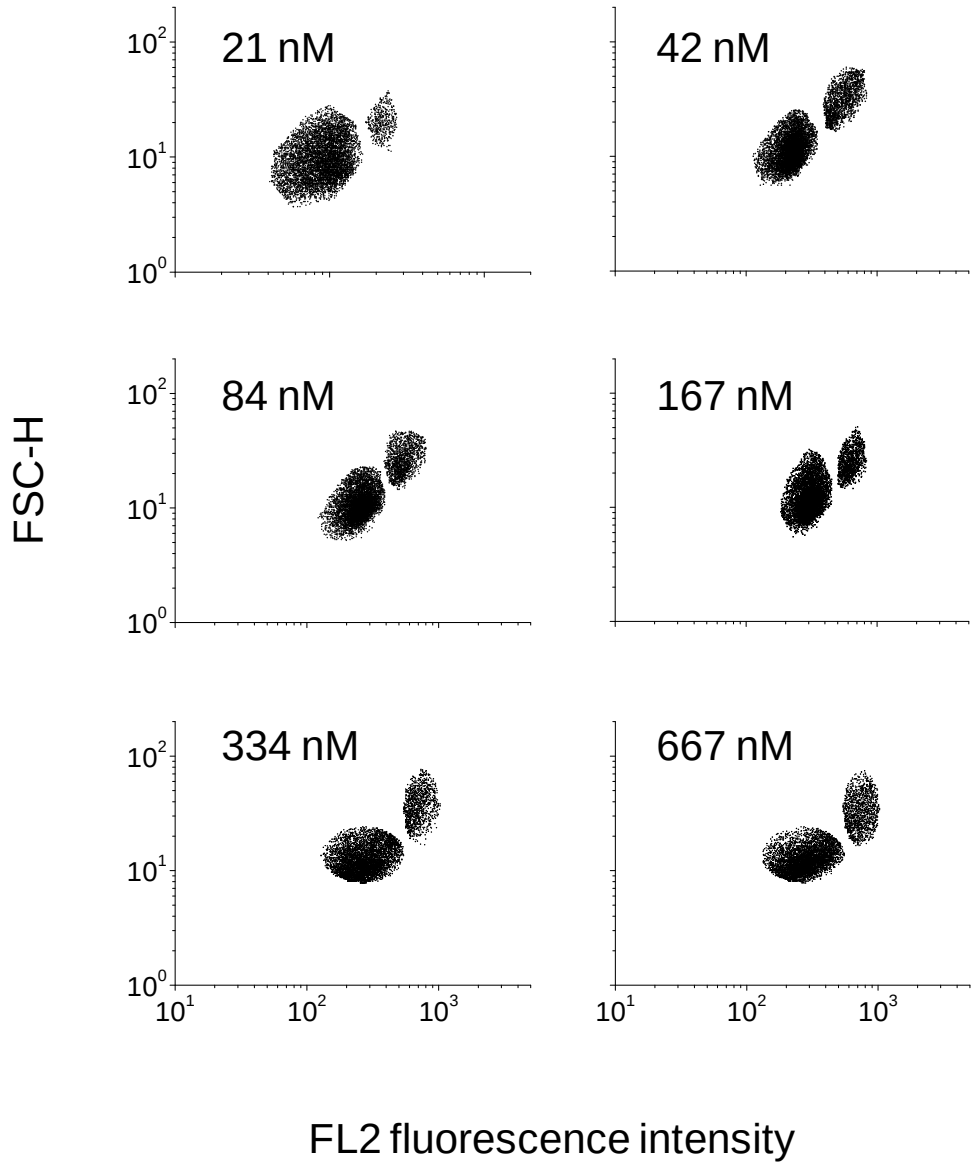

Figure 5.1 Flow cytometry dot plots of PEMC complex (PEMC/PPD10/NA/Biotin-Ab) after incubation with Cy3 labeled secondary antibody showing the forward scattering signal (FSC-H) versus the fluorescence intensity of the Cy3 labeled secondary antibody (FL2). The PEMC were first coated with $(PSS/PAH)_5$, followed by PPD10, NeutrAvidin and biotin-IgG. Different panels display the dot plot under different biotin-IgG concentration in molar unit (nM: nano molar, 10^{-9} M).

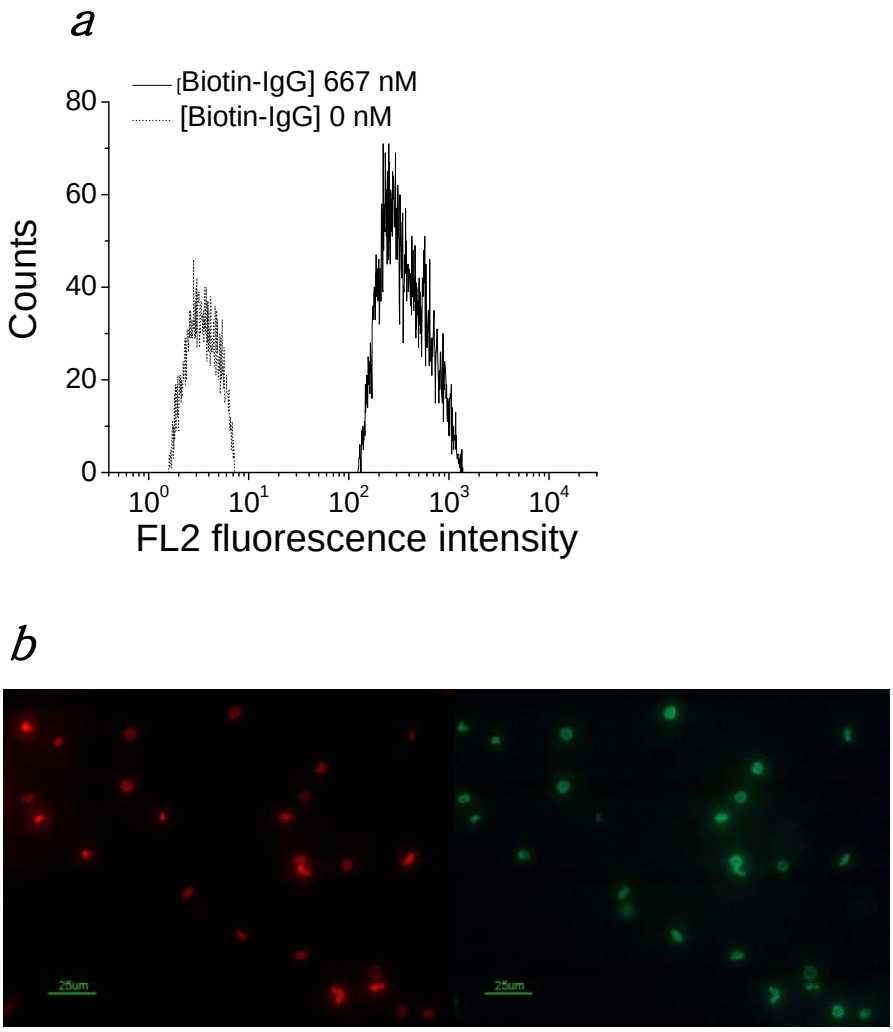

Figure 5.2 Figure (a) displays the histogram peak of 667 nM biotin-IgG coated PEMC, which is shifted to the right of that without biotin-IgG coating. Figure (b) demonstrates fluorescent image of PEMC complex after incubation with Cy3 labeled NeutrAvidin (red, left) and FITC labeled secondary antibody (green, right). The PEMC were first coated with $(PSS/PAH)_5$, followed by PPD10, NeutrAvidin and biotin-IgG. The fluorescent images confirm the simultaneous coating NeutrAvidin and biotin-IgG on the PEMC.

Figure 5.2a presents the FL2 intensity histograms extracted from the single capsule regions in Figure 5.1. This figure displays the comparison of fluorescence histogram peak between PEMC/PPD10/NA coated with 100μg/ml biotin-IgG and the control sample without biotin-IgG. A significant increase of fluorescence intensity was observed with biotin-IgG coated on PEMC/PPD10/NA. The fluorescent image (Figure 5.2b) confirms the biotin-IgG coating on the surface of PEMC/PPD10/NA.

5.2.2 Estimation of biotin-antibody binding sites on the surface of NA-PEMC

In our previous study, density of attached DSPE-PEG-biotin on PEMC was determined by HABA assay, which is commonly used for the quantitative measurement of biotin concentrations [198]. For PEMC modified with 10% biotin-PEG-lipid (PPD10), the measured biotin-PEG-lipid density is 4.2×10^7 molecules per PEMC.

Using the above known density and the number of PEMC per sample (4.7×10^4 per ml), the molar concentration of the biotin-PEG-lipid per sample was calculated to be 3.26 nM. The NA concentration (4.2 μM) added is in excess and is assumed completely cover the biotin-PEG-lipid using one side of the NA tetrameric structure. Thus the bound NA concentration was assumed to be 1.63 nM. The added biotin-IgG concentrations for subsequent coating were double diluted, starting from 667 nM to 21 nM. The concentration of biotin-IgG added should be in excess to PEMC/PPDX/NA throughout the six titration concentrations. Thus it is assumed that the initial

concentration and the final equilibrium concentration of biotin-IgG was nearly the same.

5.2.3 Langmuir fitting of binding curves

Mean fluorescence intensities (MFI) of PEMC complex (PEMC/PPD10/NA/Biotin-Ab) were measured as a function of Biotin-Ab molar concentration (Figure 5.3a-*c*). Each graph presents the binding of biotin-IgG to PEMC/PPD in the absence and presence of NeutrAvidin. In each graph, the binding curves were fit to Langmuir isotherm (Equation 5.1) for estimation of MFI_{max} and K_{app}.

$$MFI = \frac{MFI_{\max}[Biotin-antibody]}{K_{app}+[Biotin-antibody]} \quad 5.1$$

For PEMC modified with PPD0, Figure 5.3*a* demonstrates similar MFI_{max} and *MFI* increasing trend in the presence of NA as that without NA. Comparing fitting curves of all four figures, the values of MFI_{max} increase after adding the biotin-PEG-lipid on PEMC. For PEMC modified with PPD10 (Figure 5.3b) and PPD20 (Figure 5.3c), MFI_{max} significantly reduced for those PEMC complex without NA binding. For all three curves with NA, the MFI increasing rate significantly decreased when initial biotin-IgG concentration was higher than 25 μg/ml.

a

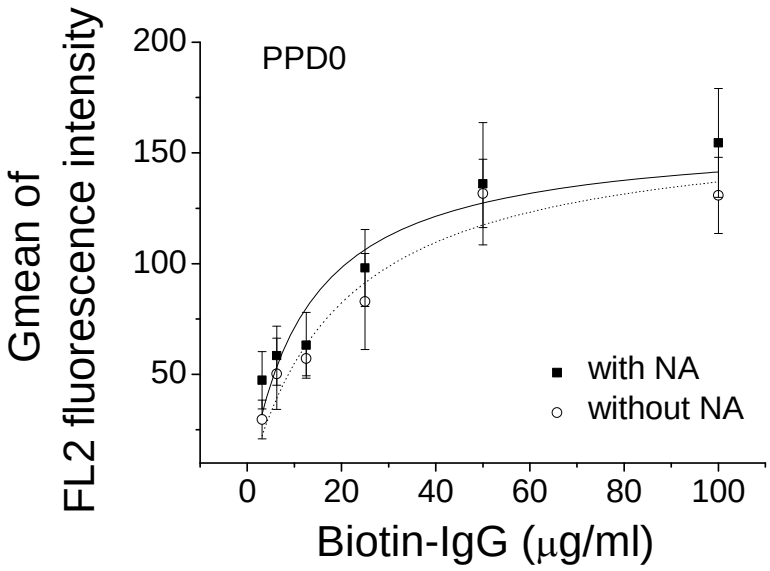
PPD0
Gmean of
FL2 fluorescence intensity
200
150
100
50
0
20
40
60
80
100
Biotin-IgG (μg/ml)
with NA
without NA

b

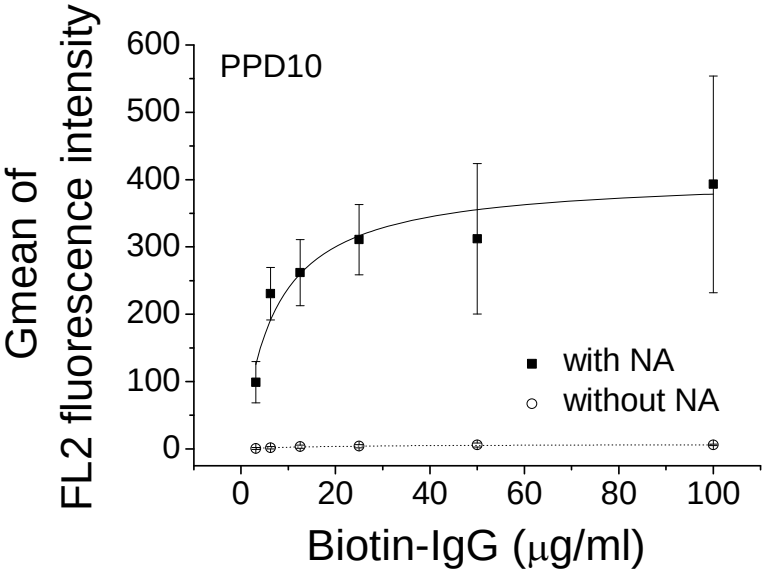
PPD10
Gmean of
FL2 fluorescence intensity
600
500
400
300
200
100
0
0
20
40
60
80
100
Biotin-IgG (μg/ml)
with NA
without NA

c

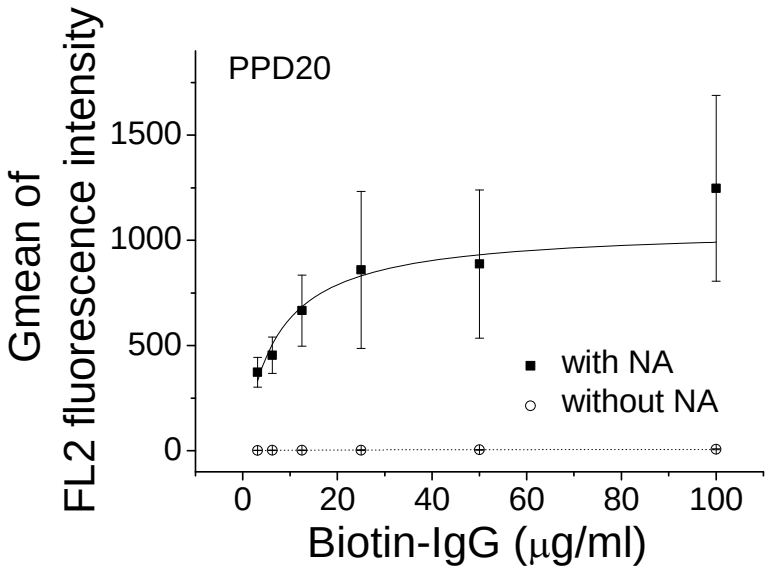

Figure 5.3 Biotin-Ab (Biotin-Rabbit IgG) binding on biofunctional PEMC. The PEMC were pre-coated with polyeletrolyte multilayers (PSS/PAH)5 and various densities of biotin-PEG-lipid (Figure 3a, without biotin-PEG-lipid, PPD0; Figure 3b PPD10; Figure3c, PPD20). The modified PEMC were incubated with NeutrAvidin and subsequently biotin-labeled antibody. Finally Cy3-secondary antibody was coated to measure the Gmean intensity (MFI) associated with each PEMC population by flow cytometry. Each panel displays the binding of biotin-IgG with NA and without NA (with NA, closed squares; without NA, closed circles). Individual data sets were analyzed by Origin nonlinear curve fit using Langmuir equation (with NA, solid curve; without NA, dash curve).

5.2.4 Estimation of MFI_{max} and K_{app}

Table 5.1 presents the estimated values for the maximal mean fluorescent intensity (MFI_{max}) and the apparent molar dissociation constant (K_{app}) of modified PEMC complex (PEMC/PPDX/NA/Biotin-Ab) and control capsules complex without adding DSPE-PEG-biotin (PEMC/PPD0/NA/Biotin-Ab, PPD0). Comparing the values of MFI_{max} of these three PEMC complex (PPD0, PPD10 and PPD20), an increasing trend of the values was found with the percentage of added biotin-PEG-lipid concentration. Also shown in Table 5.1 are the results of control samples without NA incubation (PEMC/PPDX/Biotin-Ab). MFI_{max} of PEMC complex without biotin-PEG-lipid (PPD0) remain the same with NA and without NA. PEMC modified PPD10 and PPD20 both display a huge decrease of MFI_{max} without incubation with NA, resulting in values close to noise signals.

Table 5.1: Maximal mean fluorescent intensity (MFI_{max}) and apparent dissociation constant K_{app} (in μg/ml and M) for PEMC complex. (continued)

		MFI_{max}	K_{app} (μg/ml)	K_{app} (M)
With NA	PPD0	158.9±24.66	12.36±4.73	$(8.2\pm3.2)\times10^{-8}$
	PPD10	404.89±55.16	6.98±2.33	$(4.7\pm1.6)\times10^{-8}$
	PPD20	1058.83±148.23	6.85±1.93	$(4.6\pm1.3)\times10^{-8}$

Table 5.2: Maximal mean fluorescent intensity (MFI_{max}) and apparent dissociation constant K_{app} (in μg/ml and M) for PEMC complex. (continued)

Without NA	PPD0	164.14±20.42	19.9±5.55	$(1.3\pm0.3)\times10^{-7}$
	PPD10	7.22±0.46	19.64±4.43	$(1.3\pm0.2)\times10^{-7}$
	PPD20	6.90±2.15	22.83±15.35	$(1.5\pm1)\times10^{-7}$

The addition of 10% DSPE-PEG-biotin to the POPS and POPC mixture reduces K_{app} of the modified capsules complex (PEMC/PPD10/NA/Biotin-Ab, PPD10), leading to a K_{app} of 6.98 ± 2.33 μg/ml. The results of PPD10 and PPD20 modified PEMC complex display similar values of K_{app} and are less than the control sample PEMC complex without biotin-PEG-lipid modification (PPD0, 12.36 ± 4.73 μg/ml). PEMC modified PPD10 and PPD20 both display an increased value of K_{app} comparing incubation without NA to with NA. In contrast, incubation without NA of PEMC without biotin-PEG-lipid (PPD0) display slightly increased value of K_{app} comparing to incubation with NA.

5.3 Discussion

This work verifies that biotin-antibody could bind to modified polyelectrolyte microcapsules (PEMC) with NeutrAvidin (NA) as the outmost layer. Following previous protocol [198], we fabricated functional hollow PEMC based on surface coating with POPS/POPC and DSPE-PEG-biotin (PPD). The PPD modified PEMC

was subsequently coated with NA (to form PEMC/PPDX/NA, Figure 5.4a). NeutrAvidin was immobilized with one side attached to the DSPE-PEG-biotin on PEMC and the other side for subsequent binding of biotin-antibodies (Figure 5.4b). This work confirms the binding of biotin-antibodies to PEMC/PPDX/NA (Figure 5.4c) using Cy3 labeled secondary antibody (Figure 5.4d) for fluorescence detection by flow cytometry.

Flow cytometry dot plots characterization (Figure 5.1) demonstrates that the aggregation after PEMC/PPDX/NA incubation with biotin-antibodies (biotin-IgG) was not significant, because all the six singlets regions from the dot plots account for at least 80% of the total PEMC complex counts. The binding of biotin-antibody on PEMC/PPDX/NA was confirmed by flow cytometry intensity histogram peak shifting to right, comparing with 667 nM biotin-antibody incubation and without biotin-antibody incubation (Figure 5.2a). The coating was confirmed by fluorescent images (Figure 5.2b).

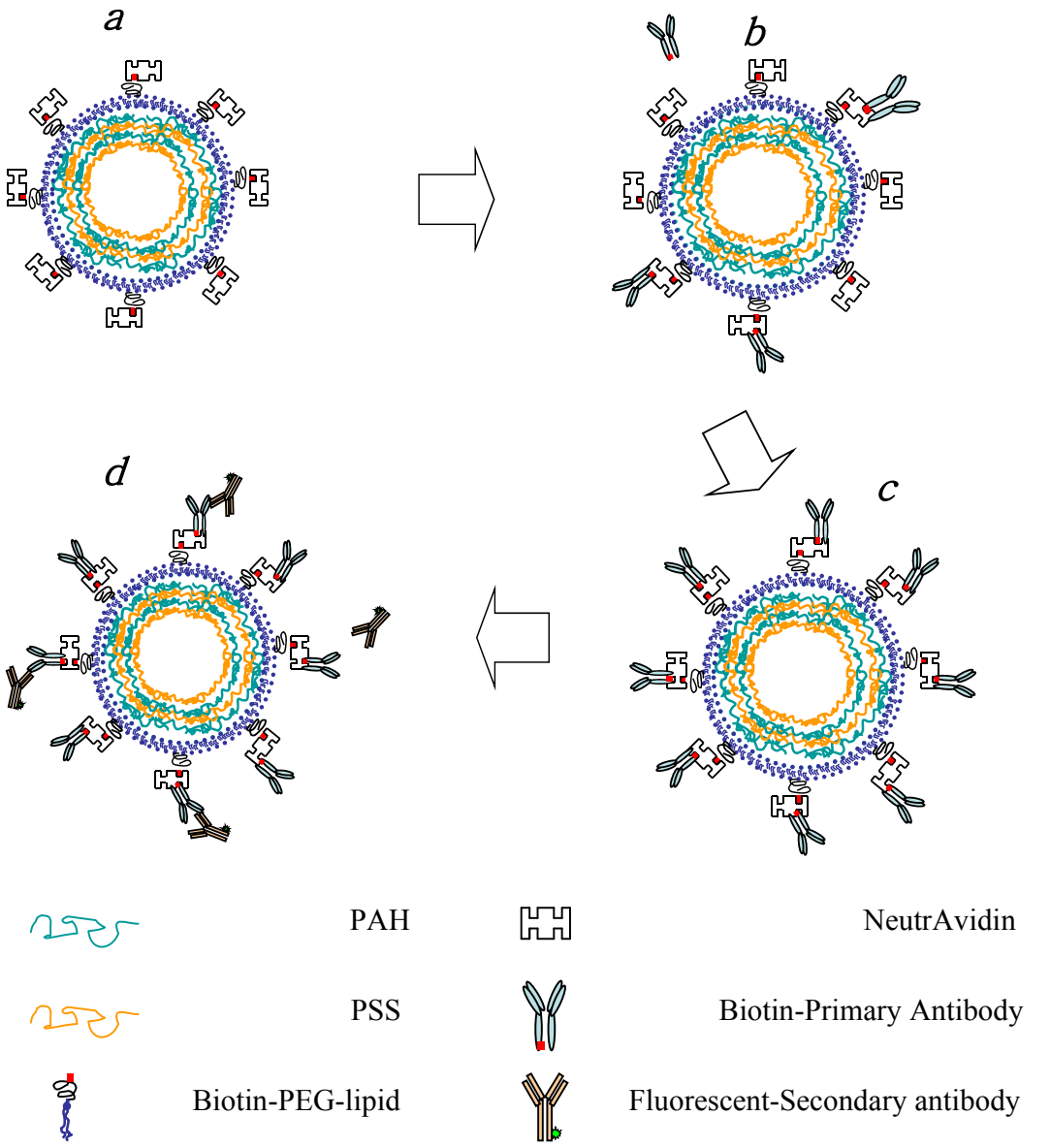

Figure 5.4 Simplified scheme of NA-PPD-PEMC (a) coated with biotin-IgG (b) to form PEMC and biotin-IgG complex (c). Cy3 secondary antibody was subsequently coated to form Cy3-labbeled PEMC complex (d) for fluorescence detection using flow cytometry

The specific binding of biotin-IgG on modified PEMC was demonstrated by comparing the estimated value of MFI_{max} between PEMC complex (PEMC/PPDX/NA/Biotin-Ab) modified with PPD and without. The value of MFI_{max} of PPD20 modified PEMC increased sevenfold as compared to PEMC complex modified with adding 10% biotin-lipid-PEG (PPD10), and threefold as compared to that without biotin-lipid-PEG (PPD0). This binding capacity difference is as expected because more PPD should induce more NeutrAvidin attachment and thus more subsequently binding of biotin-IgG. Results from the control samples without NA incubation (PEMC/PPDX/Biotin-Ab) reinforced the effect of biotin-PEG-lipid addition. With addition of 10% or 20% biotin-lipid-PEG (PPD10 or PPD20), the value of MFI_{max} dropped 23 times to noise signal level. These results also prove the presence of NA as the linker between biotin-lipid-PEG and biotin-IgG. Without NA, the biotin-IgG could not be bound to the PPD modified PEMC surface.

The apparent dissociation constant is a quantitative value, indicating how fast the interacted receptor-ligand complex would dissociate. High dissociation constant indicates low affinity of the interacted complex. In this work, PEMC complex without modification of biotin-PEG-lipid (PEMC/PPD0/NA) has the highest value of K_{app} and thus the lowest affinity to biotin-IgG. PPD10 and PPD20 modified PEMC complex display the same affinity to biotin-IgG. These values of K_{app} after addition of biotin-PEG-lipid decrease 1.8 times, compared to the control sample PPD0. This means that the PPD modified PEMC complexes are more stable than the ones without modification. It is worthy to mention that the repeatability is not high due to many rinses between layers coatings.

The apparent dissociation constant K_{app} was estimated in the unit of micrograms per milliliter (Table 5.1) and can be transformed as unit of molarity using the molecular weight of IgG (150 kD). The affinity values fall in the range of 10^{-8} M. The binding occurs when NA binds to PEMC surface, introducing differences in apparent affinity compared with NA-biotin interaction in solution (10^{-15} M). This may be due to restricted diffusion (thereby decreasing the probability of association), orientation and steric effects, and denaturation of the immobilized reactant [199].

This work continued from our previous study, which employed the LbL technique to fabricate biofunctional PEMC modified with DSPE-PEG-biotin. In this work, the modified PEMC was further coated with NeutrAvidin (to form PEMC/PPDX/NA complex) and incubated with biotin-IgG to study their affinity. Microsphere-based immunoassay was utilized to detect biotin-IgG by flow cytometry technique. It was shown that via the biotin-PEG-lipid modification, the biofunctional PEMC complex has a high specificity and affinity to biotin-IgG. Fluorescence microscopy confirmed the complete surface coverage of adsorbed Cy3-biotin-IgG layers, as well as the mono-dispersity of the microcapsules.

Chapter 6 Targeting of DSPE-PEG-Biotin modified polyelectrolyte microcapsules to 3T3.CD4 fibroblast

6.1 Introduction

Targeting of specific antibodies modified PEMC to the corresponding antigen expressed cells was investigated in this chapter. Fibroblast cell line 3T3.CD4.CXCR4 was used as a model cell line. After transfection, this cell line expresses surface antigen CCR5 and thus the positive cell line is 3T3.CD4.CCR5. 3T3.CD4.CXCR4 was served as negative control to test the unspecific binding of the modified PEMC. In our work, the antibody coated PEMC were incubated with cells on planar surfaces 37^{o}C to mimic physiological conditions. Specifically, we assessed in detail the modified PEMC interaction with cells in a time dependent way to study the efficiency of the interaction.

6.2 Results

6.2.1 Surface Morphology of BSA coated on biofunctional polyelectrolyte multilayers

The effect of serum proteins on the surface property was studied to elucidate PEMC-serum interactions occur in circulation. This effect was investigated on 2D surface with the same LbL coatings as on the surface of PEMC. The surface morphology of the BSA coated biofunctional polyelectrolyte multilayers was

characterized by AFM. Initially, $[PAH/PSS]_4$-PAH PEM and PPD10/PPD20 lipid layers were coated on planar silicon substrates. The BSA blocking buffer was subsequently incubated on the modified PEM (Figure 6.1). The control sample was $[PAH/PSS]_4$-PAH PEM films. Fig. a demonstrates the surface morphology of control sample without any biotin-PEG-lipid. It has the highest root mean square (RMS) roughness of 4.74 nm. With the modification of PPD10, the surface coated with BSA becomes smoother and the RMS roughness decreases to 0.88 nm (Fig. b). In addition, Fig. b also indicates a uniform protein coating with no significant clustering. BSA coating on the PPD20 modified surface exhibited large clustering with an RMS of 3.54 nm (Fig. c).

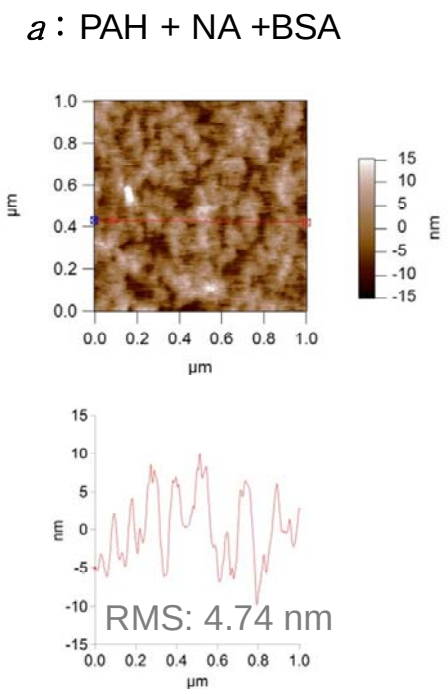

b : PPD10 + NA +BSA

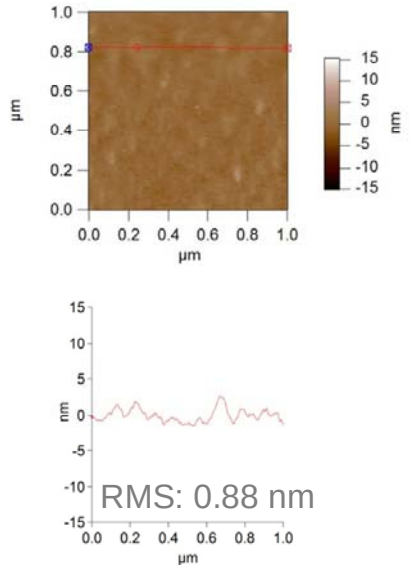

c : PPD20 + NA +BSA

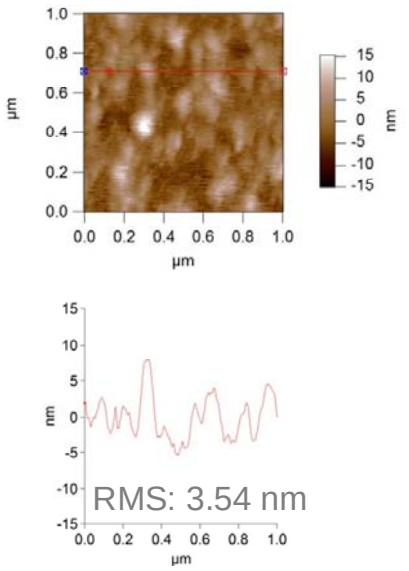

Figure 6.1 AFM images of $(PAH/PSS)_4/PAH$ (a, RMS = 4.74 nm); $(PAH/PSS)_4/PAH$ /PPD10/primary antibody in BSA (b, RMS = 0.88 nm); $(PAH/PSS)_4/PAH$/PPD10/primary antibody in BSA/ secondary antibody in BSA (c, RMS = 3.54nm).

6.2.2 Biotin-antiCCR5 IgG binding to biofunctional PEMC

On the above sections, the biofunctional PEMC was coated with biotin-Rabbit IgG for investigation the binding ability of the modified PEMC. In this experiment, the biotin-antibody utilized is biotin-antiCCR5 IgG for targeting the modified PEMC to CCR5 expressing cells. PEMC were prepared as described above in Material and Method. Briefly, MF particles were coated with 10 layers of polyelectrolyte as $(PSS/PAH)_5$. The MF was then dissolved in HCl to form the hollow PEMC before being modified with POPS/POPC/Biotin-PEG-lipid. NeutrAvidin was coated on PPD modified PEMC for further coating with biotin-antiCCR5 IgG. Finally, FITC labeled secondary antibody was coated for fluorescence detection using flow cytometer.

The PEMC exhibited the same aggregation status before and after coating biotin-antiCCR5 IgG, shown in flow cytometry dot plots (Figure 6.2). Each of the two regions is localized in the same place in both graphs. R1, which represents single PEMC, is between the forward scattering intensities (20-60 a.u.) and the sideward scattering intensities (70-170 a.u.). The doublets R2 is between the forward scattering intensities (20-60 a.u.) and the sideward scattering intensities (100-360 a.u.). R1 regions account for most of the PEMC of the total particle population (R1 in Fig. a, 73%; R1 in Fig. b, 81%). The fluorescence intensity histograms from both R1 regions are shown in Fig. c. FL1 fluorescence intensity geometric mean (Gmean) value of the control sample was 1.64±85.95 a.u., while that of the biotin-antiCCR5 IgG adsorbed PEMC is shifted to higher intensities with Gmean value 836±17.35 a.u..

a

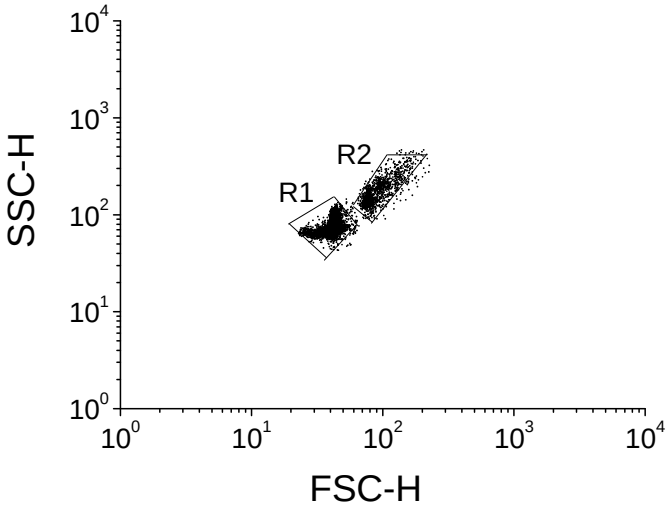
SSC-H
FSC-H
R1
R2
10^0
10^1
10^2
10^3
10^4

b

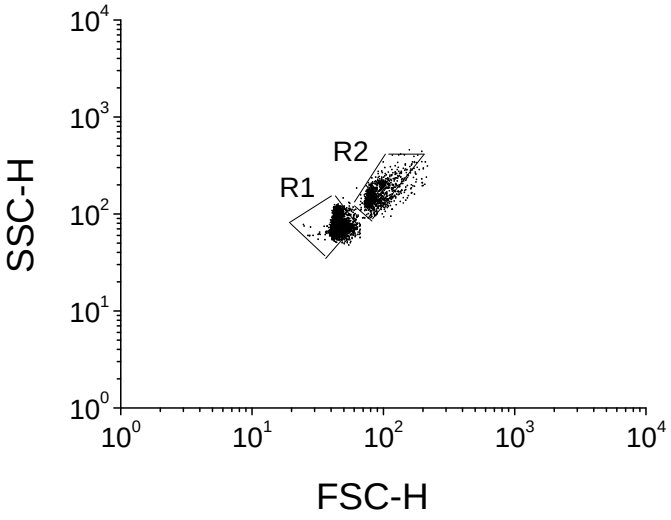
SSC-H
FSC-H
R1
R2
10^0
10^1
10^2
10^3
10^4

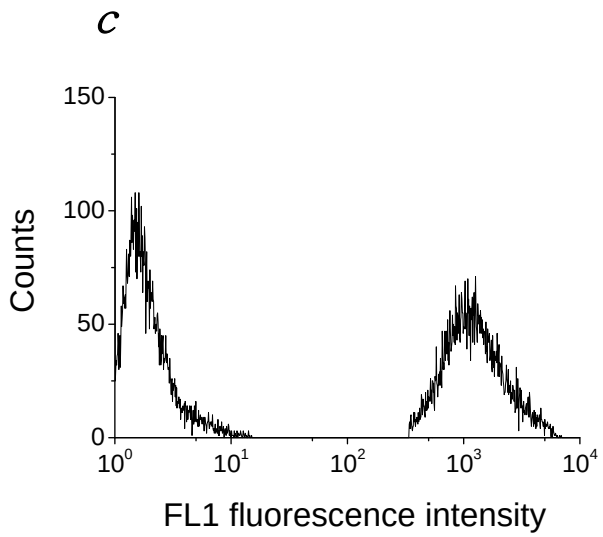

Figure 6.2 Proof of biotin-antiCCR5 IgG binding to PEMC. The PEMC were pre-coated with polyelectrolyte multilayers $(PSS/PAH)_5$ and POPS/POPC/10%biotin-PEG-lipid (PPD10). The modified PEMC were incubated with NeutrAvidin and subsequently biotin-antiCCR5 IgG. The PEMC with NeutrAvidin as the outmost layer served as the control sample. Finally FITC-secondary antibody was coated to measure the florescence associated with each PEMC population by flow cytometry. The flow cytometry images exhibit dot plots of forward scattering (FSC-H) v.s. side scattering (SSC-H): (a) control PEMC without biotin-antiCCR5 IgG, (b) binding of biotin-antiCCR5 IgG to NeutrAvidin coated PEMC. R1 and R2 represent the single and aggregated capsules respectively. The fluorescence intensities (c) of region 1 (R1) from (a) and (b) are compared, and the positive sample histogram peak is shifted to the right.

6.2.3 Interaction of biofunctional PEMC with 3T3 fibroblast cells

In the experiments of cell interaction with the modified PEMC, fibroblast cell line without CCR5 antigen (3T3.CD4.CXCR4) served as a negative control to test the unspecific binding of the PEMC. In detail, the biotin-antiCCR5 IgG modified PEMC was incubated with control cell lines and positive cell lines (3T3.CD4.CCR5) at the

same time. This incubation was performed on planar surfaces of a 24-well microplate at 37^{o}C. The cell-PEMC interaction was compared for different time intervals. The cell lines are tested with anti-CCR5 IgG first to prove the antigen expression on the cell surface (Figure 6.3).

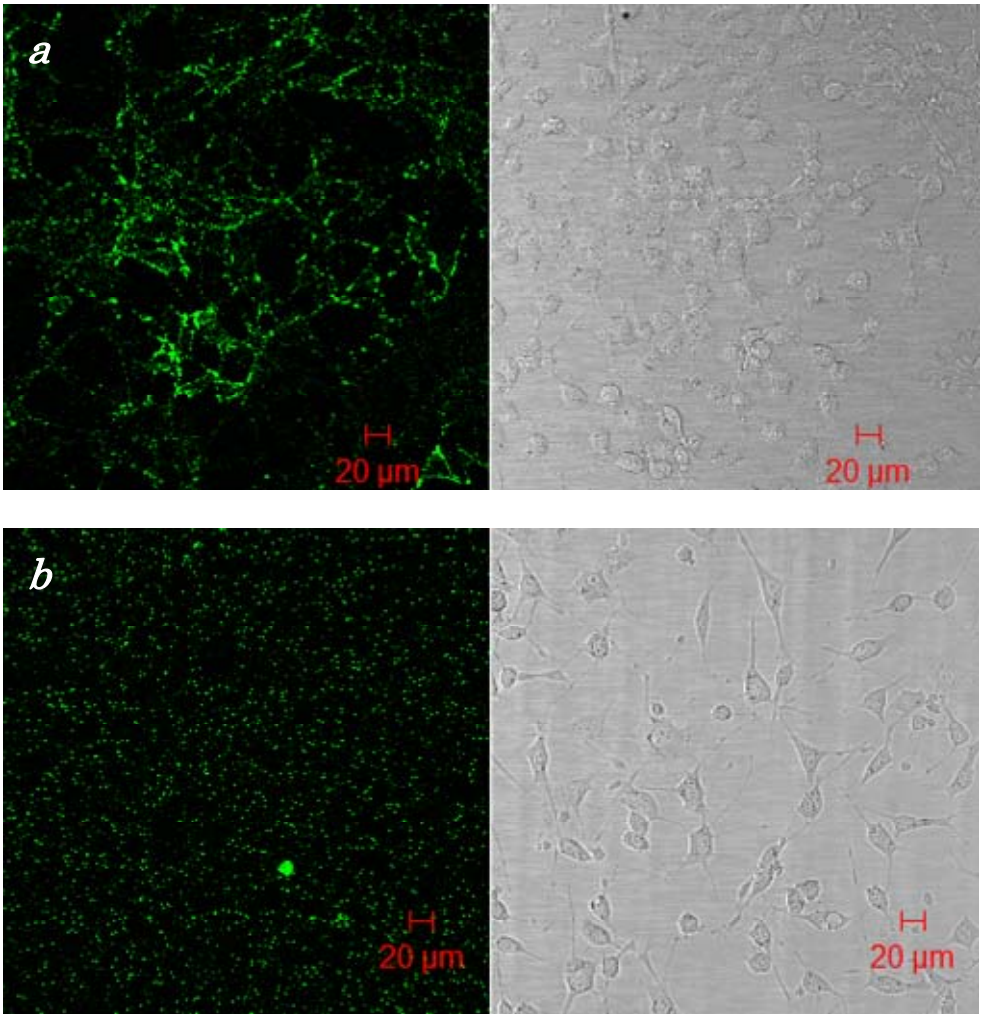

Figure 6.3 Proof of CCR5 antigen expression on 3T3.CD4 cell lines. CLSM images of the CCR5 expressed cell lines 3T3.CD4 CCR5 (a) and control cell lines 3T3.CD4 CXCR4 (b). Left : fluorescence image; right: bright field image. Both positive and control cell lines were coated with anti-CCR5 IgG and FITC-secondary antibody.

PEMC was fabricated by coating MF particles with 10 layers polyelectrolytes as $(PSS/PAH)_5$. To label the PEMC for fluorescence detection by flow cytometry, FITC-PAH replaced the 2nd and 4th layer of PAH. After that, the PEMC was further modified with POPS/POPC/10% Biotin-PEG-lipid. Subsequently, NeutrAvidin and biotin-antiCCR5 IgG (both in 1% BSA) were coated to form the biofunctional PEMC. The biofunctional PEMC was incubated with both CCR5 expressed cell lines and control cell lines. Figure 6.4a demonstrates the cell-PEMC complex size distribution after incubation and washing. There are three dot plot regions, with R1 and R2 in the same locations as that of Figure 6.2a and b, representing the PEMC location. Region R3 represents the cell-PEMC complex, which is between the forward scattering intensities (260-1000 a.u.) and the sideward scattering intensities (700-1450 a.u.). As reference, Figure 6.4b provides the dot plot for cells without any PEMC, with R3 in the same location as that from Figure 6.4a.

Figure 6.4c demonstrates the fluorescence intensity of the same R3 region from Fig. a. Figure 6.4c proves the R3 region is the cell-PEMC complex, as only cells attached with FITC-PEMC would exhibit fluorescence. For control experiment, Figure 6.4d represents the cells without fluorescence labeling (the same cells from Fig. b). Hence the R3 region of cell-PEMC complex is the interested region in these experiments. There are three experiments of different time interval incubation of 1hr, 2hr and 4hr. For each time interval, the incubations were performed on two types of cells: control cells (3T3.CD4.CXCR4 cells) and antigen expressing cells (3T3.CD4.CCR5 cells). Thus there are totally six data files with the same dot plot pattern. Figure 6.4c

demonstrates the FITC-PEMC with 3T3.CD4.CCR5 cell lines for 4 hr incubation, as one dot plot example for explaining the size distribution of cell-PEMC complex.

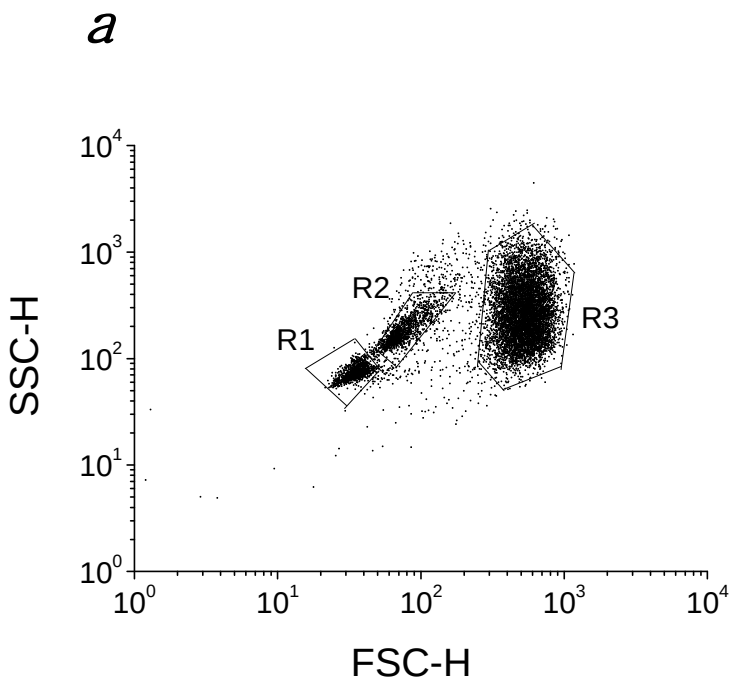

b

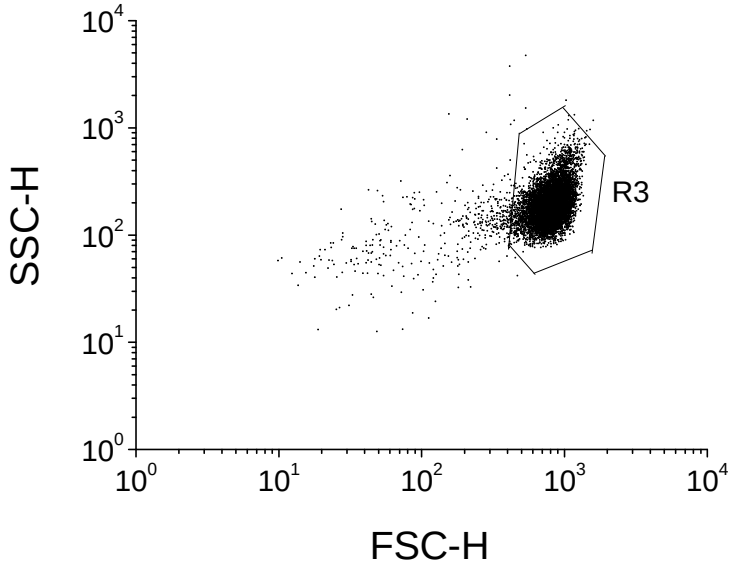
SSC-H
FSC-H
R3
10^0
10^1
10^2
10^3
10^4

c

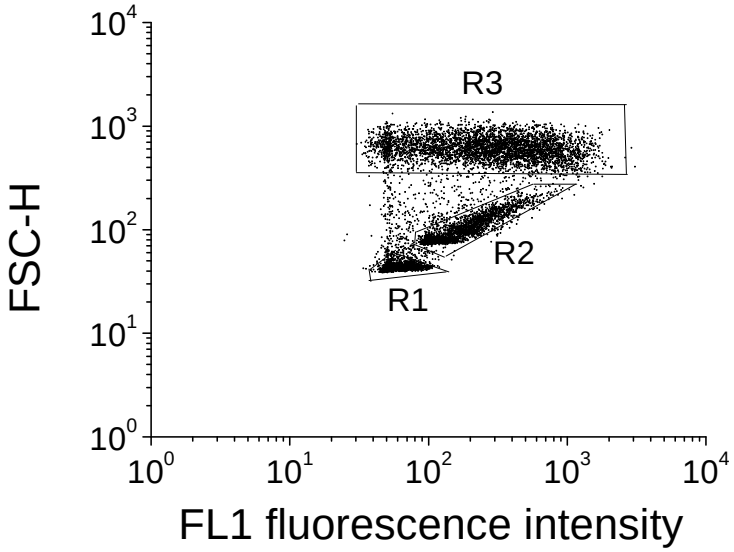
FSC-H
FL1 fluorescence intensity
R3
R2
R1
10^0
10^1
10^2
10^3
10^4

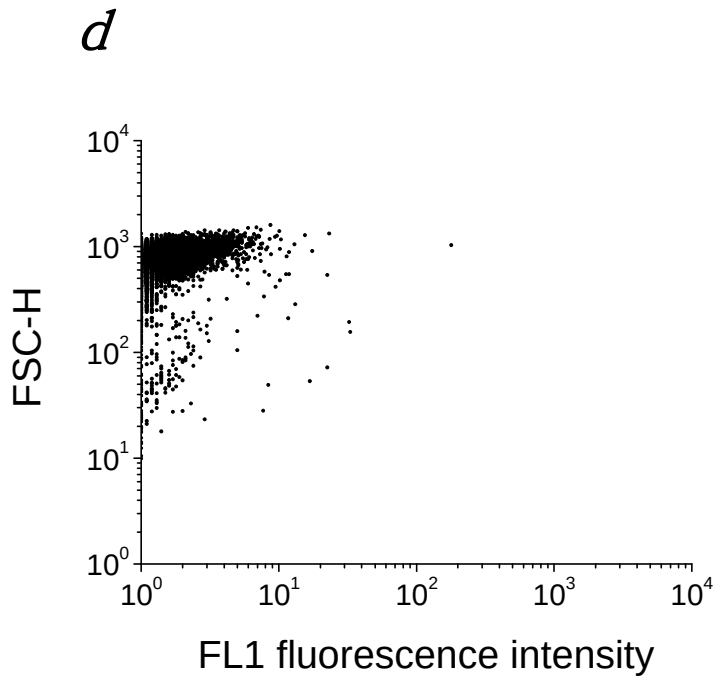

Figure 6.4 Attachment of FITC labeled biofunctional PEMC to the 3T3.CD4 cell lines. Figure (a) demonstrates size distribution of PEMC (R1 and R2 region) and cell-PEMC complex (R3 region). Figure (b): proof of R3 region as the cell lines. Figure (c): proof of attachment of FITC labeled biofunctional PEMC to the cell lines, demonstrating the FITC-PEMC with 3T3.CD4.CCR5 cell lines for 4 hr incubation. In Figure (c), R1, R2 and R3 represent the same cells population as in Figure (a). Figure (d) is the control cell lines without fluorescence for comparison to cells with FITC-PEMC in Figure (c).

The cell-PEMC interaction of different time interval was illustrated in Figure 6.5. The fluorescence intensity histograms are gated from each of the R3 regions. The gray curves represent FITC-PEMC interaction with control cell lines without CCR5 antigen (3T3.CD4.CXCR4). The black curves represent the FITC-PEMC interaction with

positive cell lines with CCR5 antigen (3T3.CD4.CCR5). The Gmean value of each histogram is listed in Table 6.1.

Table 6.1 Gmean value of fluorescence histogram of cell-PEMC complex after different incubation time

Time		Gmean of Peak 1 (M1)	Gmean of Peak 2 (M2)
1 hr	Control cells	38±27	-
	Positive cells	153±19	-
2 hr	Control cells	92±20	-
	Positive cells	153±18	-
4 hr	Region Percentage	22%	78%
	Control	48±4	207±13
	Region Percentage	11%	89%
	Positive cells	50±4	315±14

In this experiment, Gmean of fluorescence represents the amount of biotin anti-CCR5 IgG modified PEMC attached on the cell lines. At 1 hr incubation (Figure a), the peak of gray curve (Gmean value 38) is on the left to that of the black curve (Gmean value 152.65). For 2 hr incubation (Figure b), the peak of gray curve (Gmean value 92) shifted closer to that of the black curve (Gmean value 152.65). At 4 hr incubation, we observed two peaks in each intensity histograms (Figure c, gray and d, black). There are two parts of each curve separated by markers (M1 and M2). M1 represents the single particles attached per cell (M1 = 22%, Gmean value 48, Fig. c; M1= 11%,

Gmean value 50, Fig. d), while M2 represents a few particles per cell (M2 = 78%, Gmean value 207, Fig. c; M2= 89%, Gmean value 315, Fig. d).

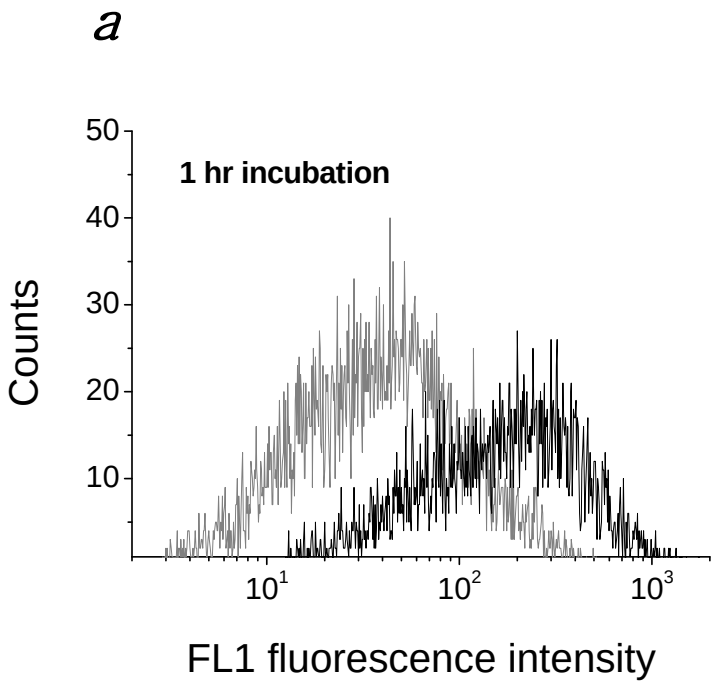

b

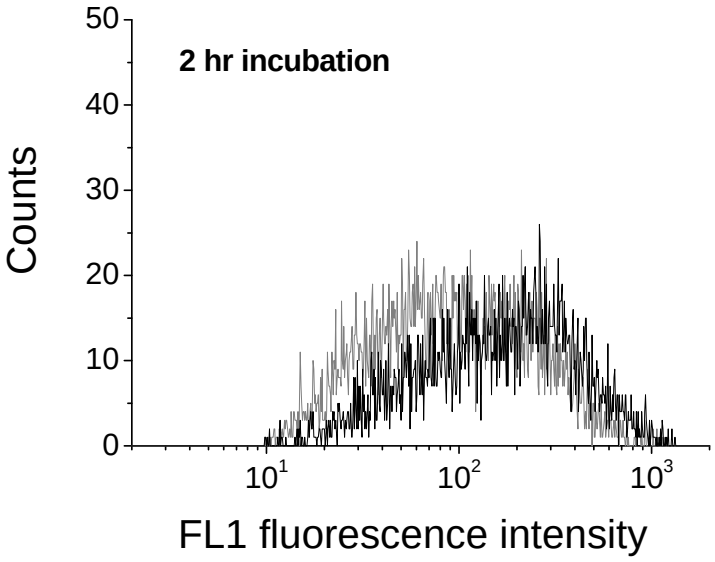
2 hr incubation
Counts
FL1 fluorescence intensity
0
10
20
30
40
50
10^1
10^2
10^3

c

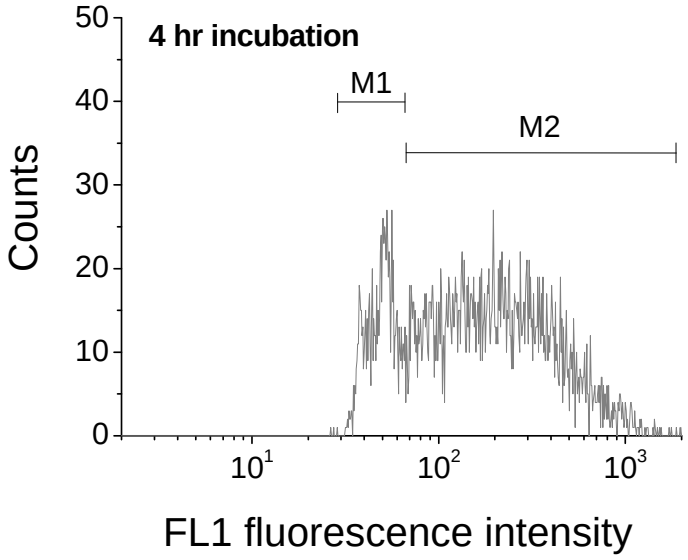
4 hr incubation
M1
M2
Counts
FL1 fluorescence intensity
0
10
20
30
40
50
10^1
10^2
10^3

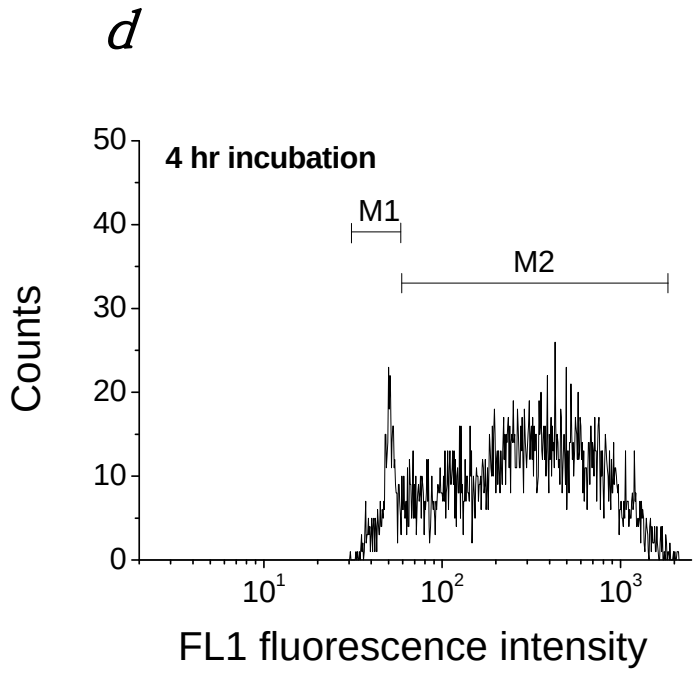

Figure 6.5 Fluorescence intensity histogram of PEMC with cells on planer surface at 37^{o}C. Graphs (a-d) represent fluorescence intensity of R3 from the respective dot plots as described in Figure 6.4. Incubation of biotin-antibody coated PEMC interaction with control cells (gray curve) and antigen expressing cells (black curve) for different time interval (a for 1hr, b for 2hr, c and d both for 4hr). In (c) and (d), each intensity histogram has 2 parts, separated by marker M1 and M2. M1 represents the cells attached with single capsules. M2 represents the cells attached with single capsules and a few capsules. The number of biofunctional PEMC bound to control cells increased with increasing incubation time interval.

Fluorescent images demonstrate the interaction of modified PEMC with antigen expressed cells. Incubation with biotin labeled isotype mouse IgG coated PEMC (control) showed low PEMC binding with cells (Fig. 6.6 a1 - a3). Interaction of non-modified PEMC (PPD0) with cells demonstrated higher PEMC binding than control (Fig. 6.6 b1 - b3), but lower binding than PPD 10 modified PEMC (Fig. 6.6 c1 - c3).

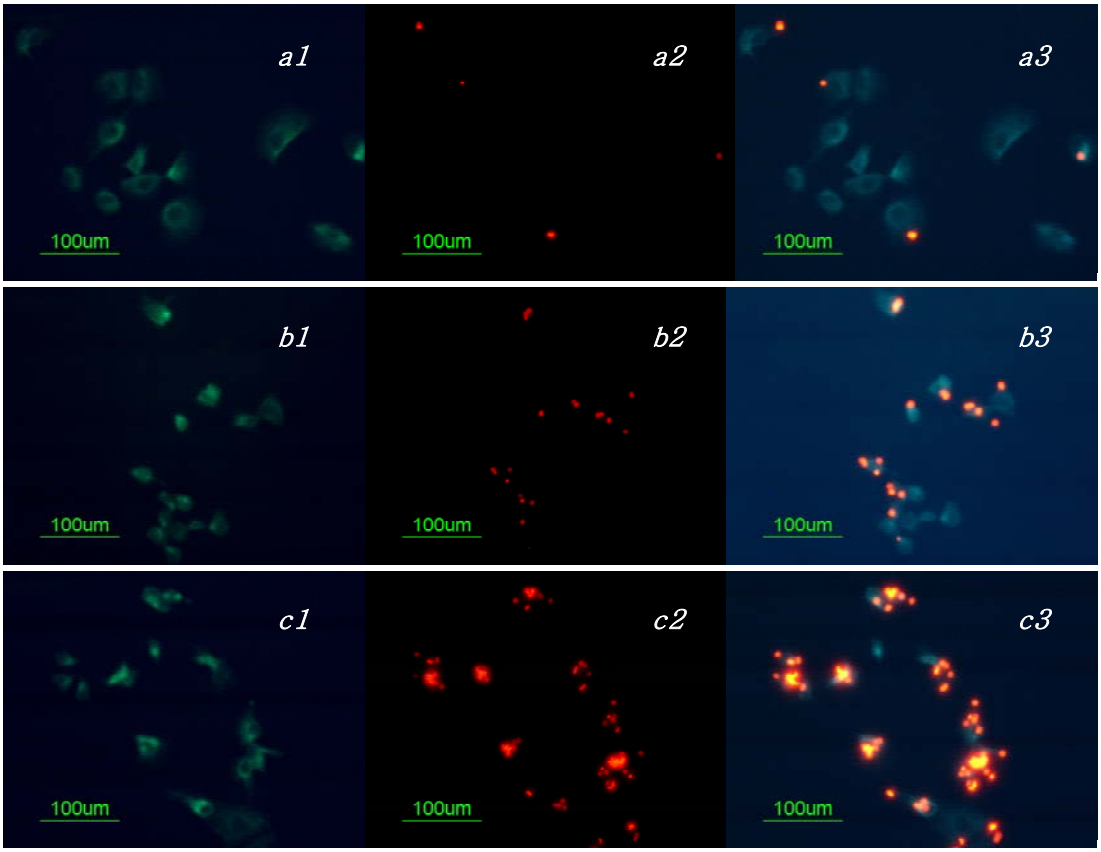

Figure 6.6 Fluorescent microscopy investigation of the interaction of PEMC with antigen expressed cell lines. The cell lines were labeled with FITC anti-cytokeratin (a1-c1, green). The PEMC were pre-coated with polyelectrolyte multilayers (PSS/PAH)5 and POPS/POPC/X% biotin-PEG-lipid (PPDX). The modified PEMC were incubated with Cy3 labeled NeutrAvidin (a2-c2, red). Subsequently the modified PEMC were incubated with biotin-isotype antibody as a control (a1-a3) and biotin-antiCCR5 IgG (b1-b3, c1-c3). Figure (b1-b3) demonstrates the interaction of cells with PEMC without modification of biotin-lipid (PPD 0). Figure (c1-c3) demonstrates interaction of cells with PEMC modified with PPD 10. Figure c is the overlay image of (a) and (b).

6.3 Discussion

This confirmation change of protein adsorption on different modified surface provides information for optimization of the surfaces. BSA adsorption on $[PAH/PSS]_4$-PAH PEM exhibited highest RMS roughness. The RMS roughness reduced significantly for the BSA coating on PPD10 modified surface. The PPD10 lipid bilayer formed a cushion between PEM and BSA and smoothed the granularity of BSA outlayer. From Chapter 4, the PPD10 modified PEMC surface presented a dense brush-like surface. PEG is uncharged, hydrophilic and possesses high chain mobility. The protein resistance property of such PPD10 surface also contributes to the reduced roughness. The BSA adsorption on PPD20 surface exhibited increased RMS roughness with visible increased granularity. According to Chapter 4, the clustering is due to the high concentration of biotin-PEG-lipid. Although PPD20 modified surfaces gave better antibody binding capacity, the aggregated surfaces are not desirable. Thus PPD10 modified surface was chosen for the study of interaction with cells.

PEMC aggregation was observed after antibodies coating on NeutrAvidin ending PEMC. The degree of aggregation of the particles can be quantified from the dot plot graph (*Figure 6.2*). R1 represents the single particle population. In R2 region the particles size and granularity increase, meaning there are some aggregations after protein coating on the particles. This phenomenon can be briefly explained by surface charge. NeutrAvidin is a deglycosylated Avidin exhibiting a more neutral pI of 6.3, which results nearly zero charged in PBS (pH=7.4). Single PEMC (R1) accounts for 73% for NeutrAvidin ending PEMC. IgG displays pI of 8, which results negatively

charge in PBS. Thus after antibodies coating, the absolute value of surface charge increased, resulting in the increase of the single PEMC to 81%.

The attachment of biotin-antiCCR5 IgG on the particles was verified by detecting FITC labeled secondary antibody adsorption (Figure 6.2c). The fluorescence intensity Gmean of the biotin-antiCCR5 IgG is 500 times of the control sample. The distinct fluorescence increase demonstrates the successful attachment of biotin-antiCCR5 IgG.

Comparing SSC-H v.s. FSC-H dot plots from Figure 6.2a and Figure 6.4a, R1 and R2 from Figure 6.4a appear in the same locations as in Figure 6.2a. Thus, R1 represents single PEMC and R2 PEMC aggregations. R3 can be concluded as the cells population because the dot plot region is at the same location as that of samples with only cells (Figure 6.4b). Comparing FSC-H v.s. FL1-H from Figure 6.4c and d, R3 region from Figure 6.4c contain cells with FITC labeled biofunctional PEMC, as an increase in FL1 fluorescence intensity displayed in comparison with cells without adding particles (Figure 6.4d).

In this experiment of cell-PEMC interaction, the specific binding means the amount of biotin anti-CCR5 IgG coated particles attached on CCR5 antigen expressing cells (3T3.CD4.CCR5). The specific binding increased 2 times from incubation 1 hr to 4 hr (Gmean intensity increased from 153 to 314). The unspecific binding refers to the amount of biotin anti-CCR5 IgG coated PEMC attached on control cells without expressing CCR5 antigen (3T3.CD4.CXCR4). With increasing incubation time from 1 hr to 4 hr, the unspecific binding became 5 times stronger (Gmean intensity increased from 38 to 207). At 1 hr, the specific binding of biofunctional PEMC to CCR5

expressed cells is 4 times than that of binding to control cells. While at 4 hr, the specific binding decreased to 1.5 times. Thus, the conclusion is that specific binding decreased with increasing incubation time.

It should be noted that M1 peaks (Figure 6.5c&d) appeared after 4 hr incubation. Comparing R1 and R3 region location from Figure 6.4c, it can be concluded that M1 peaks represent cells attached with single PEMC. For incubation 1hr and 2hr, aggregated PEMC started to attach cells sooner than single PEMC, thus the peaks of M1 in Figure 6.5a&b are not obvious. Comparing M1 population of Figure 6.5c&d, the percentage of M1 decreased by half for CCR5 cells attached with single PEMC. The results indicate that single PEMC tends to attach randomly per control cell, while on CCR5 cells their attachment is more accumulated to one cell.

In summary of the experiments conducted under physiological conditions, it was found that the interaction of biotin-antiCCR5 IgG coated PEMC with 3T3 fibroblast cells followed a time dependant pattern. In this work, the specific binding to CCR5 cells is most obvious in the first hour. The particle and cell interactions are based on the antibody and antigen specific binding, which only take effect within a few hours. This observation is important to know the efficiency of the developed delivery system. The fluorescent images confirmed that biofunctional PEMC have the potential for targeting cells with high specificity, which is an important prerequisite for effective colloidal delivery systems.

Chapter 7 Conclusions and future work

7.1 Conclusions

The overall objective of this project was to develop multifunctional polyelectrolyte microcapsules (PEMC) as potential targeted drug carriers. In this work, the layer by layer (LbL) technique was employed to fabricate biofunctional PEMC and to modify its surface with DSPE-PEG-biotin. NeutrAvidin was bound specifically to the modified biofunctional PEMC and created a surface for binding targeted molecules, which was biotin-immunoglobulin G (biotin-IgG). Finally, PEMC with biotin-IgG on the outmost layer was specifically bound to antigen expressed cells in a time dependent way.

This dissertation was focus on the surface modification of hollow PEMC with biotin-PEG-lipid. Biotin-PEG-lipid, which has three functional moieties: 1) biotin, which could be utilized for binding immunoglobulin G (IgG) via the biotin-avidin interaction, 2) PEG that can be expected to reduce unspecific protein binding and undesired cellular uptake, and 3) a lipid layer to control the surface stability. This work successfully demonstrates the possibility to combine these three functions by adsorption of biotin-PEG-lipid on hollow PEMC under economical and mild conditions through LbL technique. Liposome containing DSPE-PEG-biotin (PPDX) was adsorbed on hollow PEMC by electrostatic interaction. Aggregation of the PEMC was shown to be reduced after modification with biotin-PEG-lipid.

It was shown that the modified biofunctional surface has a high specific affinity to NeutrAvidin (NA). This work established the optimized concentration of biotin-PEG-

lipid on the PEMC surface by investigation of the surface morphology. With 10% biotin-PEG-lipid (PPD10), the PEMC surface presented a dense brush-like surface, which could provide significant reduction of non-specific protein binding, as well as high specific binding to NeutrAvidin.

With NeutrAvidin on the outmost layer of PEMC, the PEMC/PPDX/NA complex was further incubated with biotin-IgG. It was proven that NA was necessary and behaved as the linker, connecting the biotin-lipid-PEG of PEMC and subsequently coated biotin-IgG. Quantification of the affinity between PEMC/PPDX/NA complex and biotin-IgG was achieved using microsphere-based immunoassay. It was shown that via the biotin-PEG-lipid modification, the biofunctional PEMC complex had a high specificity and affinity to biotin-IgG. This study therefore provided a deep understanding of such functionalized PEMC, and not only enhanced their efficiency as potential drug carriers but widened their possible applications, such as diagnostic biosensors for drug screening. A possible application of such modified PEMC could be the development of sensitive microsphere based immunoassay for the recognition of biomolecules in suspension.

Under physiological conditions, we found the interaction of biotin-antiCCR5 IgG coated PEMC with 3T3 fibroblast cells following a time dependant pattern. This is because the interaction is based on antigen-antibody binding, which usually happens at the first few hours of attachment. In this work, the specific binding to CCR5 cells is most obvious in the first hour. Hence, it could be concluded that the particle and cell interactions were based on the antibody and antigen specific binding. This observation is important to understand the efficiency of the developed delivery system.

This study therefore provided a new and useful strategy to functionalize PEMC and should not only enhancing their efficiency as potential drug carriers as well as extending their possible applications, such as diagnostic biosensors for drug screening, or as artificial cell-like structures for bio-mimetic studies.

7.2 Future work

For establishing proof of concept of surface modification, we utilized MF particles and PAH/PSS as layer constituents. The advantage of this system is that it has been extensively studied and thus an ideal model system to establish the feasibility of functionalizing these capsules with biotin-PEG-lipid. However, it should be noted that this system can only serve as a model system due to its limitation in terms of biocompatibility. In the future, especially for biomedical applications, it will still be necessary to employ alternative polyelectrolyte and templates with higher biocompatibility such as polysaccharides, proteins, or peptides [118]. Testing of such capsules in animal models would be essential for application of these capsules as drug carriers.

Therapeutic molecules, e.g. anticancer drugs, can be encapsulated in the core of LbL capsules or be incorporated on the capsules walls. The understanding of release kinetics of the therapeutic molecules *in vitro* is necessary for developments in drug delivery applications. The modification of polyelectrolyte multilayers with biotin-PEG-lipid might affect the diffusion properties of the polyelectrolyte multilayers. In addition, the change of environmental conditions, e.g. pH and ionic strength could be ways

utilized to control the drug release. Mathematical modeling and computational simulation might be helpful for providing scientific insights in drug release from PEMC.

Another research direction would be theoretical understanding of the physical property of the polyelectrolyte thin films after the surface modification. From biophysics direction, the mechanical property of PEMC, e.g. swelling trend of a large quantity of PEMC after dissolvation of the templates, could be further considered and investigated. Further study on the permeability or rate of adsorption of molecules could also be a possible way as a proof for a homogenous coating of PEMC. From biochemistry area, advanced polymers with a number of different geometries, such as brushes, combs, and linear block maybe used to create thin films of different properties. If these surface properties could be controlled and standardized, patterning of one surface with different functions might be created on the film.

LbL techniques are economical to produce versatile surface coatings in laborotary experiments. For large scale production of capsules in large scale, several parameters need to be considered according to the quantity of the final product, such as the concentrations of polyelectrolytes and templates, pH, ionic strength, centrifuge, number of rinsing steps.

Although some drug carriers are delivered through arteries, e.g. Lipidol® used in liver cancer operation, many of them should allow facile passage through capillary veins for intravenous administration. The EPR (enhanced permeability and retention) effect of the blood vessels in targeted tissues only allows particles with a size of up to 200 nm to escape the blood vessel. Therefore, the challenge is the development of

capsules with a size of less than 200 nm. Decreasing the size of delivery vehicles augments challenges, e.g. surface functionalisation, mechanical properties and controlled release from these delivery vehicles, which will be the interest of researchers in the near future.

References

1. Drews, J. and S. Ryser, *The role of innovation in drug development.* Nature biotechnology, 1997. **15**(13): p. 1318-1319.
2. Venkatesh, S. and R.A. Lipper, *Role of the development scientist in compound lead selection and optimization.* Journal of Pharmaceutical Sciences, 2000. **89**(2): p. 145-154.
3. Prentis, R.A., Y. Lis, and S.R. Walker, *Pharmaceutical innovation by the seven UK-owned pharmaceutical companies (1964-1985).* British Journal of Clinical Pharmacology, 1988. **25**(3): p. 387-396.
4. Han, C. and B.h. Wang, eds. *Factors that impact the developability of drug candidates: an overview* Drug Delivery: Principles and Applications, ed. B. Wang, T.J. Siahaan, and R.A. Soltero. 2005. 1-12.
5. Torchilin, V.P., *Recent advances with liposomes as pharmaceutical carriers.* Nature Reviews Drug Discovery, 2005. **4**(2): p. 145-160.
6. Woodle, M.C., *Poly(ethylene glycol)-Grafted Liposome Therapeutics*. Poly(ethylene glycol) Chemistry and Biological Applications, ed. J.M. Harris; and S. Zalipsky. 1997: ACS Washington.
7. BabincovaÌ , M., et al., *AC-magnetic field controlled drug release from magnetoliposomes: Design of a method for site-specific chemotherapy.* Bioelectrochemistry, 2002. **55**(1-2): p. 17-19.
8. Cheng, C., et al., *Biotinylated thermoresponsive micelle self-assembled from double-hydrophilic block copolymer for drug delivery and tumor target.* Biomaterials, 2008. **29**(4): p. 497-505.
9. Sandström, M.C., E. Johansson, and K. Edwards, *Influence of preparation path on the formation of discs and threadlike micelles in DSPE-PEG2000/lipid systems.* Biophysical Chemistry, 2008. **132**(2-3): p. 97-103.
10. Sun, H.K., et al., *Folate receptor targeted delivery of polyelectrolyte complex micelles prepared from ODN-PEG-folate conjugate and cationic lipids.* Biotechnology Progress, 2007. **23**(1): p. 232-237.
11. Hamidi, M., et al., *Applications of carrier erythrocytes in delivery of biopharmaceuticals.* Journal of Controlled Release, 2007. **118**(2): p. 145-160.
12. Skirtach, A.G., et al., *The role of metal nanoparticles in remote release of encapsulated materials.* Nano Letters, 2005. **5**(7): p. 1371-1377.
13. Khan, D.R., *The use of nanocarriers for drug delivery in cancer therapy.* Journal of Cancer Science and Therapy, 2010. **2**(3): p. 58-62.
14. Mornet, S., *The formation of supported lipid bilayers on silica nanoparticles revealed by cryoelectron microscopy.* Nano Letters, 2005. **5**(2): p. 281-285.
15. Johnston, A.P.R., et al., *Layer-by-layer engineered capsules and their applications.* Current Opinion in Colloid and Interface Science, 2006. **11**(4): p. 203-209.

16. Peyratout, C.S. and L. Dähne, *Tailor-made polyelectrolyte microcapsules: From multilayers to smart containers.* Angewandte Chemie - International Edition, 2004. **43**(29): p. 3762-3783.
17. Sukhorukov, G.B., et al., *Multifunctionalized polymer microcapsules: Novel tools for biological and pharmacological applications.* Small, 2007. **3**(6): p. 944-955.
18. De Cock, L.J., et al., *Polymeric Multilayer Capsules in Drug Delivery.* Angewandte Chemie - International Edition, 2010. **49**(39): p. 6954-6973.
19. Decher, G. and J.D. Hong, Ber. Bunsen-Ges. Phys. Chem., 1991(95): p. 1430.
20. Lvov, Y., et al., *Assembly of multicomponent protein films by means of electrostatic layer-by-layer adsorption.* Journal of the American Chemical Society, 1995. **117**(22): p. 6117-6123.
21. Hammond, P.T., *Recent explorations in electrostatic multilayer thin film assembly.* Current Opinion in Colloid and Interface Science, 1999. **4**(6): p. 430-442.
22. Quinn, J.F., et al., *Next generation, sequentially assembled ultrathin films: Beyond electrostatics.* Chemical Society Reviews, 2007. **36**(5): p. 707-718.
23. Bertrand, P., et al., *Ultrathin polymer coatings by complexation of polyelectrolytes at interfaces: Suitable materials, structure and properties.* Macromolecular Rapid Communications, 2000. **21**(7): p. 319-348.
24. Arys, X., et al., eds. *Supramolecular Polyelectrolyte Assemblies*. Supermolecular Polymers, ed. A. Ciferri. 2005: New York.
25. Li, Q., et al., *Preparation of nanoporous polyelectrolyte multilayer films via nanoparticle templating.* Chemistry of Materials, 2006. **18**(23): p. 5480-5485.
26. Sukhorukov, G., et al., *Controlled precipitation of dyes into hollow polyelectrolyte capsules based on colloids and biocolloids.* Advanced Materials, 2000. **12**(2): p. 112-115.
27. Yu, A., et al., *Mesoporous silica particles as templates for preparing enzyme-loaded biocompatible microcapsules.* Advanced Materials, 2005. **17**(14): p. 1737-1741.
28. Katagiri, K. and F. Caruso, *Functionalization of colloids with robust inorganic-based lipid coatings.* Macromolecules, 2004. **37**(26): p. 9947-9953.
29. Kharlampieva, E. and S.A. Sukhishvili, *Hydrogen-bonded layer-by-layer polymer films.* Polymer Reviews, 2006. **46**(4): p. 377-395.
30. Kotov, N.A., *Layer-by-layer self-assembly: the contribution of hydrophobic interactions.* Nanostructured Materials, 1999. **12**(5): p. 789-796.
31. Caruso, F., et al., *Investigation of electrostatic interactions in polyelectrolyte multilayer films: Binding of anionic fluorescent probes to layers assembled onto colloids.* Macromolecules, 1999. **32**(7): p. 2317-2328.
32. Sackmann, E. and M. Tanaka, *Supported membranes on soft polymer cushions: Fabrication, characterization and applications.* Trends in Biotechnology, 2000. **18**(2): p. 58-64.
33. Boudou, T., et al., *Multiple functionalities of polyelectrolyte multilayer films: New biomedical applications.* Advanced Materials, 2010. **22**(4): p. 441-467.

34. Terrot, M.S., *Nucleic base-directed adsorption of colloids and polyelectrolytes*, in *Chemical Engineering Department*. 2007, MASSACHUSETTS INSTITUTE OF TECHNOLOGY. p. 15.
35. Yuan, W., et al., *pH-controlled construction of chitosan/alginate multilayer film: Characterization and application for antibody immobilization.* Langmuir, 2007. **23**(26): p. 13046-13052.
36. Déjugnat, C. and G.B. Sukhorukov, *pH-responsive properties of hollow polyelectrolyte microcapsules templated on various cores.* Langmuir, 2004. **20**(17): p. 7265-7269.
37. Sukhorukov, G.B., et al., *pH-controlled macromolecule encapsulation in and release from polyelectrolyte multilayer nanocapsules.* Macromolecular Rapid Communications, 2001. **22**(1): p. 44-46.
38. Cohen Stuart, M.A. and H. Tamai, *Dynamics of adsorbed polymers. 2. Thickness relaxation of poly(ethylene oxide) on glass as a function of segmental binding energy.* Langmuir, 1988. **4**(5): p. 1184-1188.
39. Patel, P.A., A.V. Dobrynin, and P.T. Mather, *Combined effect of spin speed and ionic strength on polyelectrolyte spin assembly.* Langmuir, 2007. **23**(25): p. 12589-12597.
40. Serizawa, T., M. Yamaguchi, and M. Akashi, *Enzymatic hydrolysis of a layer-by-layer assembly prepared from chitosan and dextran sulfate.* Macromolecules, 2002. **35**(23): p. 8656-8658.
41. Shaillender, M., et al., *Layer-by-layer microcapsules templated on erythrocyte ghost carriers.* International Journal of Pharmaceutics, 2011. **415**(1-2): p. 211-217.
42. Yu, D.G., et al., *Surface modification of poly(tetramethylene adipate-co-terephthalate) membrane via layer-by-layer assembly of chitosan and dextran sulfate polyelectrolyte multiplayer.* Colloids and Surfaces B: Biointerfaces, 2007. **54**(2): p. 222-229.
43. Johnston, A.P.R.A.P.R., *DNA multilayer films on planar and colloidal supports: Sequential assembly of like-charged polyelectrolytes.* Nano letters, 2005. **5**(5): p. 953-956.
44. Shchukin, D.G., et al., *Nanoassembly of Biodegradable Microcapsules for DNA Encasing.* Journal of the American Chemical Society, 2004. **126**(11): p. 3374-3375.
45. Montrel, M.M., et al., *Spectroscopic study of thin multilayer films of the complexes of nucleic acids with cationic amphiphiles and polycations: Their possible use as sensor elements.* Sensors and Actuators, B: Chemical, 1997. **42**(3 B): p. 225-231.
46. Caruso, F., et al., *2. Assembly of alternating polyelectrolyte and protein multilayer films for imiminosensing.* Langmuir, 1997. **13**(13): p. 3427-3433.
47. Dai, J., G.L. Baker, and M.L. Bruening, *Use of porous membranes modified with polyelectrolyte multilayers as substrates for protein arrays with low nonspecific adsorption.* Analytical Chemistry, 2006. **78**(1): p. 135-140.

48. Feldman, K., et al., *Probing resistance to protein adsorption of oligo(ethylene glycol)- terminated self-assembled monolayers by scanning force microscopy.* Journal of the American Chemical Society, 1999. **121**(43): p. 10134-10141.
49. Park, J. and M.J. McShane, *Dual-function nanofilm coatings with diffusion control and protein resistance.* ACS applied materials & interfaces, 2010. **2**(4): p. 991-997.
50. Wang, Y., A.S. Angelatos, and F. Caruso, *Template synthesis of nanostructured materials via layer-by-layer assembly.* Chemistry of Materials, 2008. **20**(3): p. 848-858.
51. De Geest, B.G., et al., *Polyelectrolyte microcapsules for biomedical applications.* Soft Matter, 2009. **5**(2): p. 282-291.
52. Reibetanz, U., *Flow cytometry of HEK 293T cells interacting with polyelectrolyte multilayer capsules containing fluorescein-labeled poly(acrylic acid) as a pH sensor.* Biomacromolecules, 2007. **8**(6): p. 1927-1933.
53. Donath, E., et al., *Novel hollow polymer shells by colloid-templated assembly of polyelectrolytes.* Angewandte Chemie - International Edition, 1998. **37**(16): p. 2202-2205.
54. Donath, E., et al., *Hollow polymer shells from biological templates: Fabrication and potential applications.* Chemistry - A European Journal, 2002. **8**(23): p. 5481-5485.
55. Neu, B., et al., *Biological cells as templates for hollow microcapsules.* Journal of Microencapsulation, 2001. **18**(3): p. 385-395.
56. Berth, G., et al., *Polyelectrolyte complexes and layer-by-layer capsules from chitosan/chitosan sulfate.* Biomacromolecules, 2002. **3**(3): p. 579-590.
57. Neu, B., et al., *Biological cells as templates for hollow microcapsules.* Journal of Microencapsulation, 2001. **18**(3): p. 385-395.
58. Dahne, L., et al., *Fabrication of micro reaction cages with tailored properties.* Journal of the American Chemical Society, 2001. **123**(23): p. 5431-5436.
59. Gil, P.R., et al., *Nanoparticle-modified polyelectrolyte capsules.* Nano Today, 2008. **3**(3-4): p. 12-21.
60. Antipov, A.A., et al., *Carbonate microparticles for hollow polyelectrolyte capsules fabrication.* Colloids and Surfaces A: Physicochemical and Engineering Aspects, 2003. **224**(1-3): p. 175-183.
61. Kreft, O., et al., *Red blood cell templated polyelectrolyte capsules: A novel vehicle for the stable encapsulation of DNA and proteins.* Macromolecular Rapid Communications, 2006. **27**(6): p. 435-440.
62. Wang, Y. and F. Caruso, *Mesoporous silica spheres as supports for enzyme immobilization and encapsulation.* Chemistry of Materials, 2005. **17**(5): p. 953-961.
63. Gao, C., et al., *The decomposition process of melamine formaldehyde cores: The key step in the fabrication of ultrathin polyelectrolyte multilayer capsules.* Macromolecular Materials and Engineering, 2001. **286**(6): p. 355-361.
64. Shenoy, D.B., et al., *Layer-by-layer engineering of biocompatible, decomposable core-shell structures.* Biomacromolecules, 2003. **4**(2): p. 265-272.

65. Zhang, F., et al., *Bioactive galactose-branched polyelectrolyte multilayers and microcapsules: Self-assembly, characterization, and biospecific lectin adsorption.* Langmuir, 2006. **22**(20): p. 8458-8464.
66. Yap, H.P., et al., *Compositional engineering of polyelectrolyte blend capsules.* Macromolecules, 2007. **40**(21): p. 7581-7589.
67. Ibarz, G., et al., *Controlled permeability of polyelectrolyte capsules via defined annealing.* Chemistry of Materials, 2002. **14**(10): p. 4059-4062.
68. Raichur, A.M., et al., *Adhesion of polyelectrolyte microcapsules through biotin-streptavidin specific interaction.* Biomacromolecules, 2006. **7**(8): p. 2331-2336.
69. Elsner, N., F. Dubreuil, and A. Fery, *Tuning of microcapsule adhesion by varying the capsule-wall thickness.* Physical Review E - Statistical, Nonlinear, and Soft Matter Physics, 2004. **69**(3 1): p. 031802-1-031802-6.
70. Lvov, Y., et al., *Urease Encapsulation in Nanoorganized Microshells.* Nano Letters, 2001. **1**(3): p. 125-128.
71. Ma, Y., et al., *Redox-controlled molecular permeability of composite-wall microcapsules.* Nature Materials, 2006. **5**(9): p. 724-729.
72. Antipov, A.A., G.B. Sukhorukov, and H. Möhwald, *Influence of the ionic strength on the polyelectrolyte multilayers' permeability.* Langmuir, 2003. **19**(6): p. 2444-2448.
73. De Geest, B.G., et al., *Self-rupturing and hollow microcapsules prepared from bio-polyelectrolyte- coated microgels.* Advanced Functional Materials, 2007. **17**(4): p. 531-537.
74. Khopade, A.J. and F. Caruso, *Stepwise self-assembled poly(amidoamine) dendrimer and poly(styrenesulfonate) microcapsules as sustained delivery vehicles.* Biomacromolecules, 2002. **3**(6): p. 1154-1162.
75. Zhao, Q., et al., *Polyelectrolyte microcapsules templated on poly(styrene sulfonate)-doped CaCO3 particles for loading and sustained release of daunorubicin and doxorubicin.* European Polymer Journal, 2006. **42**(12): p. 3341-3351.
76. Antipov, A.A., et al., *Sustained release properties of polyelectrolyte multilayer capsules.* Journal of Physical Chemistry B, 2001. **105**(12): p. 2281-2284.
77. Wang, C., et al., *Combination of adsorption by porous CaCO3 microparticles and encapsulation by polyelectrolyte multilayer films for sustained drug delivery.* International Journal of Pharmaceutics, 2006. **308**(1-2): p. 160-167.
78. Prevot, M., et al., *Behavior of temperature-sensitive PNIPAM confined in polyelectrolyte capsules.* ChemPhysChem, 2006. **7**(12): p. 2497-2502.
79. Schnäckel, A., et al., *Fluorescent bead arrays by means of layer-by-layer polyelectrolyte adsorption.* Soft Matter, 2007. **3**(2): p. 200-206.
80. Kreft, O., et al., *Polymer microcapsules as mobile local pH-sensors.* Journal of Materials Chemistry, 2007. **17**(42): p. 4471-4476.
81. Angelatos, A.S., et al., *Probing the permeability of polyelectrolyte multilayer capsules via a molecular beacon approach.* Langmuir, 2007. **23**(8): p. 4554-4562.

82. Shchukin, D.G., W. Dong, and G.B. Sukhorukov, *Spatially confined tungstate ion polymerization in microcapsules.* Macromolecular Rapid Communications, 2003. **24**(7): p. 462-466.
83. Tiourina, O.P., et al., *Entrapment of α-chymotrypsin into hollow polyelectrolyte microcapsules.* Macromolecular Chemistry and Physics, 2001. **202**(11): p. 209-214.
84. Kreft, O., et al., *Remote control of bioreactions in multicompartment capsules.* Advanced Materials, 2007. **19**(20): p. 3142-3145.
85. Choi, Y.W., et al., *Adsorption mechanism of a weak polyelectrolyte, PAH, onto carboxylate PS particles.* Colloids and Surfaces A: Physicochemical and Engineering Aspects, 2008. **315**(1-3): p. 7-12.
86. Kim, B.S., et al., *Dynamics and stability of dispersions of polyelectrolyte-filled multilayer microcapsules.* Journal of Chemical Physics, 2007. **126**(24).
87. Deng, C., et al., *Solvent-filled matrix polyelectrolyte capsules: Preparation, structure and dynamics.* Soft Matter, 2007. **3**(10): p. 1293-1299.
88. Petrov, A.I., A.A. Antipov, and G.B. Sukhorukov, *Base-acid equilibria in polyelectrolyte systems: From weak polyelectrolytes to interpolyelectrolyte complexes and multilayered polyelectrolyte shells.* Macromolecules, 2003. **36**(26): p. 10079-10086.
89. Georgieva, R., et al., *Permeability and conductivity of red blood cell templated polyelectrolyte capsules coated with supplementary layers.* Langmuir, 2004. **20**(5): p. 1895-1900.
90. Voigt, A., et al., *Membrane filtration for microencapsulation and microcapsules fabrication by layer-by-layer polyelectrolyte adsorption.* Industrial and Engineering Chemistry Research, 1999. **38**(10): p. 4037-4043.
91. Neu, B., H.J. Meiselman, and H. Ba?umler, *Electrophoretic mobility of human erythrocytes in the presence of poly(styrene sulfonate).* Electrophoresis, 2002. **23**(15): p. 2363-2368.
92. De Geest, B.G., et al., *Release mechanisms for polyelectrolyte capsules.* Chemical Society Reviews, 2007. **36**(4): p. 636-649.
93. Moya, S., et al., *Polyelectrolyte multilayer capsules templated on biological cells: Core oxidation influences layer chemistry.* Colloids and Surfaces A: Physicochemical and Engineering Aspects, 2001. **183-185**: p. 27-40.
94. Moya, S., et al., *Lipid coating on polyelectrolyte surface modified colloidal particles and polyelectrolyte capsules.* Macromolecules, 2000. **33**(12): p. 4538-4544.
95. Petrov, A.I., D.V. Volodkin, and G.B. Sukhorukov, *Protein-calcium carbonate coprecipitation: A tool for protein encapsulation.* Biotechnology Progress, 2005. **21**(3): p. 918-925.
96. Sukhorukov, G.B., et al., *Hollow Polyelectrolyte Shells: Exclusion of Polymers and Donnan Equilibrium.* Journal of Physical Chemistry B, 1999. **103**(31): p. 6434-6440.
97. De Geest, B.G.B.G., *Intracellularly degradable polyelectrolyte microcapsules.* Advanced materials, 2006. **18**(8): p. 1005-1009.

98. Reibetanz, U., et al., *Defoliation and plasmid delivery with layer-by-layer coated colloids.* Macromolecular Bioscience, 2006. **6**(2): p. 153-160.
99. De Koker, S., et al., *In vivo cellular uptake, degradation, and biocompatibility of polyelectrolyte microcapsules.* Advanced Functional Materials, 2007. **17**(18): p. 3754-3763.
100. An, Z., et al., *Polyelectrolyte microcapsule interactions with cells in two- and three-dimensional culture.* Colloids and Surfaces B: Biointerfaces, 2009. **70**(1): p. 114-123.
101. Kirchner, C., et al., *Cytotoxicity of nanoparticle-loaded polymer capsules.* Talanta, 2005. **67**(3): p. 486-491.
102. Muñoz Javier, A., et al., *Combined Atomic Force Microscopy and Optical Microscopy Measurements as a Method To Investigate Particle Uptake by Cells.* Small, 2006. **2**(3): p. 394-400.
103. Fischer, D., et al., *In vitro cytotoxicity testing of polycations: influence of polymer structure on cell viability and hemolysis.* Biomaterials, 2003. **24**(7): p. 1121-1131.
104. Leamon, C.P. and P.S. Low, eds. *Receptor-mediated drug delivery*. Drug Delivery: Principles and Applications, ed. B. Wang, T.J. Siahaan, and R.A. Soltero. 2005. 167-187.
105. Fischlechner, M., et al., *Engineering virus functionalities on colloidal polyelectrolyte lipid composites.* Angewandte Chemie - International Edition, 2005. **44**(19): p. 2892-2895.
106. Leßig, J., et al., *Phagocytotic Competence of Differentiated U937 Cells for Colloidal Drug Delivery Systems in Immune Cells.* Inflammation: p. 1-12.
107. Sukhorukov, G.B., *Nanoengineered polymer capsules: Tools for detection, controlled delivery, and site-specific manipulation.* Small, 2005. **1**(2): p. 194-200.
108. Ai, H.H., *Interactions between self-assembled polyelectrolyte shells and tumor cells.* Journal of biomedical materials research, 2005. **73**(3): p. 303-312.
109. Zhao, Q., et al., *Hollow chitosan-alginate multilayer microcapsules as drug delivery vehicle: doxorubicin loading and in vitro and in vivo studies.* Nanomedicine: Nanotechnology, Biology, and Medicine, 2007. **3**(1): p. 63-74.
110. Roberts, C., et al., *Using mixed self-assembled monolayers presenting RGD and (EG)3OH groups to characterize long-term attachment of bovine capillary endothelial cells to surfaces.* Journal of the American Chemical Society, 1998. **120**(26): p. 6548-6555.
111. Chan, W.C.W. and S. Nie, *Quantum dot bioconjugates for ultrasensitive nonisotopic detection.* Science, 1998. **281**(5385): p. 2016-2018.
112. Greish, K., et al., *SMA-doxorubicin, a new polymeric micellar drug for effective targeting to solid tumours.* Journal of Controlled Release, 2004. **97**(2): p. 219-230.
113. Plante, O.J., E.R. Palmacci, and P.H. Seeberger, *Automated solid-phase synthesis of oligosaccharides.* Science, 2001. **291**(5508): p. 1523-1527.
114. Cortez, C., et al., *Targeting and uptake of multilayered particles to colorectal cancer cells.* Advanced Materials, 2006. **18**(15): p. 1998-2003.

115. Cortez, C., et al., *Influence of size, surface, cell line, and kinetic properties on the specific binding of A33 antigen-targeted multilayered particles and capsules to colorectal cancer cells.* ACS nano, 2007. **1**(2): p. 93-102.
116. Zebli, B., et al., *Magnetic targeting and cellular uptake of polymer microcapsules simultaneously functionalized with magnetic and luminescent nanocrystals.* Langmuir, 2005. **21**(10): p. 4262-4265.
117. Saslawski, O., et al., *Magnetically responsive microspheres for the pulsed delivery of insulin.* Life Sciences, 1988. **42**(16): p. 1521-1528.
118. Heuberger, R., et al., *Biofunctional polyelectrolyte multilayers and microcapsules: Control of non-specific and bio-specific protein adsorption.* Advanced Functional Materials, 2005. **15**(3): p. 357-366.
119. Wattendorf, U., et al., *Stable stealth function for hollow polyelectrolyte microcapsules through a poly(ethylene glycol) grafted polyelectrolyte adlayer.* Biomacromolecules, 2008. **9**(1): p. 100-108.
120. Rezwan, K., et al., *Bovine serum albumin adsorption onto colloidal Al2O3 particles: A new model based on zeta potential and UV-Vis measurements.* Langmuir, 2004. **20**(23): p. 10055-10061.
121. Mayers, A.G., *Immobilisation chemistry of biological recognition molecules*. Biomolecular Sensors, ed. E. Gizeli and C.R. Lowe. 2002, New York: Taylor & Francis Inc.
122. Yu, L., et al., *Poly(vinyl alcohol) functionalized poly(dimethylsiloxane) solid surface for immunoassay.* Bioconjugate Chemistry, 2007. **18**(2): p. 281-284.
123. Bai, Y., et al., *Surface modification for enhancing antibody binding on polymer-based microfluidic device for enzyme-linked immunosorbent assay.* Langmuir, 2006. **22**(22): p. 9458-9467.
124. Yu, L., C.M. Li, and Q. Zhou, *Efficient probe immobilization on poly (dimethylsiloxane) for sensitive detection of proteins.* Frontiers in Bioscience, 2005. **10**(SUPPL. 3): p. 2848-2855.
125. Hu, W., et al., *In situ studies of protein adsorptions on poly(pyrrole-co-pyrrole propylic acid) film by electrochemical surface plasmon resonance.* Langmuir, 2007. **23**(5): p. 2761-2767.
126. Eteshola, E. and D. Leckband, *Development and characterization of an ELISA assay in PDMS microfluidic channels.* Sensors and Actuators, B: Chemical, 2001. **72**(2): p. 129-133.
127. Vareiro, M.M.L.M., et al., *Surface plasmon fluorescence measurements of human chorionic gonadotrophin: Role of antibody orientation in obtaining enhanced sensitivity and limit of detection.* Analytical Chemistry, 2005. **77**(8): p. 2426-2431.
128. Xu, H., J.R. Lu, and D.E. Williams, *Effect of surface packing density of interfacially adsorbed monoclonal antibody on the binding of hormonal antigen human chorionic gonadotrophin.* Journal of Physical Chemistry B, 2006. **110**(4): p. 1907-1914.
129. Wen, H.W., et al., *Investigation of NeutrAvidin-tagged liposomal nanovesicles as universal detection reagents for bioanalytical assays.* Talanta, 2006. **68**(4): p. 1264-1272.

130. Sharma, M.K. and M.L. Gilchrist, *Templated assembly of biomembranes on silica microspheres using bacteriorhodopsin conjugates as structural anchors.* Langmuir, 2007. **23**(13): p. 7101-7112.
131. Teramura, Y. and H. Iwata, *Islets surface modification prevents blood-mediated inflammatory responses.* Bioconjugate Chemistry, 2008. **19**(7): p. 1389-1395.
132. Huang, N.P., et al., *Biotin-derivatized poly(L-lysine)-g-poly(ethylene glycol): A novel polymeric interface for bioaffinity sensing.* Langmuir, 2002. **18**(1): p. 220-230.
133. Angerer, L., N. Davidson, and W. Murphy, *An electron microscope study of the relative positions of the 4S and ribosomal RNA genes in HeLa cell mitochondrial DNA.* Cell, 1976. **9**(1): p. 81-90.
134. Vermette, P., et al., *Control over PEGylated-liposome aggregation by NeutrAvidin-biotin interactions investigated by photon correlation spectroscopy.* Langmuir, 2002. **18**(2): p. 505-511.
135. Furlong, D.N., *Quartz crystal microbalance study of DNA immobilization and hybridization for nucleic acid sensor development.* Analytical Chemistry, 1997. **69**(12): p. 2043-2049.
136. Ma, L., et al., *Incorporation of basic fibroblast growth factor by a layer-by-layer assembly technique to produce bioactive substrates.* Journal of Biomedical Materials Research - Part B Applied Biomaterials, 2007. **83**(1): p. 285-292.
137. Angelatos, A.S., K. Katagiri, and F. Caruso, *Bioinspired colloidal systems via layer-by-layer assembly.* Soft Matter, 2006. **2**(1): p. 18-23.
138. Toepke, M.W. and D.J. Beebe, *PDMS absorption of small molecules and consequences in microfluidic applications.* Lab on a Chip - Miniaturisation for Chemistry and Biology, 2006. **6**(12): p. 1484-1486.
139. K. Ariga and T. Kunitake, eds. *In Sequential catalysis in Organized Multienzyme Films*. Protein architecture: interfacing molecular assemblies and immobilization biotechnology ed. H.M. Y. Lvov. 2000, Marcel Dekker: New York,. Page 169-191.
140. Zhou, X. and J. Zhou, *Protein microarrays on hybrid polymeric thin films prepared by self-assembly of polyelectrolytes for multiple-protein immunoassays.* Proteomics, 2006. **6**(5): p. 1415-1426.
141. Goldsby, R.A., *Kuby's Immunology, (4th Edn.)*. 2000.
142. Zhang, H., et al., *Binding affinities/avidities of antibody-antigen interactions: Quantification and scale-up implications.* Biotechnology and bioengineering, 2006. **95**(5): p. 812-829.
143. Garcia, A.A., *Bioseparation Process Science*. 1999.
144. Goldberg, M.E. and L. Djavadi-Ohaniance, *Methods for measurement of antibody/antigen affinity based on ELISA and RIA.* Current Opinion in Immunology, 1993. **5** (2): p. 278-281.
145. Schreiber, G., *Protein-protein interactions*. Biomolecular Sensors, ed. E. Gizeli and C.R. Lowe. 2002, New York: Taylor & Francis Inc.

146. Toellner, L., et al., *Virus-coated layer-by-layer colloids as a multiplex suspension array for the detection and quantification of virus-specific antibodies.* Clinical Chemistry, 2006. **52**(8): p. 1575-1583.
147. Schwartz, A., *Standardizing flow cytometry: Construction of a standardized fluorescence calibration plot using matching spectral calibrators.* Cytometry, 1996. **26**(1): p. 22-31.
148. Volodkin, D., et al., *Composite multilayered biocompatible polyelectrolyte films with intact liposomes: Stability and temperature triggered dye release.* Soft Matter, 2007. **4**(1): p. 122-130.
149. Richter, R.P., R. Bérat, and A.R. Brisson, *Formation of solid-supported lipid bilayers: An integrated view.* Langmuir, 2006. **22**(8): p. 3497-3505.
150. Krishna, G., T. Shutava, and Y. Lvov, *Lipid modified polyelectrolyte microcapsules with controlled diffusion.* Chemical Communications, 2005(22): p. 2796-2798.
151. Baksh, M.M., M. Jaros, and J.T. Groves, *Detection of molecular interactions at membrane surfaces through colloid phase transitions.* Nature, 2004. **427**(6970): p. 139-141.
152. Torchilin, V.P., ed. *Immobilization of specific proteins on liposome surface: systems for drug targeting*. 1st Ed. ed. Liposome Technology, ed. G. Gregoriadis. Vol. Vol.3. 1984, CRC Press: Boca Raton, FL, USA. 75-94.
153. Fang, Y., *Membrane protein microarrays.* Journal of the American Chemical Society, 2002. **124**(11): p. 2394-2395.
154. Gromelski, S., *The formation of lipid bilayers on surfaces.* Colloids and Surfaces B: Biointerfaces, 2009. **74**(2): p. 477-483.
155. Troutier, A.L. and C. Ladavière, *An overview of lipid membrane supported by colloidal particles.* Advances in Colloid and Interface Science, 2007. **133**(1): p. 1-21.
156. Vats, K., *Peripheral protein organization and its influence on lipid diffusion in biomimetic membranes.* ACS chemical biology, 2010. **5**(4): p. 393-403.
157. Katagiri, K. and F. Caruso, *Monodisperse polyelectrolyte-supported asymmetric lipid-bilayer vesicles.* Advanced Materials, 2005. **17**(6): p. 738-743.
158. Radler, J., *Functionalization of solids by ultrathin soft polymer films and polymer/lipid film composites: Modeling of cell surfaces and cell recognition processes.* Current opinion in solid state & materials science, 1997. **2**(3): p. 330-336.
159. Battle, A.R., et al., *Novel engineered ion channel provides controllable ion permeability for polyelectrolyte microcapsules coated with a lipid membrane.* Advanced Functional Materials, 2009. **19**(2): p. 201-208.
160. Khopade, A.J. and F. Caruso, *Surface-modification of polyelectrolyte multilayer-coated particles for biological applications.* Langmuir, 2003. **19**(15): p. 6219-6225.
161. An, Z., H. Möhwald, and J. Li, *pH controlled permeability of lipid/protein biomimetic microcapsules.* Biomacromolecules, 2006. **7**(2): p. 580-585.

162. Köhler, G., et al., *Stability and fusion of lipid layers on polyelectrolyte multilayer supports studied by colloidal force spectroscopy.* European Biophysics Journal, 2007. **36**(4-5): p. 337-347.
163. Harris, J.M., *Introduction to Biotechnical and Biomedical Applications of Poly (Ethylene Glycol)*. Poly(Ethylene Glycol) Chemistry, ed. J.M. Harris. 1992, New York: Plenum.
164. Prime, K.L. and G.M. Whitesides, *Adsorption of proteins onto surfaces containing end-attached oligo(ethylene oxide): A model system using self-assembled monolayers.* Journal of the American Chemical Society, 1993. **115**(23): p. 10714-10721.
165. Langer, R. and D.A. Tirrell, *Designing materials for biology and medicine.* Nature, 2004. **428**(6982): p. 487-492.
166. Andrade, J.D., V. Hlady, and S.I. Jeon, eds. *Hydrophilic Polymers*. Advances in Chemistry, ed. J.E. Glass. Vol. 248. 1996, American Chemical Society: Washington, D.C. 51-59.
167. Berna, M., et al., *Novel monodisperse PEG - Dendrons as new tools for targeted drug delivery: Synthesis, characterization and cellular uptake.* Biomacromolecules, 2006. **7**(1): p. 146-153.
168. Kale, A.A. and V.P. Torchilin, *Design, synthesis, and characterization of pH-sensitive PEG-PE conjugates for stimuli-sensitive pharmaceutical nanocarriers: The effect of substitutes at the hydrazone linkage on the pH stability of PEG-PE conjugates.* Bioconjugate Chemistry, 2007. **18**(2): p. 363-370.
169. Kingshott, P., H. Thissen, and H.J. Griesser, *Effects of cloud-point grafting, chain length, and density of PEG layers on competitive adsorption of ocular proteins.* Biomaterials, 2002. **23**(9): p. 2043-2056.
170. Ostuni, E., et al., *A survey of structure-property relationships of surfaces that resist the adsorption of protein.* Langmuir, 2001. **17**(18): p. 5605-5620.
171. Pasche, S., et al., *Poly(l-lysine)-graft-poly(ethylene glycol) Assembled Monolayers on Niobium Oxide Surfaces: A Quantitative Study of the Influence of Polymer Interfacial Architecture on Resistance to Protein Adsorption by ToF-SIMS and in Situ OWLS.* Langmuir, 2003. **19**(22): p. 9216-9225.
172. Boulmedais, F., et al., *Polyelectrolyte multilayer films with pegylated polypeptides as a new type of anti-microbial protection for biomaterials.* Biomaterials, 2004. **25**(11): p. 2003-2011.
173. Park, K.D., et al., *Bacterial adhesion on PEG modified polyurethane surfaces.* Biomaterials, 1998. **19**(7-9): p. 851-859.
174. Razatos, A., et al., *Force measurements between bacteria and poly(ethylene glycol)-coated surfaces.* Langmuir, 2000. **16**(24): p. 9155-9158.
175. Gan, J., *Fabrication of cell pattern on poly(dimethylsiloxane) by vacuum ultraviolet lithography.* Colloids and Surfaces B: Biointerfaces, 2010. **76**(1): p. 381-385.
176. Tang, J., *The regulation of stem cell differentiation by cell-cell contact on micropatterned material surfaces.* Biomaterials, 2010. **31**(9): p. 2470-2476.

177. Cheung, Y.K., *Microscale control of stiffness in a cell-adhesive substrate using microfluidics-based lithography.* Angewandte Chemie (International ed. in English), 2009. **48**(39): p. 7188-7192.
178. Vermette, P. and L. Meagher, *Interactions of phospholipid- and poly(ethylene glycol)-modified surfaces with biological systems: Relation to physico-chemical properties and mechanisms.* Colloids and Surfaces B: Biointerfaces, 2003. **28**(2-3): p. 153-198.
179. Israelachvili, J., *The different faces of poly(ethylene glycol).* Proceedings of the National Academy of Sciences of the United States of America, 1997. **94**(16): p. 8378-8379.
180. Lasic, D.D., *The Conformation of Polymers at Interfaces*. Poly(ethylene glycol) Chemistry and Biological Applications, ed. J.M. Harris; and S. Zalipsky. 1997: ACS Washington.
181. McPherson, T., et al., *Prevention of protein adsorption by tethered poly(ethylene oxide) layers: Experiments and single-chain mean-field analysis.* Langmuir, 1998. **14**(1): p. 176-186.
182. Lin, Y.S., V. Hlady, and C.G. Gölander, *The surface density gradient of grafted poly(ethylene glycol): Preparation, characterization and protein adsorption.* Colloids and Surfaces B: Biointerfaces, 1994. **3**(1-2): p. 49-62.
183. Prime, *Adsorption of proteins onto surfaces containing end-attached oligo(ethylene oxide): a model system using self-assembled monolayers.* Journal of the American Chemical Society, 1993. **115**(23): p. 10714-10721.
184. Pasche, S., *MECHANISMS OF PROTEIN RESISTANCE OF ADSORBED PEG-GRAFT COPOLYMERS*. 2004, SWISS FEDERAL INSTITUTE OF TECHNOLOGY ZURICH: Zürich.
185. König, H.M., et al., *Supramolecular PEG-co-oligo(p-benzamide)s prepared on a peptide synthesizer.* Journal of the American Chemical Society, 2007. **129**(3): p. 704-708.
186. Makamba, H., *Stable permanently hydrophilic protein-resistant thin-film coatings on poly(dimethylsiloxane) substrates by electrostatic self-assembly and chemical cross-linking.* Analytical Chemistry, 2005. **77**(13): p. 3971-3978.
187. Pasche, S., et al., *Effects of ionic strength and surface charge on protein adsorption at PEGylated surfaces.* Journal of Physical Chemistry B, 2005. **109**(37): p. 17545-17552.
188. Samuel, Z. and J.M. Harris, eds. *Introduction to Chemistry and Biological Applications of Poly(ethylene glycol)* Poly(ethylene glycol) Chemistry and Biological Applications, ed. J.M. Harris. 1997, ACS Washington. 1-13.
189. Fischlechner, M., et al., *Fusion of enveloped virus nanoparticles with polyelectrolyte-supported lipid membranes for the design of bio/ nonbio interfaces.* Nano Letters, 2007. **7**(11): p. 3540-3546.
190. Malvern, I.L., *Zetasizer Nano Series User Manual*. 2005, Worcs, U.K.
191. Shapiro, H.M., *Practical Flow Cytometry* 2003, New York: Wiley-Liss
192. BD-Biosciences, *Introduction to Flow Cytometry: A Learning Guide*. 2000.
193. Asylum Research, I., *MFP-3D™ Atomic Force Microscope Installation and Operation Manual*. 2004.

194. Inc., D.I., *NanoScope®, Command Referece Manual*, Santa Barbara, CA.
195. Zeiss, C., *LSM 510 META Laser Scanning Microscope*.
196. Stine, R., et al., *Heat-stabilized phospholipid films: Film characterization and the production of protein-resistant surfaces.* Langmuir, 2005. **21**(24): p. 11352-11356.
197. Iannone, M.A. and T.G. Consler, *Effect of microsphere binding site density on the apparent affinity of an interaction partner.* Cytometry Part A, 2006. **69**(5): p. 374-383.
198. Gao, J., et al., *Bio-functionalisation of polyelectrolyte microcapsules with biotinylated polyethylene glycol - grafted liposomes.* Macromolecular Bioscience, 2011. **11**.
199. Forde, A. and J. Coley, eds. *Choosing and characterizing antibodies*. Immunoassays, ed. J.P. Gosling. 2000, Oxford: New York.